Examination of curcumin-induced heat shock protein gene expression in *Xenopus laevis* A6 kidney epithelial cells

by

Saad Khan

A thesis
presented to the University of Waterloo
in fulfillment of the
thesis requirement for the degree of
Master of Science
in
Biology

Waterloo, Ontario, Canada, 2010

Author's Declaration

I hereby declare that I am the sole author of this thesis. This is a true copy of the thesis, including any required final revisions, as accepted by my examiners.

I understand that my thesis may be made electronically available to the public.

Abstract

The heat shock response is a cellular homeostatic mechanism that is activated in response to stressful stimuli (e.g. heat shock, heavy metals, disease states etc.), which causes an increase in unfolded protein, which triggers the expression of heat shock protein (*hsp*) genes. HSPs are molecular chaperones that assist in protein synthesis, folding and degradation and prevent stress-induced protein aggregation. Since stressor-induced tissue damage is associated with different disease states, indirect evidence suggested that HSP inducers may be therapeutically beneficial for certain diseases. Curcumin, a phenolic compound found in the Indian spice, *Curcuma longa* (Turmeric), was shown to have anti-inflammatory, anti-tumor and anti-amyloid properties. In the present study, it was determined that curcumin inhibited the ubiquitin-proteasome system (UPS) activity and induced the accumulation of HSPs in the frog model system, *Xenopus laevis*. Treatment of A6 kidney epithelial cells with curcumin enhanced ubiquitinated protein levels and inhibited chymotrypsin-like activity. Furthermore, HSP30 and HSP70 accumulation was observed in cells exposed to 10 - 50 μM curcumin for 24 h in a concentration-dependent manner with maximal levels of HSP30 and HSP70 in cells treated with 30 μM curcumin. Time-dependent increases in HSP30 and HSP70 accumulation were also observed in cells treated with 30 μM curcumin for 2 to 24 h. The accumulation of HSP30 and HSP70 in cells recovering from curcumin exposure increased up to 24 h after treatment. The simultaneous treatment of A6 cells with 10 μM curcumin and mild heat shock (30 ºC) for 6 h resulted in an enhanced accumulation of HSP30 and HSP70, which was greater than with each stressor alone. This pattern of combined stressor-induced HSP30 and HSP70 accumulation increased from 2 to 6 h, after which it decreased from 10 to 24 h. The activation of HSF1 may be involved in curcumin-induced *hsp* gene expression in A6 cells since KNK437, a heat shock factor-1 inhibitor, inhibited the

accumulation of HSP30 and HSP70. Immunocytochemical analysis employing the use of laser scanning confocal microscopy (LSCM) revealed that curcumin-induced HSP30 was detectable primarily in the cytoplasm in a punctate pattern with minimal detrimental effects on the actin cytoskeleton. Elevation of the incubation temperature from 22 to 30 °C greatly enhanced the curcumin-induced cytoplasmic accumulation of HSP30 in a granular pattern. Lastly, curcumin treatment also conferred a state of thermotolerance in A6 cells such that they were able to maintain proper actin cytoskeleton in subsequent thermal challenges. This phenomenon was controlled at the transcriptional level since pretreatment of cells with KNK437, repressed HSP30 accumulation and cytoprotection. These findings are of importance given the interest in identifying agents that can upregulate HSP levels with minimal effects on cell structure or function as a therapeutic treatment of certain protein folding diseases.

Acknowledgements

I have had a time of a lifetime as a member of the Heikkila lab and have collected many cherished memories. I would like to thank first and foremost, my supervisor, Dr. John J. Heikkila for this opportunity as well as his patience, guidance and advice throughout the past two years. In addition, I would like to thank my committee members, Dr. Bernard R. Glick and Dr. Mungo Marsden for taking the time out of their busy schedules to review my work and provide helpful feedback. I would also like to thank all the members of Club Heikkila past and present: Jordan Young, Shantel Walcott, Ashley Rammeloo, Jara Brunt, Jin Duan and Ahmed el-Zahabi for making this a memorable experience. I would also like to extend a big thank you to Linda Zepf, the best graduate advisor to my knowledge, for providing her administrative assistance and advice, whenever I needed it. I would also like to acknowledge Dale Weber for his help with confocal microscopy, thank you for constantly checking in on me. I would also like to thank my special friend Harman for her unrelenting support and motivation throughout my Master's degree. Last but not least, I would like to thank my family and friends for providing continuous love and support throughout my undergraduate and Master's degree.

Table of Contents

Author's Declaration ..... **ii**

Abstract ..... **iii**

Acknowledgements ..... **v**

Table of Contents ..... **vi**

List of Figures ..... **viii**

List of Tables ..... **ix**

List of Abbreviations ..... **x**

1. Introduction **1**

1.1. Heat Shock Response 1

1.2. Heat Shock Proteins 4

1.2.1. Function of HSPs 4

1.2.2. Small heat shock proteins 4

1.2.3. Heat shock protein 70 6

1.3. Stress-induced regulation of *hsp* gene expression 8

1.3.1. Heat shock transcription factor 8

1.3.2. HSF1 structure 9

1.3.3. Transcriptional regulation of *hsp* genes via HSF1 12

1.4. *Xenopus laevis* as a model organism 15

1.5. *Xenopus laevis* HSP30 16

1.6. *Xenopus laevis* HSP70 17

1.7. Association of HSP with cancer and neurodegenerative diseases 18

1.8. Protein Degradation 19

1.8.1. Ubiquitin-proteasome pathway 20

1.8.2. Protein Ubiquitination 20

1.8.3. The Proteasome 21

1.8.4. Proteasomal Inhibition 21

1.9. Curcumin 22

1.10. Research Objectives 25

2. Materials and Methods 27

2.1. Maintenance and treatment of *Xenopus laevis* A6 kidney epithelial cells 27

2.2. Protein isolation, quantification and immunoblot analysis 28

2.2.1. Protein isolation and quantification 28

2.2.2. Immunoblot analysis 29

2.3. Densitometry and statistical analysis 31

2.4. Immunocytochemistry and laser scanning confocal microscopy 31

2.5. Cell-Based Proteasome Assay 33

3. Results 35

3.1. Curcumin-induced increase in ubiquitinated protein in A6 cells 35

3.2. Effect of curcumin on chymotrypsin-like activity of A6 cells 35

3.3. Analysis of heat shock induced HSP30 and HSP70 accumulation in *Xenopus* cultured cells 40

3.4. Curcumin-induced HSP accumulation in A6 cells occurs in a concentration and time-dependent manner 40

3.5. HSP30 and HSP70 levels in A6 cells recovering from curcumin treatments 45

3.6. Involvement of HSF activation in the accumulation of HSP30 and HSP70 in curcumin treated A6 cells treated 50

3.7. Effect of mild heat shock on curcumin-induced HSP accumulation 50

3.8. Localization of HSP30 in heat shock and curcumin-treated A6 cells 56

3.9. The effect of curcumin and mild heat shock on the acquisition of thermotolerance in A6 cells 61

4. Discussion 76

References 85

List of Figures

Figure 1. The heat shock response 2
Figure 2. General structure of HSF1. 10
Figure 3. Stress-induced regulation of heat shock response. 13
Figure 4. The chemical structure of curcumin. 23
Figure 5. Effect of curcumin and MG132 on ubiquitinated protein levels in A6 cells. 36
Figure 6. Effect of curcumin and MG132 on chymotrypsin-like activity of A6 cells. 38
Figure 7. HSP30, HSP70 and actin accumulation in A6 cells subjected to heat shock. 41
Figure 8. Curcumin-induced HSP30 and HSP70 accumulation in *Xenopus laevis* A6 cells. 43
Figure 9. Time course of curcumin-induced HSP30 and HSP70 accumulation in A6 cells. 46
Figure 10. HSP30 and HSP70 accumulation in A6 cells recovering from curcumin treatment. 48
Figure 11. Effect of KNK437 on curcumin-induced HSP30 and HSP70 accumulation in A6 cells. 51
Figure 12. Analysis of HSP30 and HSP70 accumulation in A6 cells treated simultaneously with curcumin plus mild heat shock. 54
Figure 13. Time course of HSP30 and HSP70 accumulation in A6 cells treated with concurrent curcumin and mild heat shock. 57
Figure 14. Immunocytochemical detection of intracellular HSP30 accumulation in A6 cells exposed to two different heat shock temperatures. 59
Figure 15. Intracellular localization of curcumin-induced HSP30 accumulation. 62
Figure 16. Localization of HSP30 accumulation in A6 cells treated singularly or simultaneously with a mild heat shock plus curcumin. 64
Figure 17. Time course of intracellular HSP30 accumulation in A6 cells treated with a mild heat shock plus curcumin treatment. 66
Figure 18. Cytoprotective effects of pre-treating A6 cells with heat shock prior to a 37 ºC thermal challenge. 68
Figure 19. Cytoprotective effects of pre-treating A6 cells with curcumin prior to a 37 ºC thermal challenge. 71
Figure 20. Cytoprotective effects of pre-treating A6 cells simultaneously with a mild heat shock plus curcumin prior to a 37 ºC thermal challenge. 74

List of Tables

Table 1. Dilution specifications for antibodies used in Western blot analysis 31

List of Abbreviations

ALS	amyotrophic lateral sclerosis
ANOVA	analysis of variance
APS	ammonium persulfate
ATCC	american type culture collection
BCA	bicinchoninic acid
BCIP	5-bromo-4-chloro-3-indolyl phosphate
BiP	immunoglobulin-binding protein
BSA	bovine serum albumin protein standard
C	control
CT-like	chymotrypsin-like
Cur	curcumin
DAPI	4,6-diamidino-2-phenylindole
DMSO	dimethylsulphoxide
EDTA	ethylene-diamine-tetraacetic acid
FBS	fetal bovine serum
HBSS	Hank's balanced salt solution
HEPES	4-(2-hydroxyethyl)-1-piperazineethanesulfonic acid
HSC	heat shock cognate
HSE	heat shock element
HSF	heat shock factor
HSP	heat shock protein
hsp	heat shock protein gene
HSR	heat shock response
KNK437	N-formyl-3, 4-methylenedioxy-benzylidene-γ-butyrolactam
L-15	Leibovitz-15 media
LSCM	laser scanning confocal microscopy
MBT	midblastula transition
MG132	carbobenzoxy-L-leucyl-L-leucyl-L-leucinal
NBT	4-nitro blue tetrazolium
PBS	phosphate buffered saline
SDS-PAGE	sodium dodecyl sulfate polyacrylamide gel electrophoresis
TBS-T	tris buffered saline solution – Tween20
TEMED	tetra-methyl-ethylene-diamine
Tris buffer	tris(hydroxymethyl)aminomethane
TRITC	rhodamine-tetramethylrhodamine-5-isothiocyanate phalloidin
UPS	ubiquitin-proteasome system

1. Introduction

Organisms are constantly challenged by conditions that cause chronic and acute stress and have evolved networks of responses that identify, monitor and respond to these stressful stimuli (Morimoto, 2008). At the molecular level, biochemical properties responsible for protein function and stability are disrupted as a result of exposure to stressful stimuli, both environmental and physiological, causing the proteins to unfold into unstable conformations (Morimoto, 1998; Balch et al., 2008). Polypeptides with abnormal folding are prone to cytotoxic aggregation, which can result in aberrant cellular processes and/or disease (Morimoto, 2008). As a result, cells have evolved two main mechanisms to protect themselves against cytotoxic aggregation: the heat shock response and ubiquitin-proteasome degradation pathway.

1.1. Heat Shock Response

The heat shock response is a universal cellular homeostatic mechanism, well characterized in prokaryotes and eukaryotes. It was first discovered by Ferrucio Ritossa in the salivary glands of *Drosophila* in 1962 (Jolly and Morimoto, 2000; Katschinski, 2004). It is activated in response to stressful stimuli including elevated temperatures, heavy metals or disease states (Fig. 1; Morimoto, 2008). These stresses can induce an accumulation of unfolded protein, which can interfere with regular cellular processes. Accumulation of unfolded protein triggers the up-regulation of heat shock protein (*hsp*) genes through the activation of heat shock factor 1(HSF1) (Morimoto, 1998; 2008).

Figure 1. The heat shock response. Induction of the heat shock response (HSR) in cells is a result of a variety of factors which in turn upregulate the production of heat shock proteins (HSPs) (Adapted from Morimoto, 2008).

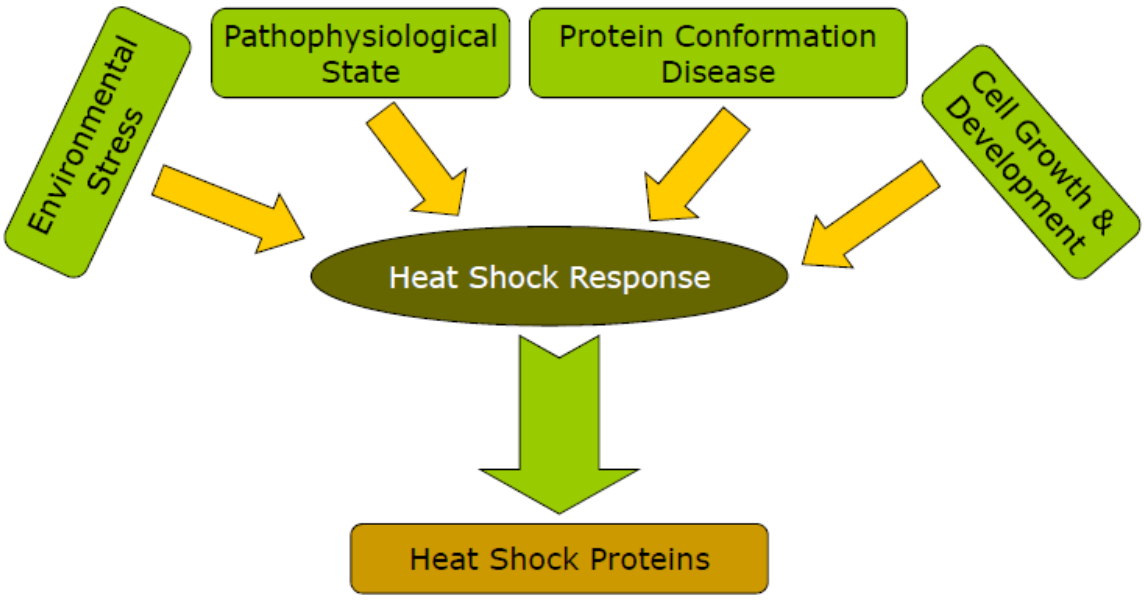
Environmental Stress
Pathophysiological State
Protein Conformation Disease
Cell Growth & Development
Heat Shock Response
Heat Shock Proteins

1.2. Heat Shock Proteins

1.2.1. Function of HSPs

Heat shock proteins (HSPs) are a large group of molecular chaperones that are involved in many cellular processes including protein synthesis, folding/assembly, membrane translocation and degradation in normally growing cells. HSPs also bind to denatured proteins and assist in refolding proteins to their native state or target them for degradation in order to prevent stress-induced protein aggregation. HSPs have been well documented in a wide variety of organisms from bacteria to man (Katschinski, 2004). There are 6 different HSP gene families that have been characterized to date and are grouped based on size and include small HSPs (sHSPs), HSP40, HSP60, HSP70, HSP90 and HSP100 (Katschinski, 2004; Morimoto, 2008). They can be constitutively expressed, strictly stress inducible or both inducible and constitutively regulated (Morimoto, 2008). HSP expression patterns vary between organisms, tissues types, and developmental stages (Lindquist, 1986; Heikkila et al., 1997; Heikkila, 2010).

1.2.2. Small heat shock proteins

The small heat shock protein (sHSP) family is made up of HSPs ranging in size from 16 to 42 kDa and includes the lens protein α-crystallin. Unlike other HSP families, sHSPs are an evolutionarily divergent family of proteins with the exception of 80 - 100 amino acid conserved α-crystallin domain (MacRae, 2000; Van Montfort et al., 2001). The number, size and sequence of the family members vary from species to species (Arrigo and Landry, 1994; Stromer et al., 2003). Despite the lack of conservation, most sHSPs have either two or three functional domains. These regions include the conserved α-crystallin domain, an amino-terminal extension and a carboxy-terminal extension. The secondary structure of the α-crystallin domain primarily

consists of β-strands organized into β-sheets required for dimer formation, the basic functional units of sHSPs (Buchner et al., 1998; MacRae, 2000). The N-terminal extension is poorly conserved except for the Trp-Asp-Pro-Phe (WDPF) sequence, which makes a α-helix and may play a role in oligomer formation (Lambert et al., 1999; Ganea, 2001). The C-terminal extension, which is poorly conserved and variable in length, has been shown to be essential for stabilization of the quaternary structure as well as chaperone activity (MacRae, 2000; Fernando and Heikkila, 2000). Research has found that in many organisms, with the exception of the nematode, the amino-terminal end has little effect on chaperone function whereas deletion of amino acids from the carboxy-terminal end of sHSPs results in a dramatic reduction in chaperone activity (Takemoto et al., 1993; Fernando and Heikkila, 2000; Abdulle et al., 2002).

SHSPs are some of the most strongly induced HSPs when compared to other HSPs (Arrigo and Landry, 1994; Haslbeck, 2002). SHSPs accumulate in different organs and tissues and levels vary in a tissue-, developmental stage- and stress-specific manner (Ciocca et al., 1993). For example, HSP25 is most abundant in lens, heart, stomach, colon, lung and bladder in rodents (Klemenz et al., 1993), whereas HSP27 is detected in muscle, nervous, connective tissue and female reproductive tract in humans (Ciocca et al., 1993). Developmental or tissue-specific controls in gene expression may be regulated at the level of chromatin structure or organization (Heikkila, 2003). Intracellular localization of sHSPs changes according to the physiological state of the cells and to the type and intensity of the stressor (Adhikari et al., 2004; Gellalchew and Heikkila, 2005).

SHSPs form highly polymeric structures (Freeman and Yamamoto, 2002), which are 9 to 30 subunits in size and are necessary for their chaperone function in vivo (Ohan et al., 1998; Heikkila, 2003). This organization is conserved in a number of organisms including yeast,

insects, crustaceans, mammals and amphibians. As a result sHSPs are competent at binding partially denatured proteins in an energy-independent manner, keeping them in a folding competent state so they may be refolded by other ATP-dependent chaperones such as HSP70. Like other HSPs, the sHSP family has both constitutive and inducible members in many animal development systems including *Drosophila*, mouse, rat, shrimp and nematode (Heikkila, 2003). It has also been shown that following heat or chemical stress, p38 mitogen-activated protein kinase (MAPK) has a role in phosphorylating sHSPs, including HSP30C in *Xenopus laevis* (Fernando et al., 2003). In the case of HSP30C, phosphorylation inactivates it as a molecular chaperone and causes the release of its substrate (Fernando et al., 2003).

Various functions that have been suggested for sHSPs include resistance against apoptosis, acquisition of thermotolerance, actin capping/decapping activity, modulation of redox parameters, and cellular differentiation (Arrigo, 1998; MacRae, 2000; Van Montfort et al., 2001; Heikkila, 2004). As a result, the role of sHSPs in several medical conditions such as multiple sclerosis, oncogenesis and neurodegenerative diseases are being investigated (Birnabaum and Kotilinek, 1997; Jolly and Morimoto, 2000; Westerheide and Morimoto, 2005).

1.2.3. Heat shock protein 70

HSP70 is a large family of conserved molecular chaperones that has been detected in all organisms with multiple family members (Katschinski, 2004; Daugaard et al., 2007). Members of the HSP70 family are responsible for regulating the folding of proteins under normal and stressful conditions. It is one of the most comprehensively studied gene families and contains several functional members including cytoplasmic stress-inducible HSP70, cytoplasmic constitutively expressed heat shock cognate 70 (HSC70), mitochondrial p75 and ER-resident

immunoglobulin binding protein (BiP) (Morimoto, 1998). Its members interact with exposed hydrophobic surfaces of unfolded or partially folded proteins and refold them in an ATP-dependent manner (Katschinski, 2004). In addition to possessing a chaperone function, HSP70 also inhibits apoptosis by recruiting and deactivating caspases (Beere et al., 2000; Daugaard et al., 2007).

HSP70 contains a highly conserved ATPase domain, a peptide binding domain and a G/C rich domain required for binding with various other co-chaperones (Beere et al., 2000; Daugaard et al., 2007). The N-terminal ATPase domain is involved in binding and release of non-native proteins. Additionally, a Glu-Glu-Val-Asp (EEVD) motif is present in the C-terminal region and allows HSP70 to interact with other HSPs and co-chaperones such as HSP40 (Katschinski, 2004; Daugaard et al., 2007). Binding at this motif maybe also be responsible for HSP70 function and target protein specificity.

HSP70 family members have been shown to assist in protein folding, translocation of proteins across cell membranes and degradation of denatured and misfolded proteins (Katschinski, 2004; Daugaard et al., 2007). Even though some HSP70 family members are expressed in a stress-dependent manner, human cytosolic HSP70 is expressed in a tissue-specific and cell-cycle dependent manner during normal steady-state conditions as well (Daugaard et al., 2007). Upregulation of *hsp70* gene expression has been reported in cells encountering stressful conditions including elevated temperature and chemical exposure. During these periods of stress, HSP70 protects the cell from aggregation of unfolded protein and also directs the refolding of these proteins (Boorstein et al., 1994). HSP70 has also been shown to play an inhibitory role in stress kinase pathways (Sreedhar and Csermely, 2004) and prevention of apoptosis (Mosser et al., 2000; Beere, 2001).

1.3. Stress-induced regulation of *hsp* gene expression

Stress inducible *hsp* genes are regulated primarily at the transcriptional level via the interaction of the heat shock transcription factor (HSF) with the cis-acting heat shock element (HSE). The HSE consists of multiple inverted repeats of the pentamer sequence 5'-nGAAn-3', which are generally present in the 5' promoter of most *hsp* genes (Morimoto, 1998; Katschinski, 2004; Voellmy, 2004).

1.3.1. Heat shock transcription factor

Drosophila melanogaster, *Sacchromyces cervisiae* and *Caenorhabditis elegans* express a single type of HSF that mediates the induction of the HSR, while vertebrate animals and plants express multiple HSFs with specialized functions (Morimoto and Santoro, 1998; Voellmy, 2004). Thus far, four HSFs have been identified and characterized in vertebrates (HSF1 – 4). While HSF1, HSF2 and HSF4 are expressed in mammals, HSF3 appears to be an avian specific-transcription factor (Voellmy, 2004; Yamamoto et al., 2009). HSF1 is considered the primary eukaryotic transcription factor responsible for the stress-induced expression of *hsp* genes and is functionally equivalent to the HSF found in *Drosophila* and yeast (Morimoto, 1998; Heikkila, 2004). Detectable levels of HSF2 have only been observed in embryonic tissues and specifically contribute to the developmental regulation of *hsp* gene expression (Rallu et al., 1997; Voellmy, 2004). Recent data collected using chromatin immunoprecipitation (ChIP) showed that both HSF1 and HSF2 are recruited to the *hsp70* promoter in response to heat shock and hemin treatment (Ostling et al., 2007). In addition, evidence acquired using RT-PCR suggested that in the presence of HSF1, HSF2 contributes to the transcriptional regulation of multiple *hsp* genes

including mouse *hsp25*, *hsp40*, *hsp70*, and *hsp110* in response to heat shock and proteasome inhibition (Ostling et al., 2007). HSF3 is required for stress-induced *hsp* gene expression in birds and the combined functional roles of avian HSF1 and HSF3 seem to be equivalent to mammalian HSF1 activity (Nakai, 1999; Voellmy, 2004). Finally, HSF4 has two isoforms; HSF4a and HSF4b and is expressed in a tissue-specific manner. HSF4a appears to function as a repressor of *hsp* gene expression while, HSF4b appears to activate transcription (Tanabe et al., 1999; Pirkkala, 2001).

1.3.2. HSF1 structure

As mentioned previously, HSF1 is the stress-responsive member of the HSF family and is responsible for the activation of the HSR in higher organisms (Heikkila, 2004; Voellmy, 2004). The structure of HSF1 is highly conserved, consisting of 100 amino acids in a helix-turn-helix DNA binding motif, as well as a carboxy-terminal transcriptional transactivation domain and an oligomerization domain consisting of a hydrophobic repeat sequence (HR-A/B) essential for trimer formation (Fig. 2; Morimoto, 1998; Voellmy, 2004). An additional hydrophobic repeat sequence (HR-C) absent in yeast HSF and mammalian HSF4 is located adjacent to the transcription activation domain. Under normal conditions interactions between HR-A/B and HR-C contribute to the suppression of HSF1 trimerization, while a conserved sequence located between HR-A/B and HR-C is thought to negatively regulate DNA-binding and transcriptional activation.

Figure 2. General structure of HSF1. Schematic representation of HSF1 structural motifs that correspond to the helix-turn-helix DNA binding domain, hydrophobic repeat sequences (HR-A/B and HR-C), the carboxy terminal transcription activation domain, and regulatory domains associated with the suppression of HSF1 activity (adapted from Voellmy, 2004).

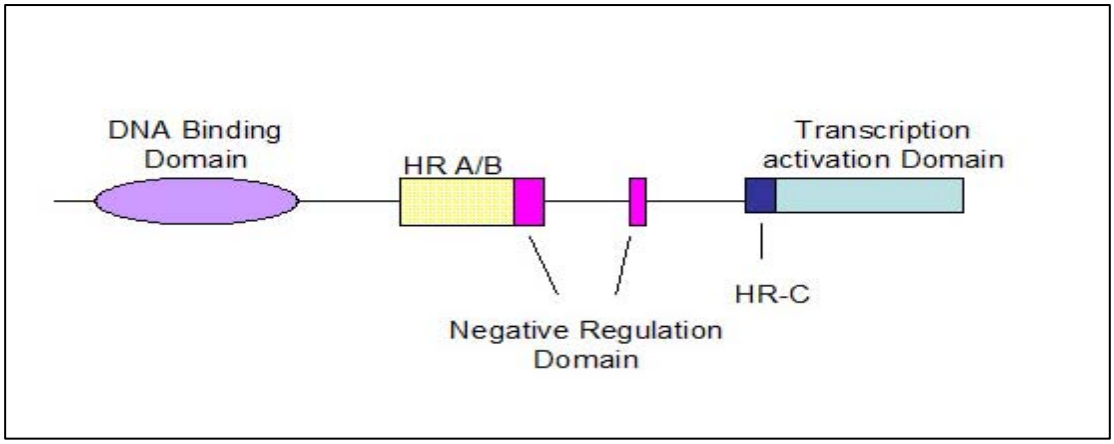
DNA Binding
Domain
HR A/B
Transcription
activation Domain
HR-C
Negative Regulation
Domain

1.3.3. Transcriptional regulation of *hsp* genes via HSF1

Normally HSF1 is bound to HSP70 and/or HSP90 and exists as an inactive monomer in the cytoplasm and/or nucleus (Voellmy, 2004). In response to an increase in the intracellular levels of denatured proteins, HSP90 and HSP70 are recruited to aid in protein folding and prevent their aggregation, thereby allowing HSF1 monomers to trimerize (Fig. 3; Voellmy, 2004). This trimerization results in the activation of the HSF1 and subsequent localization to the nucleus to initiate transcription of *hsp* genes by RNA polymerase II (Feige et al., 1996). Activated HSF1 is further modified post-translationally by phosphorylation, sumoylation and/or aceytlation at conserved amino acid residues. Phosphorylation can regulate the activation and inactivation of HSF1. Although the mechanism is not completely understood, it appears that constitutively phosphorylated serine residues suppress HSF1 activation, while inducible phosphorylated serine residues promote HSF1 activity (Holmberg et al., 2002; Voellmy, 2004). Sumoylation, the post-translational process by which a small ubiquitin-like modifier (SUMO) is added to proteins, occurs in a phosphorylation-dependent manner at conserved lysine residues in response to stress. It plays a role in regulating DNA binding activity and transcriptional activation of HSF1 (Hong et al., 2001; Anckar et al., 2006). Recently, an inhibitor of HSF1-HSE binding activity, N-formyl-3, 4-methylenedioxy-benzylidene-γ-butyrolactam, more commonly known as KNK437, was found to inhibit induction of various HSPs including HSP105, HSP70 and HSP40 in human colon cancer cells (Yokota et al., 2000). In mammals, KNK437 was shown to inhibit heat shock induced HSF1 activation or the interaction between HSF1 and HSE (Ohnishi et al., 2004). Finally, it was demonstrated in our laboratory that KNK437 inhibited *hsp* gene expression induced by heat shock as well as sodium arsenite, cadmium chloride, herbimycin A and proteasome inhibitors, MG132 and celastrol, in *Xenopus laevis* A6 cells

Figure 3. Stress-induced regulation of heat shock response. (1,2) External stressful stimuli cause native proteins in the cell to unfold. (3) HSP70 and HSP90 are bound to HSF-1 under normal conditions in the cell. (4) HSP70 and HSP90 are recruited to prevent aggregation of unfolded proteins. (5) This allows HSF-1 monomers to trimerize and translocate to the nucleus. (6) The HSF-1 trimer then binds to the heat shock element at the 5' promoter of *hsp* genes. (7) HSF-1 binding to the HSE results in the transcription of stress-induced HSPs.

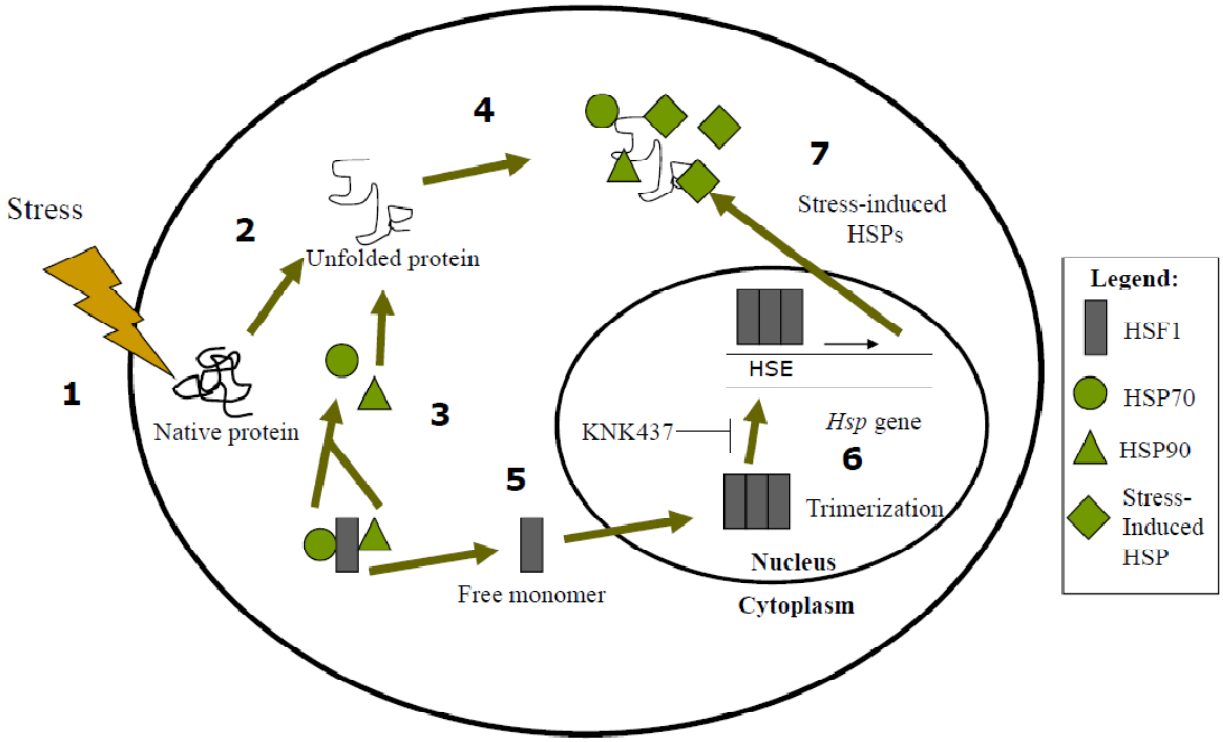
Stress
1
Native protein
2
Unfolded protein
3
4
5
Free monomer
6
KNK437
HSE
Hsp gene
Trimerization
7
Stress-induced HSPs
Nucleus
Cytoplasm
Legend:
HSF1
HSP70
HSP90
Stress-Induced HSP

(Manwell and Heikkila, 2007; Voyer and Heikkila, 2008; Woolfson and Heikkila, 2009; Walcott and Heikkila, 2010;Young and Heikkila, 2010).

1.4. Xenopus laevis as a model organism

The South African clawed frog, *Xenopus laevis* has been used extensively as a model system for amphibian development. As aquatic animals they have a high tolerance for dynamic environmental conditions and possess physiological traits that are common to most vertebrates thus ensuring that data collected through these systems is applicable to mammals (Burggren and Warburton, 2007). There are 18 species within the *Xenopus* genus, and 7 subspecies of *Xenopus laevis. Xenopus* generally prefer stagnant pools and gulp air for respiration. *Xenopus* is relatively inexpensive to rear and produces eggs that are large, approximately 1 mm in diameter and suitable for microinjection (Etkin, 1982; Sive et al., 2000; Heikkila et al., 2007). Furthermore *X. laevis* eggs are externally fertilized and the embryos develop rapidly at room temperature. Many *X. laevis* genes have been isolated and characterized and the findings obtained from studies using *X. laevis* are generally applicable to humans.

Xenopus continuous cell lines are useful tools for in vitro molecular analyses. A number of *Xenopus* cell lines have been developed over the years including A6, B3.2, KR, XF, XL2, XL110, XL-177 and XTC-2 (Smith and Tata, 1991). The most popular cell line used today is the A6 somatic cell line, which was also used in the present study. The *X. laevis* A6 kidney epithelial cell line was isolated from the renal tubules of the adult *Xenopus* by Rafferty (1969). It is easy to maintain and has a quick doubling time, making it an ideal tool for cellular and molecular biology research. Unlike other untransformed *Xenopus* cell lines, A6 cells continue to divide after reaching confluency. The A6 kidney epithelial cell line has been used widely in diverse

areas of research, from genetic profiling under zero gravity to the function of Cystic Fibrosis transmembrane conductance regulator channels, and the role of renal epithelial sodium channels in hypertension (Guerra et al., 2004; Ikuzawa et al., 2007; Wang et al., 2009). Finally, the induction of the heat shock response following exposure to environmental stressors such as heat shock, sodium arsenite, hydrogen peroxide, cadmium chloride and herbimycin A has been well characterized in *X. laevis* A6 kidney epithelial cells (Briant et al., 1997; Ohan et al., 1998; Phang et al., 1999; Muller et. al, 2004; Gellalchew and Heikkila, 2005; Woolfson and Heikkila, 2009; Heikkila, 2010).

1.5. *Xenopus laevis* HSP30

HSP30 is a member of the sHSP superfamily of proteins. There have been 5 *X. laevis* gene family members in two gene clusters identified to date. All of the *hsp30* genes are intronless and share a conserved α-crystallin domain. They are denoted *A – E*. The first gene cluster containing *hsp30A* and *hsp30B* genes was first identified by Bienz (1984). *Hsp30A* contains a 21 base pair insertion in the coding region that includes a translational termination signal which results in the production of a 10 kDa protein. The *hsp30B* gene contains a frameshift mutation and was considered a pseudogene. The second gene cluster, which contains *hsp30C* and *hsp30D*, was isolated and completely sequenced by Krone et al. (1992) and found to encode 24 kDa fully functional HSP30 proteins (Krone et al., 1992; Heikkila, 2003). Only the promoter and the N-terminal coding region of *hsp30E* were isolated from this gene cluster. *Hsp30C*, the most extensively studied *hsp30* gene in *Xenopus*, contains 2 TATA boxes, 3 HSEs and a CCAAT box within its 5' promoter regions while the 3' UTR is AT-rich and contain both polyadenylation element and an mRNA instability region (Heikkila, 2003).

During *Xenopus* development, *hsp30C* was first heat-inducable at the late neurula/early taildbud stage, while *hsp30D* was not inducible until midtailbud (Heikkila, 2003). Whole mount in situ hybridization and immunocytochemical analysis of heat shock-treated midtailbud embryos revealed a preferential accumulation of *hsp30* mRNA and protein in the cement gland, lens placode, somites and proctodeum (Lang et al., 1999). It was also determined that both HSP30C and HSP30D were capable of molecular chaperone activity by inhibiting heat-induced target protein aggregation and maintaining heat- or chemically-denatured luciferase in a folding competent state (Fernando and Heikkila, 2000; Fernando et al., 2002; Abdulle et al., 2002).

Various cellular stresses including heat shock, sodium arsenite, herbimycin A, cadmium chloride and hydrogen peroxide have all been shown to induce *hsp30* gene expression in *X. laevis* A6 cells and/or embryos (Briant et al., 1997; Ohan et al., 1998; Phang et al., 1999; Muller et. al, 2004; Woolfson and Heikkila, 2009; Young et al., 2009; Heikkila, 2010). Upon stressful conditions, such as heat stress at 33 °C or treatment with 30 – 50 μM sodium arsenite, HSP30 accumulation in A6 cells is primarily cytoplasmic in a granular or punctuate pattern, but is also localized in the perinuclear region as determined by immunocytochemistry and laser scanning confocal microscopy (Gellalchew and Heikkila, 2005; Manwell and Heikkila, 2007).

1.6. *Xenopus laevis* HSP70

The members of the *Xenopus* HSP70 family analyzed to date consist of constitutively expressed heat shock cognate 70 (HSC70), stress-inducible HSP70 and immunoglobulin binding protein (BiP) also known as glucose-regulated protein 78 (Grp78). HSC70 and HSP70 are expressed in the cytoplasm, while BiP is found in the endoplasmic reticulum. To date, four members of the stress-inducible *Xenopus hsp70* genes (*hsp70A*, *hsp70B*, *hsp70C* and *hsp70D*)

have been isolated by Bienz (1984). Coding regions of *hsc70.I*, *hsc70.II* and *BiP* have been isolated and characterized by our laboratory (Ali et al., 1996a; 1996b; Miskovic et al., 1997).

During development *hsp70* mRNA is first heat inducible after the midblastula transition (MBT), which marks the activation of the zygotic genome even though HSF was detectable and heat activatable in cleavage stage embryos (Krone and Heikkila, 1988; Ovsenek and Heikkila, 1990). Whole mount in situ hybridization revealed that while *hsp70* mRNA was not readily detectable during normal development, heat shock induced *hsp70* mRNA was enriched in a tissue-specific manner (Lang et al., 2000). For example, heat shock-treated early tailbud embryos demonstrated *hsp70* mRNA accumulation in the lens placode, cement gland, heart, somites, spinal cord and proctoderm. Previously in our laboratory, it was also shown that HSP70 was induced in A6 cells by a variety of stressors including heat shock, sodium arsenite, herbimycin A, hydrogen peroxide, ethanol and cadmium (Darasch et al., 1988; Briant et al., 1997; Heikkila, 2004; Muller et al., 2004; Woolfson and Heikkila, 2009; Young et al., 2009).

1.7. Association of HSP with cancer and neurodegenerative diseases

Overexpression or deregulation of cytoprotective HSPs such as HSP27 and HSP70 have been implicated in a variety of human cancers including breast, lung and prostate cancer (Malusecka et al., 2001; Melendez et al., 2006; So et al., 2007). It is believed that HSPs protect cancer cells from cell death and that higher levels likely contribute to acquisition of chemoresistance in certain types of cancers (Brodsky and Chiosis, 2006; So et al., 2007). In recent studies, inhibition of HSP70 and HSP90 by antisense RNAs inhibited growth and induced apoptosis in transformed cells (Whitesell et al., 1994; Nylandsted et al., 2000; Westerheide and Morimoto, 2005). This approach may provide a novel therapeutic modality for cancer.

Numerous neurodegenerative diseases have also been linked to HSP and proteasome dysfunction that are pathologically defined by abnormal deposition of misfolded polypeptides, which subsequently form cytotoxic aggregates (Westerheide et al., 2004; Zhang and Sarge, 2007). These diseases include polyglutamine diseases such as Huntington's disease along with amyotrophic lateral sclerosis (ALS), Alzheimer's and Parkinson's disease to name a few. Thus, it seems possible that therapeutic approaches may involve the use of HSPs to suppress the amount of unfolded proteins, which in turn will reduce the level of toxic aggregates in neuronal cells. In fact, previous studies suggest that chaperone activity provided by overexpression of HSPs can inhibit aggregate formation in HeLa cells (Zhang and Sarge, 2007). Given this finding, there has been a great amount of interest in the characterization of various inducers of the HSR for therapeutic purposes.

1.8. Protein Degradation

Eukaryotic cells employ two main protein degradation pathways to maintain protein homeostasis: the lysosomal degradation pathway and the ubiquitin-proteasome system (UPS). The lysosomal degradation pathway plays a minor role in the non-specific degradation of cellular proteins and is primarily responsible for hydrolysis of extracellular proteins (Lee and Goldberg, 1998a). Although lysosomal degradation is important, it is in fact the ATP-dependent ubiquitin-proteasome system (UPS) which is responsible for the majority (80 – 90 %) of protein hydrolysis in the cell (Lee and Goldberg, 1998a).

1.8.1. Ubiquitin-proteasome pathway

The ubiquitin-proteasome pathway is the principle mechanism used by all cells to degrade proteins and maintain protein homeostasis in the cell. It is essential for many fundamental processes in the cell including cellular differentiation, cell cycle progression, proliferation and apoptosis (Mani and Gelmann, 2005; Landis-Piwowar et al., 2006). The pathway is broken down into two successive steps: addition of ubiquitin molecules onto the protein targeted for degradation and the subsequent degradation of the ubiquitinated proteins by the 26S proteasome (Yang et al., 2008).

1.8.2. Protein Ubiquitination

Eukaryotic cells initially ubiquitinate proteins that are targeted for degradation through the UPS. Ubiquitin is a 76 amino acid protein that serves as a marker for proteasome degradation when it is attached to lysine residues. The process of ubiquitination is controlled by a set of ubiquitin-activating and conjugating enzymes (E1 – E4) (Yang et al., 2008; Lehman, 2009). Firstly, ubiquitin-activating enzyme (E1) activates ubiquitin in an ATP-dependent manner through the adenylation and formation of a thiol-ester bond at its C-terminus. Subsequently, ubiquitin is transferred to a cysteine residue within one of several distinct ubiquitin-conjugating enzymes (E2). With the aid of a third enzyme, an E3 ubiquitin ligase, ubiquitin is transferred to a lysine residue of a substrate protein. This mechanism continues until the substrate protein is polyubiquitinated (Hershko and Ciechanover, 1998). E4 enzymes facilitate the formation of these polyubiquitin chains (Koegl et al., 1999). Following, ubiquitination, the substrate protein is then delivered by ubiquitin receptor proteins to the proteasome.

1.8.3. The Proteasome

The 26S proteasome is a complex of multiple protein subunits containing the 20S proteolytic core and the 19S and 11S regulatory subunits. The 20S subunit is capable of hydrolyzing most unfolded proteins and is composed of two catalytic β rings surrounded by two non-catalytic α-rings. The catalytic β rings contains multiple peptidase activities including the chymotrypsin-like (CT-like), trypsin-like (T-like) and peptidyl-glutamyl peptide hydrolyzing-like (PGPH-like) (Groll et al., 1997; Ciechanover, 1998). The 19S and 11S regulatory subcomplexes bind to either end of the 20S core and serve to control which proteins will be degraded by identifying ubiquitinated proteins and then subsequently deubiquitinating them and passing them onto the 20S catalytic core for degradation. The 20S core degrades proteins into oligopeptides and ubiquitin is released and recycled.

1.8.4. Proteasomal Inhibition

Inhibition of the ubiquitin-proteasome pathway has been associated with a variety of neurological and protein-misfolding diseases including Alzheimer's, Parkinson's and Huntington's Disease (Masliah et al., 2000; Ross and Pickart, 2004). Recently in *Xenopus* and other eukaryotic organisms, inhibition of the proteasome has also been associated with an increase in *hsp* gene expression (Bush et al., 1997; Young and Heikkila, 2010). Carbobenzoxy-leucyl-L-leucyl-L-leucinal (MG132), lactacystin, and celastrol are proteasome inhibitors that primarily inhibit chymotrypsin-like activity of the 20S proteasome. These proteasomal inhibitors have been shown to induce the accumulation of HSP30 and HSP70 in *Xenopus laevis* A6 cells (Walcott and Heikkila, 2010; Young and Heikkila, 2010).

1.9. Curcumin

Curcumin is an active ingredient in the Indian spice, Turmeric, which is obtained from the rhizome of the plant *Curcuma longa* (Fig. 4). Turmeric has been widely used in Ayurvedic Indian Medicine as an herbal remedy to treat common eye infections, mosquito bites, burns, fever and various other skin diseases (Ammon and Wahl, 1991). Curcumin has also been shown to possess various beneficial properties including anti-inflammatory, antioxidant, chemopreventative, and chemotherapeutic activities (Aggarwal et al., 2003; Duvoix et al., 2003; Campbell and Collett, 2005; Shishodia et al., 2005). In vitro studies have shown that curcumin inhibits the production of pro-inflammatory macrophage-derived cytokines in blood monocytes and alveolar macrophages thereby inhibiting inflammation (Abe et al., 1999). In vivo studies involving rat models also demonstrated that curcumin inhibited inflammation caused by cyclophosphamide-induced acute lung injury (Venkatesan and Chandrakasan, 1995). Also several animal studies found that curcumin has a dose-dependent chemopreventive effect in colon, duodenal, stomach and oral carcinogenesis (Maheshwari et al., 2006). In addition to its role as a chemotherapeutic agent, curcumin also functions as a chemosensitizer and enhances the activity of other anti-carcinogenic agents (Garg et al., 2005). Combined treatment of curcumin and TRAIL (TNF-related apoptosis inducing ligand) at low concentrations induced tumor cell death, while individually neither compounds induced apoptosis (Deeb et al., 2005). Curcumin treatment also led to decreased expression of anti-apoptotic members of the Bcl-2 family such as Inhibitor of Apoptosis (IAP), thus leading to the induction of programmed cell death (Shishodia et al., 2005).

Figure 4. The chemical structure of curcumin.

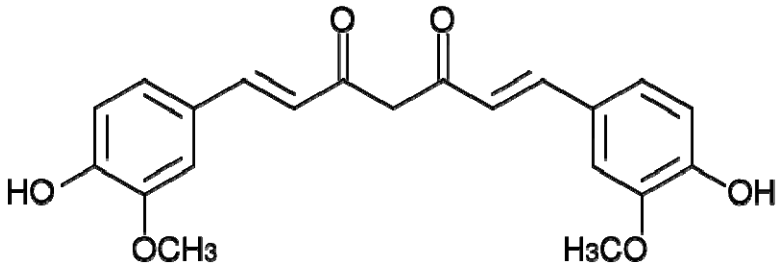
O
O
HO
OCH3
H3CO
OH

Recently, it was shown that human leukemia K562 cells treated with 30 – 80 μM curcumin underwent apoptosis (Teiten et al., 2009). Curcumin-induced suppression of carcinogenesis is thought to be due to the inhibition of nuclear factor-κB (NF- κB), which is controlled by the proteasome-mediated proteolytic degradation pathway (Cohen et al., 2006). Moreover, curcumin was found to increase the relative levels of ubiquitinated proteins and inhibit the chymotrypsin-like activity of the 26S proteasome in SW480 and HCT-116 human colon cancer cells (Milacic et al., 2008). Additionally, curcumin was reported to induce anti-metastatic properties in lung adenocarcinoma cells through the induction of *hsp* genes identified by means of microarray analysis (Chen et al., 2001; Chen et al., 2004). Curcumin was also implicated in the induction of *hsp70* gene expression in human colorectal carcinoma cells and human leukemia K562 cells (Chen et al., 2001; Teiten et al., 2009).

1.10. Research Objectives

Thus far, the effects of curcumin on *hsp* gene expression have been minimally characterized in mammalian systems. Given the potential health benefits of curcumin, the primary goal of this thesis was to examine the effect of curcumin on proteasome activity and the pattern of HSP accumulation in *Xenopus laevis* A6 kidney epithelial cells. More specifically, the objectives of this research are as follows:

a) To examine the effect of curcumin on proteasome activity in A6 cells.
b) To determine the effect of curcumin and heat shock, by itself and in combination, on the patterns of *hsp30* and *hsp70* gene expression.
c) To examine the effects of recovery from curcumin exposure on the accumulation of HSP30 and HSP70 protein via immunoblot analysis.

d) To determine if curcumin-induced HSP30 and HSP70 accumulation is mediated by HSF1 activation.

e) To monitor curcumin-induced accumulation and intracellular localization of HSP30 and to determine whether curcumin can induce thermolerance in *X. laevis* A6 cells using immunocytochemistry and laser scanning confocal microscopy.

2. Materials and Methods

2.1. Maintenance and treatment of *Xenopus laevis* A6 kidney epithelial cells

X. laevis A6 cells were obtained from the American Type Culture Collection (ATCC, Rockville, MD) and were grown in 55 % Leibovitz L-15 Media containing 10 % (v/v) fetal bovine serum and 1 % penicillin (100 U/ml) and streptomycin (100 μg/ml; all purchased through Sigma-Aldrich, Oakville, ON) at 22 °C in T75 cm^2 BD falcon culture flasks (BD Biosciences, Mississauga, ON). Upon confluency, cells were washed with 1 ml of versene [0.02 % (w/v) KCl, 0.8 % (w/v) NaCl, 0.02 % (w/v) KH_2PO_4, 0.115 % (w/v) Na_2HPO_4, 0.02 % (w/v) sodium ethylenediaminetetraacetic acid (Na_2 EDTA)], followed by a 1 min incubation with 2 ml of fresh versene. Then 1 ml of 1X trypsin (Sigma-Aldrich) diluted in 100 % Hank's Balanced Salt Solution (HBSS; Sigma-Aldrich) was added until cells began to detach from the flask. Ten ml of fresh L-15 media was then added to the detached cells. The cell suspension was then divided evenly into additional flasks. Cell treatments were performed 2 days after cell splitting to allow the cells to reach 90-100 % confluence.

Flasks of A6 cells subjected to heat stress were immersed in temperature-regulated water baths at 30 °C or 33 °C for 2 or 6 h. It took 20 min for the media to reach the given temperature. A6 cells used for protein analysis were placed at 22 °C for 2 h after heat shock treatments prior to harvest. Curcumin (Sigma-Aldrich) treatments of A6 cells were performed at 22 °C or 30 °C using dilutions from a 100 mM curcumin stock solution dissolved in dimethyl sulfoxide (DMSO; Sigma-Aldrich) and stored at -20 °C. A6 cells were also treated with 30 μM MG132 (Sigma-Aldrich; stock solution of 21 mM was dissolved in DMSO and stored at -20 °C). Also, some A6 cells were pre-treated with 100 μM KNK437 (Calbiochem, Gibbstown, NJ; stock solution of 5 mg/ml was dissolved in DMSO) for 6 h before curcumin treatments. KNK437 was left in these

flasks during the curcumin treatments. Cells were rinsed using 65 % HBSS and removed via scraping in 1 ml of 100 % HBSS. Cells were centrifuged at 21,920 x g for 1 min and the resulting pellets were stored at -80 °C until protein isolation.

2.2. Protein isolation, quantification and immunoblot analysis

2.2.1. Protein isolation and quantification

Protein was isolated from A6 cells using a lysis buffer solution at pH 7.4 containing 200 mM sucrose, 2 mM EDTA, 40 mM NaCl, 30 mM HEPES, 1% (w/v) SDS and 1 % protease inhibitor cocktail (Promega, Madison, WI). It should be noted here that the lysis buffer used for samples in preparation for Western blotting with mouse anti-ubiquitin antibody contained 10 mM N-ethylmaleimide (Sigma-Aldrich) to inhibit ubiquitin conjugating enzymes. The cells were homogenized in the lysis buffer by sonication (output 4.5, 60% duty cycle) on ice for 15 bursts using a Fisher Scientific Sonic Dismembrator 100 (Fisher Scientific, Ottawa, ON) and subsequently centrifuged at 21, 920 x g for 30 min at 4 °C. The supernatant containing the protein sample was removed.

Protein was quantified using a bicinchoninic acid (BCA) Protein Assay Kit (Pierce, Rockford, IL). A bovine serum albumin (BSA; BioShop, Burlington, ON) protein standard was created by diluting BSA in distilled water at concentrations ranging from 0 to 2 mg/ml. Protein samples were diluted to a concentration of 1:2 in distilled water. Ten µL of BSA standards and protein samples were transferred in triplicate into a 96 well clear polystyrene plate. Then 80 µL of BCA reagent A and B (Pierce) at a ratio 50:1 were added to the BSA and protein samples. The plate was incubated at 37 °C for 30 min and then read at 562 nm using a Versamax Tunable microplate reader (Molecular Devices, Sunnyvale, CA). A standard curve was created using the

concentrations of the BSA protein standards which was used to determine the concentration of the protein samples. Protein samples were stored at -20 °C until further use.

2.2.2. Immunoblot analysis

Immunoblot analysis was performed using 20 or 60 µg of protein (the higher amount was used for the analysis of ubiquitinated protein) and sodium dodecyl sulfate-polyacrylamide gel electrophoresis (SDS-PAGE). Separating gels [10-12% (v/v) acrylamide, 0.32% (v/v) n'n'-bis methylene acrylamide, 0.375 M Tris (pH 8.8), 1% (w/v) SDS, 0.2% (w/v) ammonium persulfate (APS), 0.14% (v/v) tetramethylethylenediamine (TEMED)] were prepared, poured and allowed to polymerize for 25 min with 100% ethanol layered on top. Ethanol was poured off and the stacking gel [4% (v/v) acrylamide, 0.11% (v/v) n'n'-bis methylene acrylamide, 0.125 M Tris (pH 6.8), 1% (w/v) SDS, 0.4% (w/v) APS, 0.21 % (v/v) TEMED] was prepared, poured and allowed to polymerize for 25 min. A6 cell protein samples were aliquoted in loading buffer [0.0625M Tris (pH 6.8), 10% (v/v) glycerol, 2% (w/v) SDS, 5% (v/v) β-mercaptoethanol, 0.00125% (w/v) bromophenol blue] was added, to a final concentration of 1X. Samples and molecular weight markers (BioRad, Mississauga, ON) were denatured via boiling for 10 min, cooled on ice for 5 min and pulse-centrifuged prior to loading. Polyacrylamide gels were electrophoresed on a BioRad Mini Protean III gel system (BioRad) with 1X running buffer [25mM Tris, 0.2M glycine, 1 mM SDS] at 90 V until samples reached the separating gel, at which time the voltage was turned up to 160 V until the dye front reached the bottom of the gel.

Pure nitrocellulose transfer blot membranes (BioRad) and filter paper (BioRad) were cut to 5.5 cm x 8.5 cm, and membranes were incubated for 30 min in transfer buffer [25 mM Tris, 192 mM glycine, 20% (v/v) methanol]. After electrophoresis, the stacking gel was cut away and

the remainder of the gel was soaked in transfer buffer for 15 min. Protein was transferred to a nitrocellulose membrane with a Trans-Blot Semi-Dry Transfer Cell (BioRad) at 25 volts for 20 min. Blots were then stained with Ponceau S stain [0.19% (w/v) Ponceau S (Sigma-Aldrich), 5% (v/v) acetic acid] for 10 min to determine transfer efficiency. The membrane was destained with MilliQ water and then photographed. The membrane was subsequently blocked in 5 % blocking solution [20 mM Tris (pH 7.5), 0.1% Tween 20 (Sigma-Aldrich), 300 mM NaCl, 5% (w/v) Nestle® Carnation skim milk powder] for 1 h to prevent non-specific binding. Immunodetection was carried out via either the use of polyclonal rabbit anti-*Xenopus* HSP30 antibody (Fernando and Heikkila, 2000); 1:1000 dilution, the polyclonal rabbit anti-*Xenopus* HSP70 antibody (Gauley et al., 2008); 1:350 dilution, the polyclonal rabbit anti-actin antibody (Sigma-Aldrich); 1:200 dilution or the polyclonal mouse anti-ubiquitin antibody (Zymed, San Francisco, CA); 1:150 dilution (Table 1). Excess unbound antibody was removed by rinsing the membrane (2 x 10 seconds) with 1X TBS-T [20 mM Tris, 300 mM NaCl, (pH 7.5), 0.1% (v/v) Tween 20]. The membrane was washed with fresh TBS-T for 15 min, followed by two 10 min washes. The membrane was then incubated for 1 h with blocking solution containing the secondary antibody (alkaline phosphatase-conjugated goat-anti-rabbit or mouse (BioRad)). The secondary antibody dilution was dependent on the primary antibody employed, which is outlined in Table 1. For detection, the membrane was incubated in alkaline phosphatase detection buffer [alkaline phosphatase buffer (100 mM Tris base, 100 mM NaCl, 50 mM $MgCl_2$ (pH 9.5)), 0.3% 4-nitro blue tetrazolium (NBT; Roche, Indianapolis, IN), 0.17% 5-bromo-4-chloro-3-indolyl phosphate, toluidine salt (BCIP; Roche)] until the bands were visible.

Table 1. Dilution specifications for antibodies used in Western blot analysis

Primary Antibody		Secondary Antibody		Comments
Name	**Dilution**	**Name**	**Dilution**	
Rabbit anti-*Xenopus* HSP30	1:1000	Goat anti-rabbit IgG AP-conjugate	1:2000	1° antibody prepared by Heikkila lab
Rabbit anti-*Xenopus* HSP70	1:350	Goat anti-rabbit IgG AP-conjugate	1:3000	1° antibody prepared by Abgent (San Diego, CA)
Rabbit anti-actin	1:200	Goat anti-rabbit IgG AP-conjugate	1:3000	1 ° antibody obtained from Sigma-Aldrich
Mouse anti-ubiquitin	1:150	Goat anti-mouse IgG AP-conjugate	1:1000	1° antibody obtained from Zymed

2.3. Densitometry and statistical analysis

Densitometric analyses within the range of linearity were performed using ImageJ (1.42q) software on all blots examining the effect of curcumin as described previously (Walcott and Heikkila, 2010). Briefly, experiments were repeated in triplicate, and the average densitometric values were expressed as a percentage of the maximum hybridization band or as a percent inhibition for KNK437 experiments. The data were graphed with standard error of the mean represented as vertical error bars. Statistical analysis through one way analysis of variance (ANOVA) followed by Tukey's Multiple comparison post-test were performed with this data to determine if statistically significant differences existed between samples. Confidence levels used were 90% ($p < 0.1$; Δ) and 95% ($p < 0.05$; *).

2.4. Immunocytochemistry and laser scanning confocal microscopy

Cells were prepared for imaging by laser scanning confocal microscopy (LSCM) on 22 x 22 mm glass coverslips in sterile petri dishes. In order to clean the glass coverslips, they were placed in small Coplin jars to ensure full contact with the base solution [49.5% (v/v) ethanol, 0.22M NaOH] for 30 min with periodic shaking at room temperature. The coverslips were then

rinsed under running distilled water for 3 h and dried on Whatman paper. A6 cells were grown on flame sterilized cover slips for 24 h at 22 °C. A6 cells were incubated at 30 °C or 33 °C for 2 h followed by a 2 h recovery period at 22 °C. A6 cells were also treated with 10 μM or 30 μM curcumin at 22 °C. Following the treatments, the cells were rinsed with phosphate buffered saline [PBS; 1.37 M NaCl, 67 mM Na_2HPO_4, 26 mM KCl, 14.7 mM KH_2PO_4, 1 mM $CaCl_2$, 0.5 mM $MgCl_2$, pH 7.4] and fixed using 3.7% (w/v) paraformaldehyde (pH 7.4 in PBS; BDH, Toronto, ON) for 15 min. A6 cells were rinsed 3 times with PBS for 5 min each and permeabilized using 0.3% Triton X-100 (Sigma-Aldrich) for 10 min. A6 cells were then rinsed 3 times with PBS and incubated in 3.7 % (w/v) bovine serum albumin fraction V (BSA; Fischer Scientific) for 1 h or overnight on the shaker at 4 °C. The BSA fraction V was filter-sterilized using a 0.45 μm filter (Pall Filtration Corp., St. Laurent, QC) to remove debris that might negatively affect the imaging. The following day cells were incubated with affinity-purified rabbit anti-*Xenopus* HSP30 antibody (1:500) in 3.7 % BSA for 1h. Following three washes with PBS, indirect labeling of A6 cells was performed using fluorescent-conjugated secondary antibody, goat anti-rabbit Alexa Fluor 488 (Invitrogen Molecular Probes, Carlsbad, CA) at 1:2000 in 3.7 % BSA for 30 min in the dark. To visualize the actin cytoskeleton, A6 cells were incubated with rhodamine-tetramethylrhodamine-5-isothiocyanate phalloidin (TRITC; Invitrogen Molecular Probes) for 15 min at 1:60 in 3.7 % BSA in the dark. The cover slips were dried and mounted on glass slides with Vectashield mounting medium containing 4, 6-diamidino-2-phenylindole (DAPI; Vector Laboratories Inc., Burlingame, CA) to stain nuclei. Coverslips were permanently attached to glass slides by using clear nail polish and examined by laser scanning confocal microscopy by using a Zeiss Axiovert 200 microscope and LSM 510 META software (Carl Zeiss Canada Ltd., Mississauga, ON).

2.5. Cell-Based Proteasome Assay

To evaluate the effect of curcumin on proteasomal activity in A6 cells, The Proteasome-Glo Chymotrypsin-Like cell based luminescent assay kit was obtained from Promega (Promega, Madison, WI). Proteasome-Glo Cell-Based Reagents each contain a specific luminogenic proteasome substrate (Suc- Leu-Leu-Val-Tyr-Glo substrate for chymotrypsin-like activity) in a buffer optimized for cell permeabilization, proteasome activity and luciferase activity. The proteasome cleavage generates an aminoluciferin substrate that is consumed by luciferase to produce a luminescent signal at a rate proportional to proteasome activity. Proteasome-Glo™ Cell-Based Buffer and Luciferin Detection Reagent were equilibriated to room temperature in the dark and mixed with the Suc-Leu-Leu-Val-Tyr-aminoluciferin (Suc-LLVY-aminoluciferin) substrate to produce the Proteasome-Glo™ Reagent, which was used to detect the chymotrypsin-like activity. Flasks of A6 cells were treated with 10 μM or 30 μM curcumin at 22 °C for 24 h. A 30 μM MG132 treatment was used as a positive control. After treatments, cells were washed with 2 ml of versene and then with 1 ml of 1X trypsin until the cells began to detach from the T75 cm^2 BD falcon culture flask. Nine ml of fresh L-15 media was then added to the flask and the media was pipetted up and down to rinse the flask surface and allow for even distribution. The cell suspension was then removed from the flask and placed into a 15 ml falcon tube. Cells were pelleted at 4 °C by gentle centrifugation at 2,400 x g for 5 min. Following centrifugation excess media was removed and pellets were washed in 5 ml of fresh L-15 media and then centrifuged again at 2,400 x g for 5 min at 4 °C. A6 cells were then resuspended in 5 ml of fresh L-15 media. For each sample, the total number of cells per ml was determined using a Bright-Line haemocytometer (Hausser Scientific, Horsham, PA).

Approximately 15,000 cells per well were added to white-walled 96 well plates along with an L-15 blank. Proteasome-Glo™ Reagent was allowed to reach room temperature before being added to the 96-well plate in a 1:1 ratio (100 µL sample: 100 µL reagent). The contents of the plate were then mixed for 2 min on the shaker and allowed to incubate at room temperature for 45 min before detection of luminescence. The luminescence of each sample was measured using the Victor^3 luminometer (Perkin Elmer Inc., Waltham, MA) containing a filter set at 340/480 nm. Values were then compared to a blank control (Proteasome-Glo cell-based reagent + L-15 media) and a no-treatment control (Proteasome-Glo cell-based reagent + L-15 containing DMSO). Measurements were repeated 3 times and statistical analysis was performed through analysis of variance (ANOVA) followed by Tukey's Multiple comparison post-test.

3. Results

3.1. Curcumin-induced increase in ubiquitinated protein in A6 cells

Previous studies showed that curcumin inhibited proteasome activity in human colon cancer cells (Milacic et al., 2008). One method to assess proteasome inhibition in A6 cells treated with curucmin is to determine if there is an increase in the relative level of ubiquitinated protein. Previously in our laboratory, the proteasomal inhibitors, MG132 and lactacystin induced an increase in the accumulation of ubiquitinated proteins in A6 cells (Young and Heikkila, 2010). In the present study, the relative levels of ubiquitinated proteins in cells treated with 30 μM curcumin for 14 or 24 h at 22 °C were higher than observed in control cells (Fig. 5A). Densitometric analysis determined that there was a 3.7- and 4.7-fold increase in the accumulation of ubiquitinated protein in cells treated with 30 μM curcumin for 14 and 24 h, respectively, when compared to control (Fig. 5B). Densitometric analysis also revealed that a 10-fold increase in ubiquitinated protein was observed in cells treated with the proteasome inhibitor, MG132 for 24 h, when compared to control.

3.2. Effect of curcumin on chymotrypsin-like activity of A6 cells

An additional method to evaluate the effect of curcumin on proteasomal activity in A6 cells was to measure chymotrypsin (CT)-like activity using a cell-based assay. As shown in Figure 6, cells treated with 30 μM curcumin at 22 °C for 14 or 24 h showed a 24 % and 76 % decrease, respectively, in CT-like activity when compared to the control cells maintained at 22 °C. Curcumin-mediated proteasome inhibition was also compared to the effects of MG132, which acts a substrate analog of CT-like activity in the 20S proteasome. An 85 % reduction in chymotrypsin-like activity occurred in cells treated with 30 μM MG132 for 24 h.

Figure 5. Effect of curcumin and MG132 on ubiquitinated protein levels in A6 cells. [A] Cells were maintained at either 22 °C (C), treated with 30 μM curcumin (Cur) for 14 or 24 h, or treated with 30 μM MG132 for 24 h at 22 °C. Protein was transferred to nitrocellulose membrane from SDS polyacrylamide gels and probed with a mouse anti-ubiquitin monoclonal antibody as described in Materials and methods. The positions of molecular mass standards in kDa are shown in the first lane (M). A section of a representative Ponceau S stained membrane that brackets a 42-kDa band (asterisk) is included to demonstrate efficient protein transfer. **[B]** Image J software was used to perform densitometric analysis of the signal intensity for ubiquitinated protein bands of western blot images. The data are expressed as a percentage of the maximum band (30 μM MG132) while the standard error is represented by vertical error bars. The level of significance of the differences between samples was calculated by one-way ANOVA with a Tukey's post-test. Significant differences between the control and other samples are indicated as * ($p < 0.05$). These data are representative of three separate experiments.

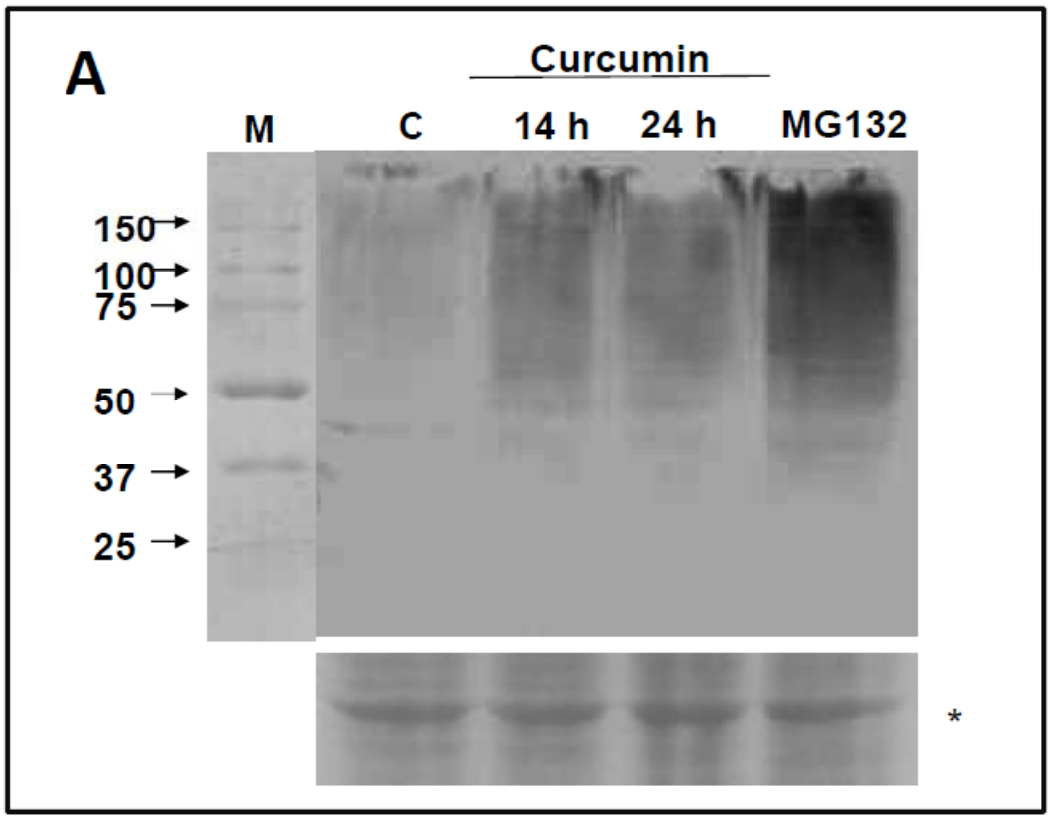
A
Curcumin
M
C
14 h
24 h
MG132
150
100
75
50
37
25
*

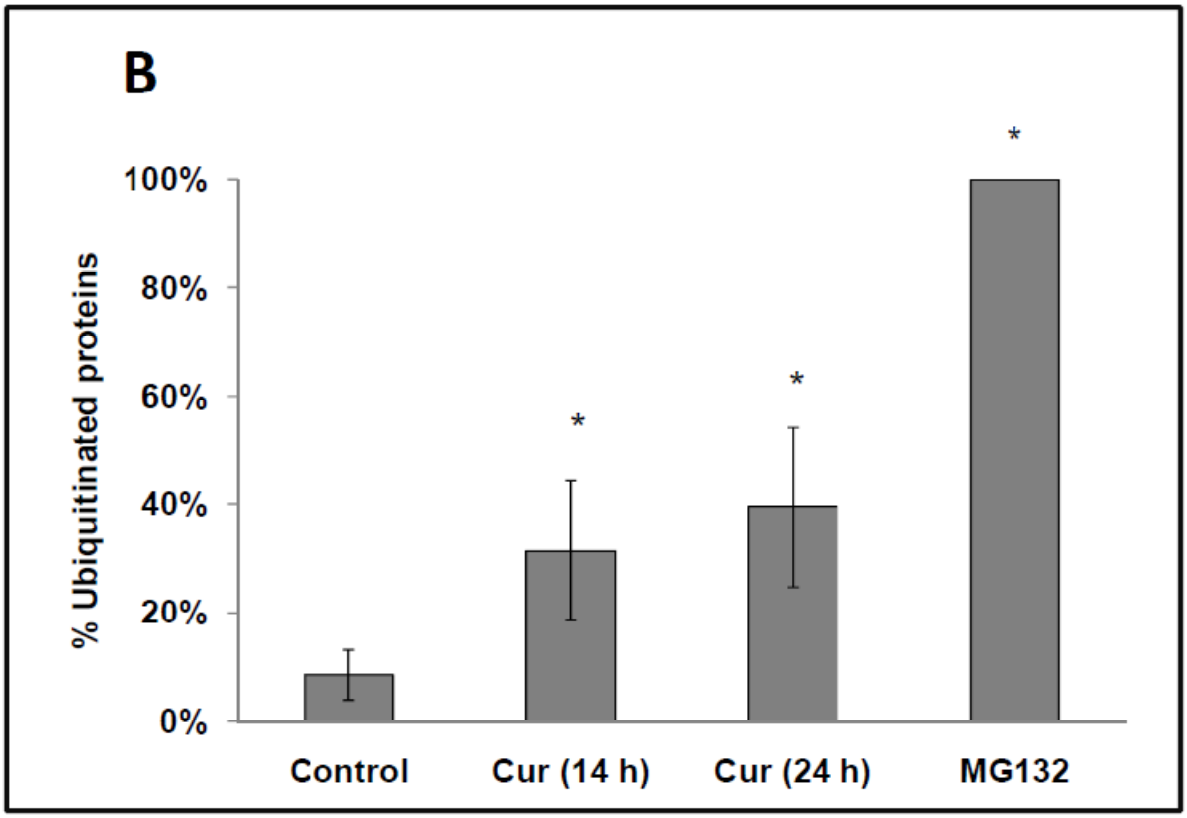
B
% Ubiquitinated proteins
100%
80%
60%
40%
20%
0%
*
*
*
Control
Cur (14 h)
Cur (24 h)
MG132

Figure 6. Effect of curcumin and MG132 on chymotrypsin-like activity of A6 cells. Cells were either maintained at 22 °C (Control), treated with 30 μM curcumin (Cur) for 14 or 24 h, or treated with 30 μM MG132 for 24 h (MG132) at 22 °C. Cells were suspended in L-15 media and 15,000 cells per well were placed in a 96-well plate. A cell-based chymotrypsin (CT)-like assay was used to monitor the proteolytic activity. The level of significance of the differences between samples and maximum (control) was calculated by one-way ANOVA with a Tukey's post-test and indicated as * ($p < 0.05$). These data are representative of three separate experiments.

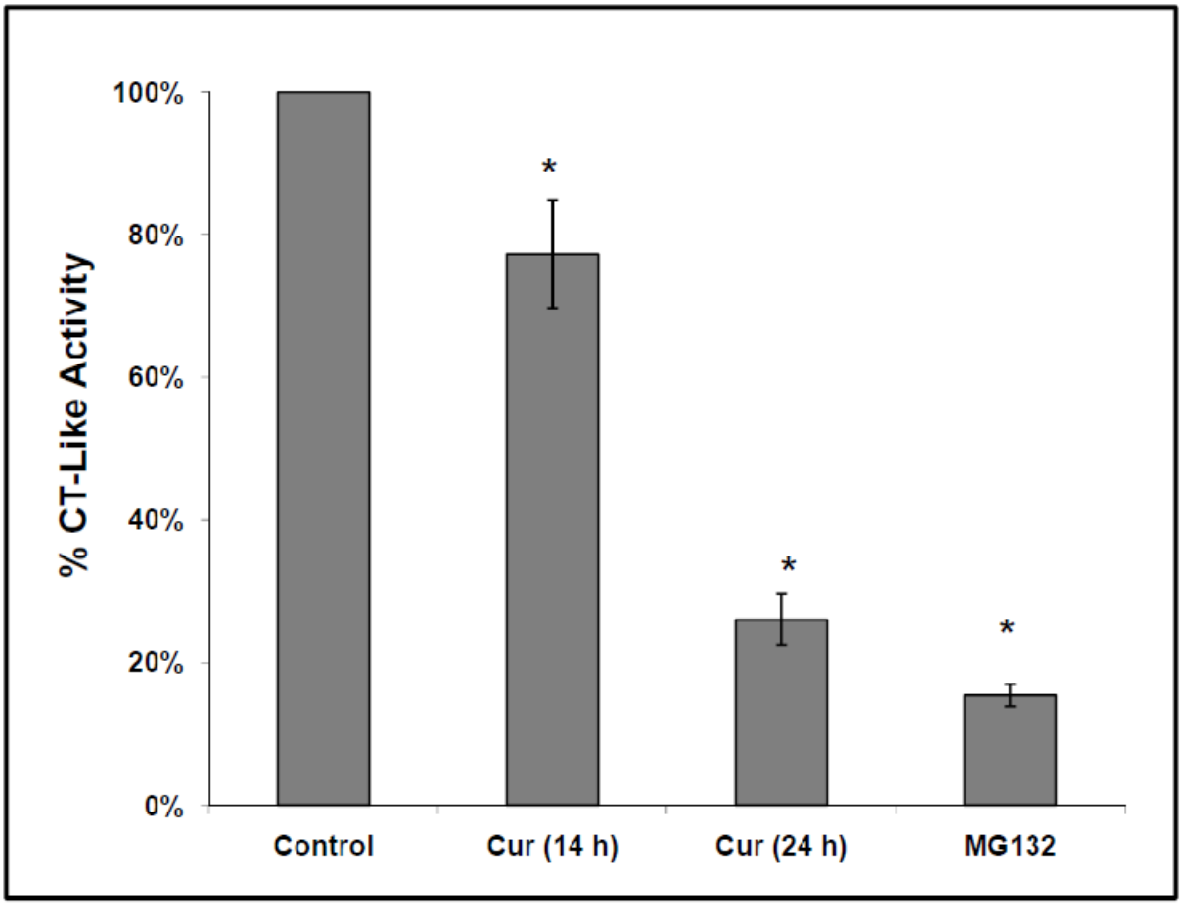
% CT-Like Activity
100%
80%
60%
40%
20%
0%
*
*
*
Control
Cur (14 h)
Cur (24 h)
MG132

3.3. Analysis of heat shock induced HSP30 and HSP70 accumulation in *Xenopus* cultured cells

A number of studies previously conducted in our laboratory using *X. laevis* A6 cells have shown that both HSP30 and HSP70 accumulated in response to elevated temperatures (Ohan et al., 1998; Phang et al., 1999; Fernando and Heikkila, 2000; Gellalchew and Heikkila, 2004; Young et al., 2009). As shown in Figure 7, enhanced levels of HSP30 and HSP70 but not actin were detected in cells subjected to heat shock at 33 °C for 2 h followed by a 2 h recovery at 22 °C. It should be noted that the anti-HSP30 antibody utilized in this study, which was prepared against the entire coding sequence of HSP30C, detected multiple members of the HSP30 family in immunoblot analysis (Fernando and Heikkila, 2000).

3.4. Curcumin-induced HSP accumulation in A6 cells occurs in a concentration and time-dependent manner

In the next phase of the study, A6 cells were treated with different concentrations of curcumin to examine their effects on the relative level of HSP30 and HSP70 accumulation. Western blot analysis revealed that the relative levels of HSP30 and HSP70 increased in cells treated with increasing concentrations of curcumin from 5 to 30 μM for 24 h (Fig. 8A). Densitometric analysis revealed that in comparison to cells incubated with 5 μM curcumin for 24 h, HSP30 and HSP70 accumulation increased approximately 20-fold in cells that were treated with 30 μM curcumin (Fig. 8B). Upon treatment with 50 μM curcumin, cells exhibited abnormal morphology with elongated cellular projections and a loss of intercellular connections. This was accompanied by a 72 and 67 % decrease in HSP30 and HSP70 levels, respectively, compared to

Figure 7. HSP30, HSP70 and actin accumulation in A6 cells subjected to heat shock. Cells were maintained at 22 °C or treated at 33 °C for 2 h followed by a 2 h recovery at 22 °C. After treatment, cells were harvested and total protein was isolated. Twenty μg of protein was then resolved on a 12% SDS-polyacrylamide gel. Protein was transferred to nitrocellulose membranes and probed with anti-HSP30, anti-HSP70 or anti-actin polyclonal antibodies as described in Material and methods. These data are representative of three separate experiments.

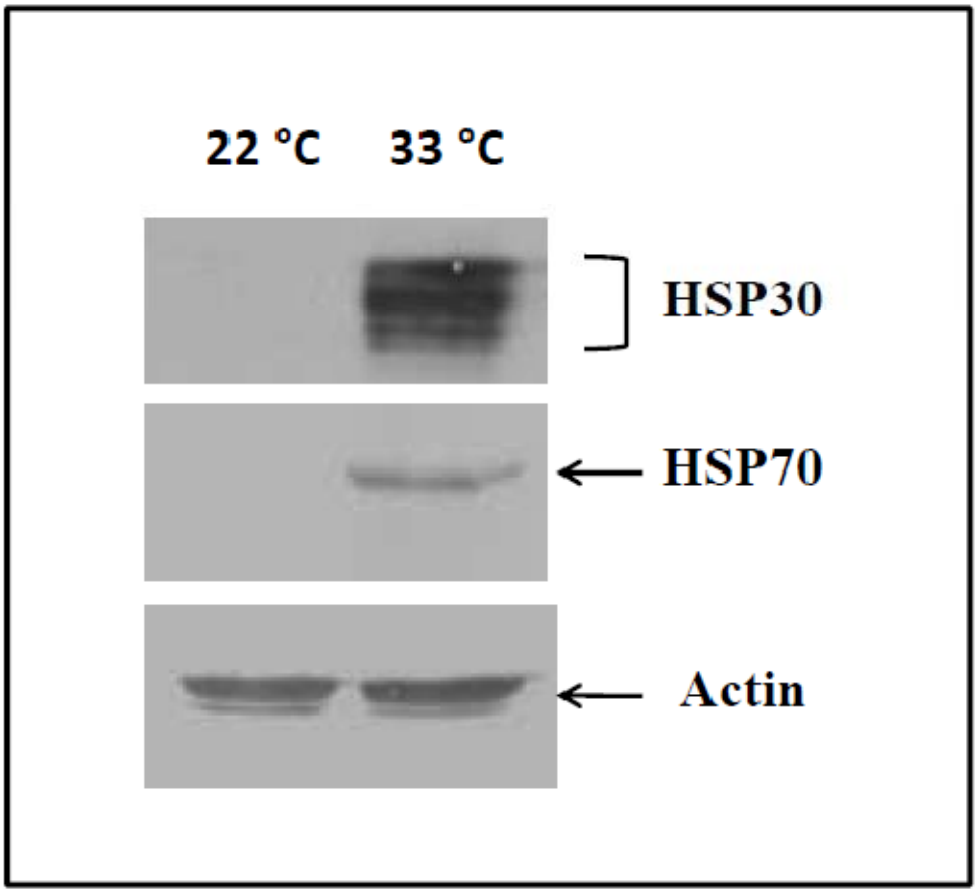
22 °C
33 °C
HSP30
HSP70
Actin

Figure 8. Curcumin-induced HSP30 and HSP70 accumulation in *Xenopus laevis* A6 cells. **[A]** Cells were maintained at 22 °C (C) or curcumin (Cur)-treated (5, 10, 20, 30 or 50 μM) for 24 h. After treatment, cells were harvested and total protein was isolated. Twenty μg of protein was then resolved on a 12% SDS-polyacrylamide gel. Protein was transferred to nitrocellulose membranes and probed with anti-HSP30, anti-HSP70 or anti-actin polyclonal antibodies as described in Material and methods. **[B]** Image J software was used to perform densitometric analysis of the signal intensity for HSP30 (white) and HSP70 (black) protein bands of western blot images. The data are expressed as a percentage of the maximum band (30 μM curcumin for HSP70 and HSP30) while the standard error is represented by vertical error bars. The level of significance of the differences between samples was calculated by one-way ANOVA with a Tukey's post-test. Significant differences between the control and other concentrations of curcumin are indicated as * ($p < 0.05$) or Δ ($p < 0.1$). These data are representative of three separate experiments.

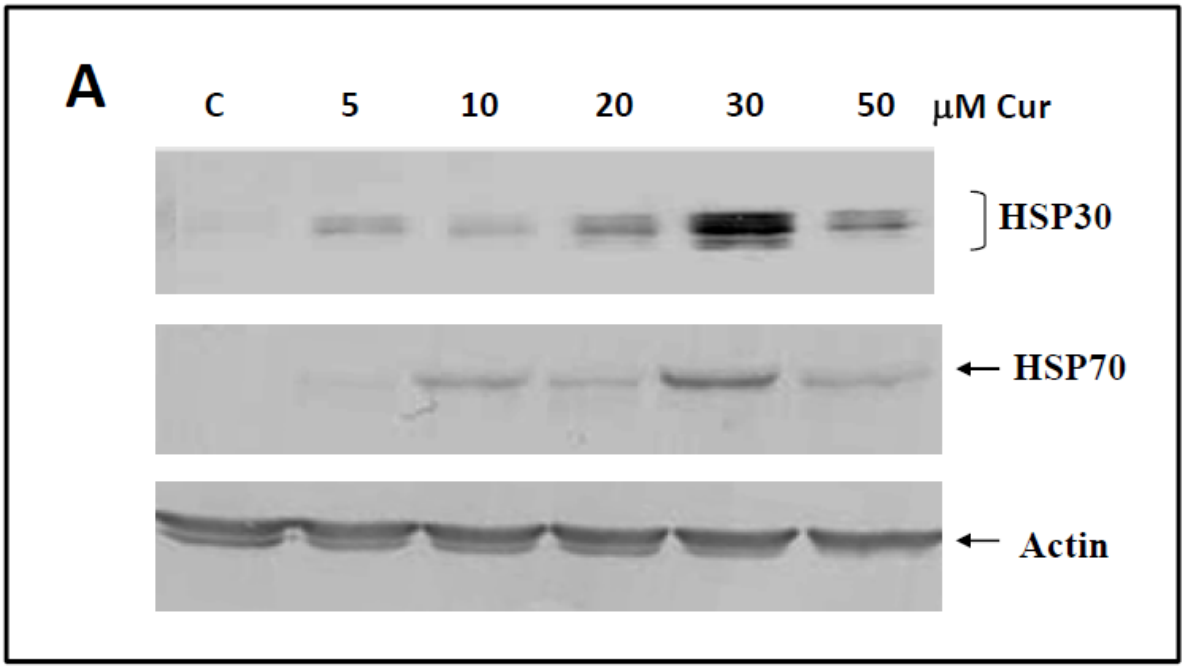
A
C
5
10
20
30
50
μM Cur
HSP30
HSP70
Actin

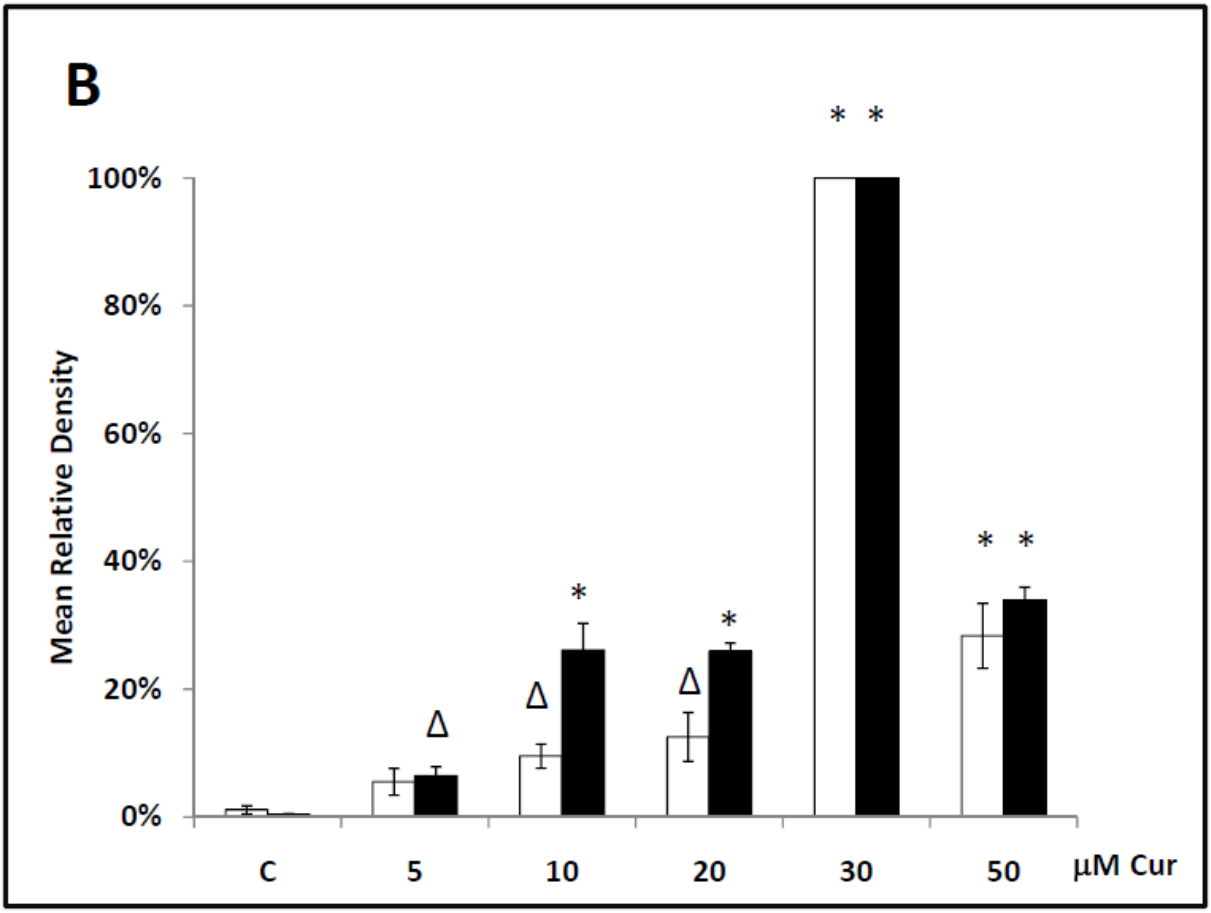
B
100%
80%
60%
40%
20%
0%
Mean Relative Density
C
5
10
20
30
50
μM Cur

cells treated with 30 μM curcumin. In all of these treatments actin levels remained relatively unchanged.

In time course studies, HSP30 and HSP70 accumulation was first observed in cells treated with 30 μM curcumin at 22 °C for 10 h (Fig. 9A). HSP30 levels increased over time with optimal accumulation between 18 and 24 h. Densitometric analysis revealed that in comparison to cells treated with curcumin for 10 h, an 8-fold increase in HSP30 accumulation occurred in cells treated for 18 h (Fig. 9B). Similar to HSP30 levels, HSP70 accumulation increased as the length of curcumin exposure increased from 10 to 24 h (Fig. 9A). Densitometric analysis demonstrated that in comparison to cells treated with curcumin for 10 h, a 2.5-fold increase in HSP70 accumulation occurred in cells treated for 24 h (Fig. 9B). Actin levels remained relatively unchanged throughout the course of treatments.

3.5. HSP30 and HSP70 levels in A6 cells recovering from curcumin treatments

In recovery experiments, A6 cells were treated with 30 μM curcumin for 14 h at 22 °C and were then allowed to recover in fresh L-15 media at 22 °C for different time periods ranging from 0 to 48 h. Western blot analysis revealed that HSP30 and HSP70 accumulation increased up to the 24 h recovery period, after which the relative levels of these HSPs decreased (Fig. 10A). Also, the relative levels of actin remained unchanged throughout the course of these treatments. Subsequent densitometric analysis revealed that HSP30 levels increased 3-fold in cells recovering from curcumin for 2 and 8 h when compared to cells exposed to curcumin with no recovery period. There was a 10-fold increase observed in cells when the recovery time was increased up to 24 h. Similarly, densitometric analysis exhibited that HSP70 levels increased 2-

Figure 9. Time course of curcumin-induced HSP30 and HSP70 accumulation in A6 cells. **[A]** Cells were maintained at 22 °C (C) or exposed to 30 μM curcumin for time intervals ranging from 2 to 24 h. Cells were harvested and total protein was isolated. Twenty μg of protein were then analyzed by Western blot analysis using anti-HSP30, anti-HSP70 or anti-actin polyclonal antibodies as described in Material and methods. **[B]** Image J software was used to perform densitometric analysis of the signal intensity for HSP30 (white) and HSP70 (black) protein bands of western blot images. The data are expressed as a percentage of the maximum band (30 μM curcumin for 24 and 18 h for HSP70 and HSP30 respectively) while the standard error is represented by vertical error bars. The level of significance of the differences between samples compared to control was calculated by one-way ANOVA with a Tukey's post-test. Significant differences between the control and time intervals are indicated as * ($p < 0.05$) or Δ ($p < 0.1$). These data are representative of three separate experiments.

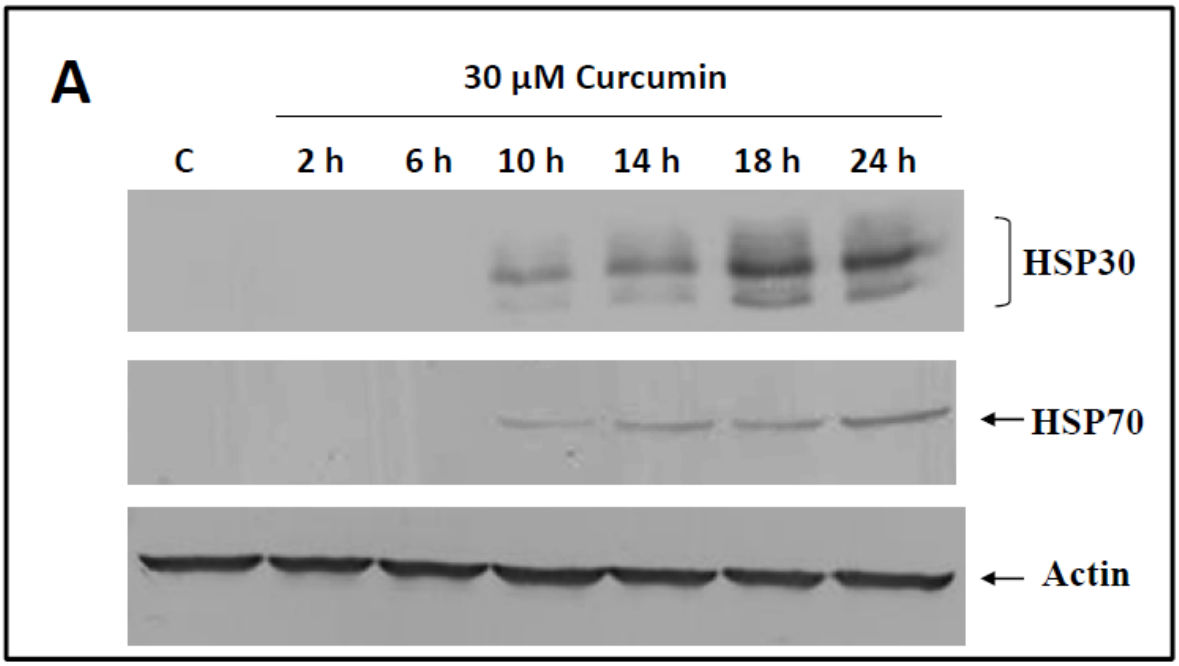
A
30 μM Curcumin
C
2 h
6 h
10 h
14 h
18 h
24 h
HSP30
HSP70
Actin

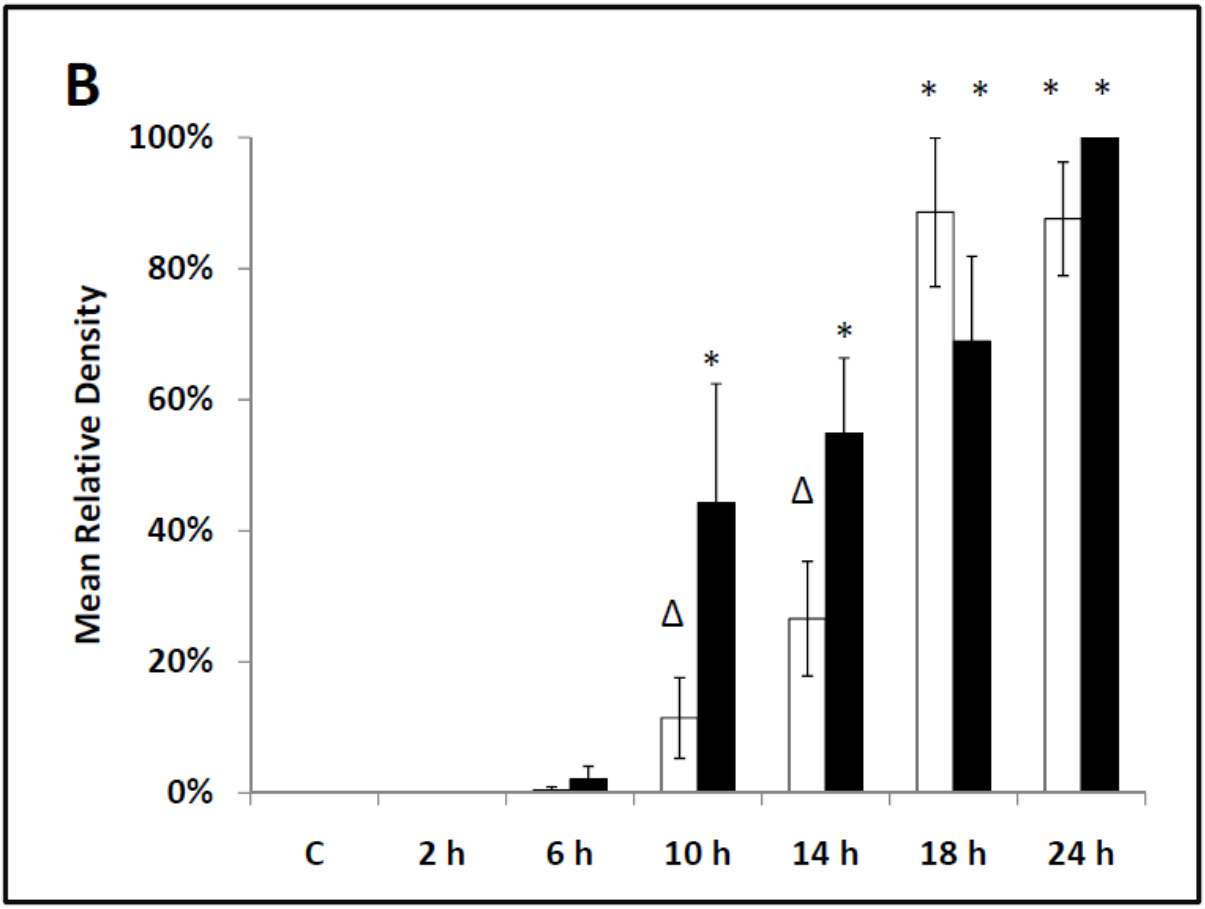
B
Mean Relative Density
100%
80%
60%
40%
20%
0%
C
2 h
6 h
10 h
14 h
18 h
24 h
*
Δ

Figure 10. HSP30 and HSP70 accumulation in A6 cells recovering from curcumin treatment. [A] Cells were maintained at 22 °C, or exposed to 30 μM curcumin for 14 h. Curcumin-treated cells were allowed to recover in fresh L-15 media at 22 °C for different time intervals ranging from 2 to 48 h. Cells were harvested and total protein was isolated and analyzed by immunoblotting using anti-HSP30, anti-HSP70 or anti-actin polyclonal antibodies as described in Material and methods. **[B]** Image J software was used to perform densitometric analysis of the signal intensity for HSP30 (white) and HSP70 (black) protein bands of western blot images. The data are expressed as a percentage of the maximum band (30 μM curcumin for 14 h with 24 h recovery for HSP30 and HSP70) while the standard error is represented by vertical error bars. The level of significance of the differences between samples was calculated by one-way ANOVA with a Tukey's post-test. Significant differences between the control and other treatments are indicated as * ($p < 0.05$). These results are representative of 3 separate experiments.

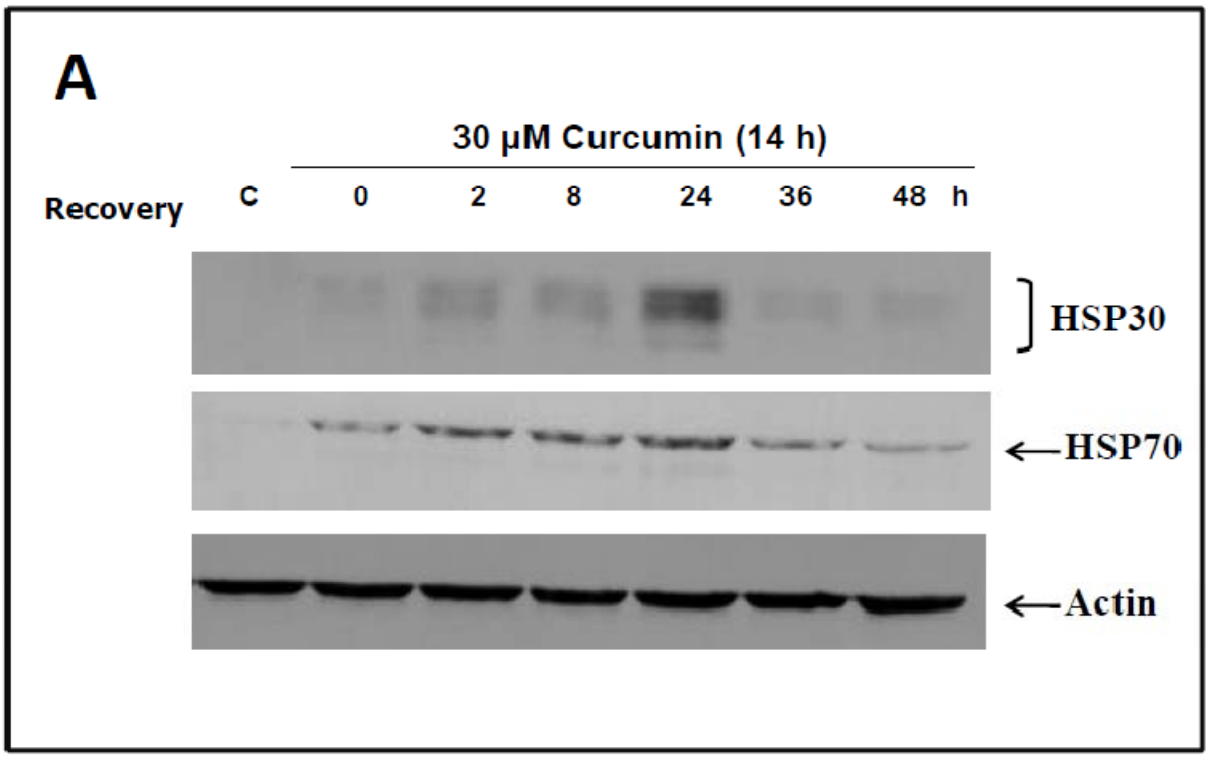
A
30 μM Curcumin (14 h)
Recovery
C
0
2
8
24
36
48 h
HSP30
HSP70
Actin

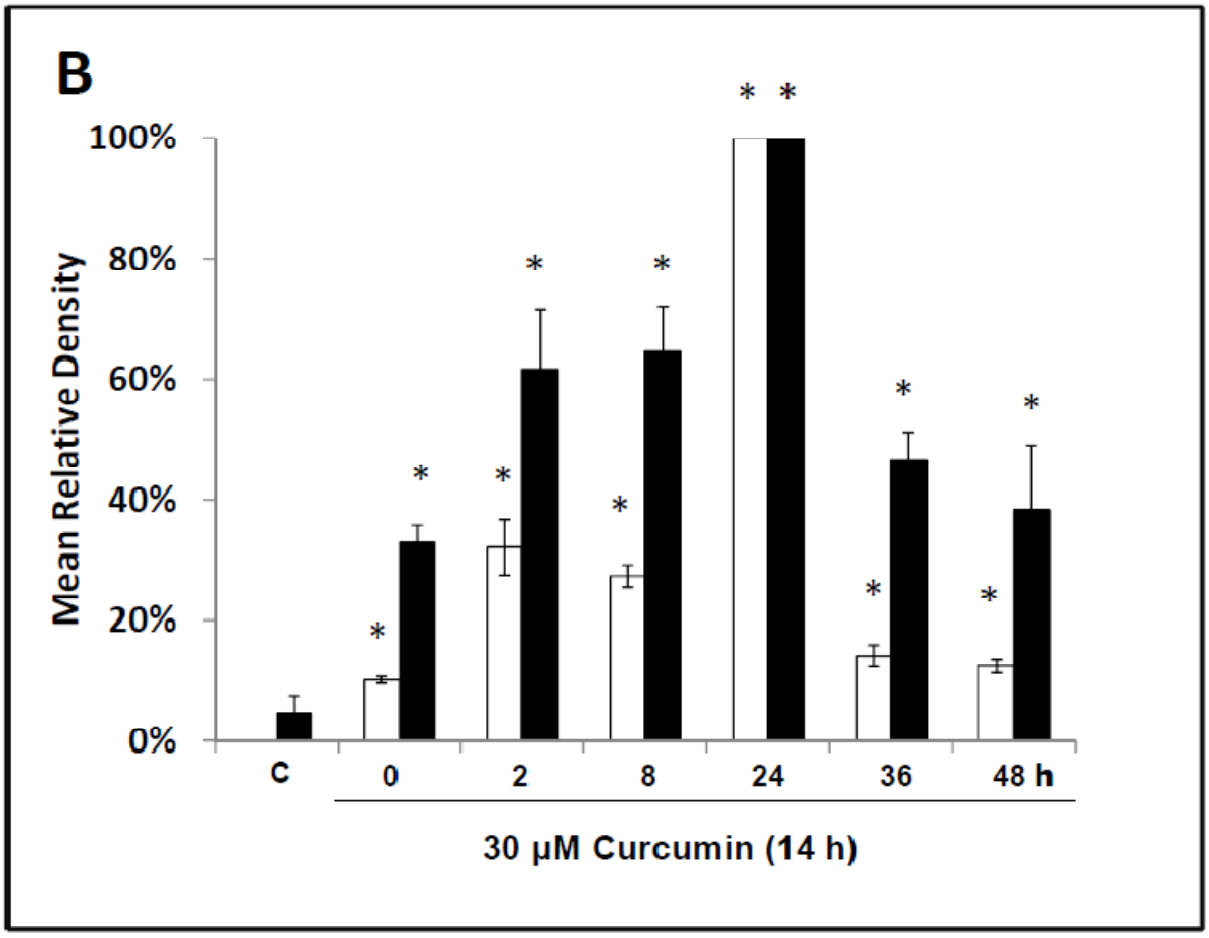
B
Mean Relative Density
100%
80%
60%
40%
20%
0%
C
0
2
8
24
36
48 h
30 μM Curcumin (14 h)

and 3-fold in cells recovering for curcumin for 8 and 24 h when compared to curcumin-treated cells with no recovery time.

3.6. Involvement of HSF activation in the accumulation of HSP30 and HSP70 in curcumin treated A6 cells treated

A HSF1 inhibitor, KNK437, was employed to determine if curcumin-induced accumulation of HSP30 and HSP70 in A6 cells involved HSE-HSF1 binding activity. Previously, our laboratory demonstrated that KNK437 pretreatment inhibited both heat shock and chemical stress-induced *hsp* gene expression in *Xenopus laevis* A6 cells (Manwell and Heikkila, 2007; Voyer and Heikkila, 2008). As shown in Figure 11, when cells were pretreated with KNK437 prior to a curcumin treatment, there was a complete inhibition of HSP30 and HSP70 accumulation (Fig. 11A). Actin levels remained relatively unchanged throughout the course of the treatments. Subsequent densitometric analysis demonstrated that KNK437 caused inhibition of curcumin-induced HSP30 and HSP70 accumulation by 100 % and 94.8 %, respectively (Fig. 11C).

3.7. Effect of mild heat shock on curcumin-induced HSP accumulation

In the present study, I characterized the effect of treating A6 cells simultaneously with curcumin and mild heat shock on HSP30 and HSP70 accumulation. Cells were exposed to 10 μM curcumin alone or in combination with a mild heat shock of 30 °C for 6 h followed by a 2 h recovery at 22 °C. Neither a 6 h 30 °C heat shock nor a 6 h 10 μM curcumin treatment alone resulted in any detectable accumulation of HSP30 protein, whereas the simultaneous treatment with the two stressors resulted in an enhanced accumulation of HSP30 (Fig. 12A). While relatively low levels of HSP70 accumulation were observed in cells treated with a 30 °C heat

Figure 11. Effect of KNK437 on curcumin-induced HSP30 and HSP70 accumulation in A6 cells. [A] Cells were maintained at 22 °C, or exposed to 30 μM curcumin for 14 or 24 h with (+) or without (-) a 6 h pre-treatment with 100 μM KNK437 (KNK). KNK was present during the stress treatments. Cells were harvested and total protein was isolated and analyzed by immunoblotting using anti-HSP30, anti-HSP70 or anti-actin polyclonal antibodies as described in Material and methods. **[B]** Image J software was used to perform densitometric analysis of the signal intensity for HSP30 (white) and HSP70 (black) protein bands of western blot images. The data are expressed as a percentage of the maximum band (30 μM curcumin for 24 h without pre-treatment with KNK for HSP30 and HSP70) while the standard error is represented by vertical error bars. The level of significance of the differences between samples was calculated by one-way ANOVA with a Tukey's post-test. Significant differences between the control and other treatments are indicated as * ($p < 0.05$). These results are representative of 3 separate experiments. **[C]** The ability of KNK437 to inhibit HSP30 and HSP70 protein accumulation at each time point is graphed as % inhibition while the standard error is represented by vertical error bars. These results are representative of 3 separate experiments.

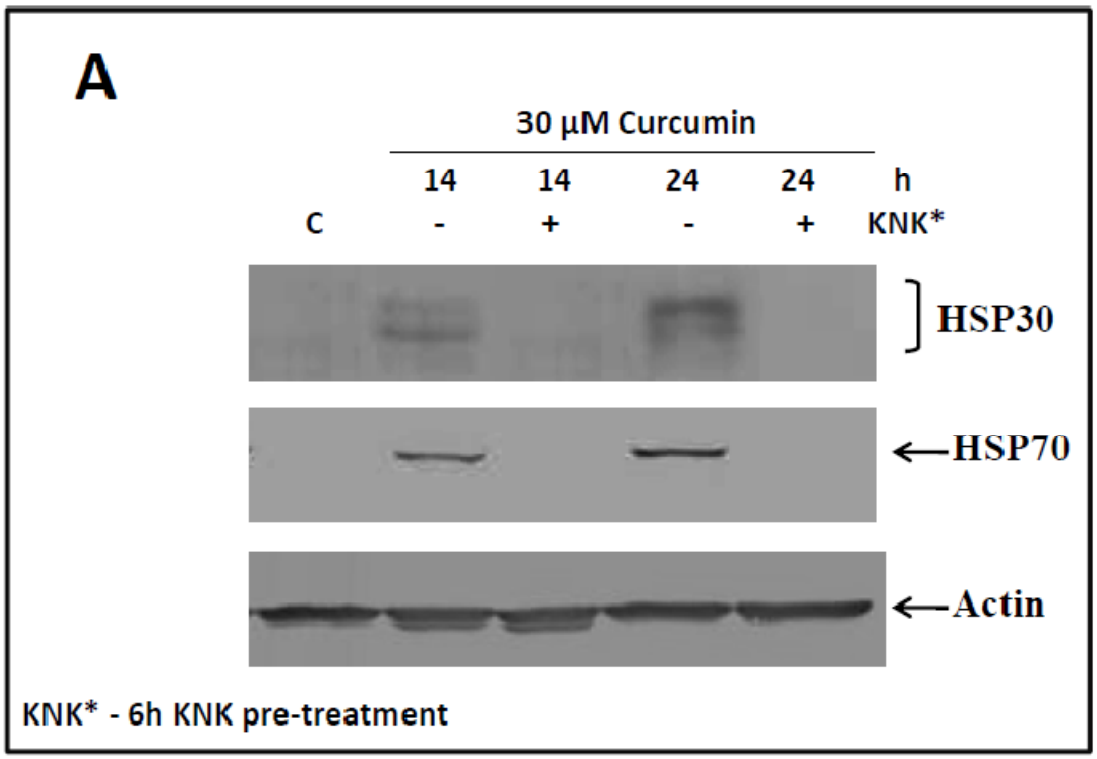
A
30 µM Curcumin
14
14
24
24
h
C
-
+
-
+
KNK*
HSP30
HSP70
Actin
KNK* - 6h KNK pre-treatment

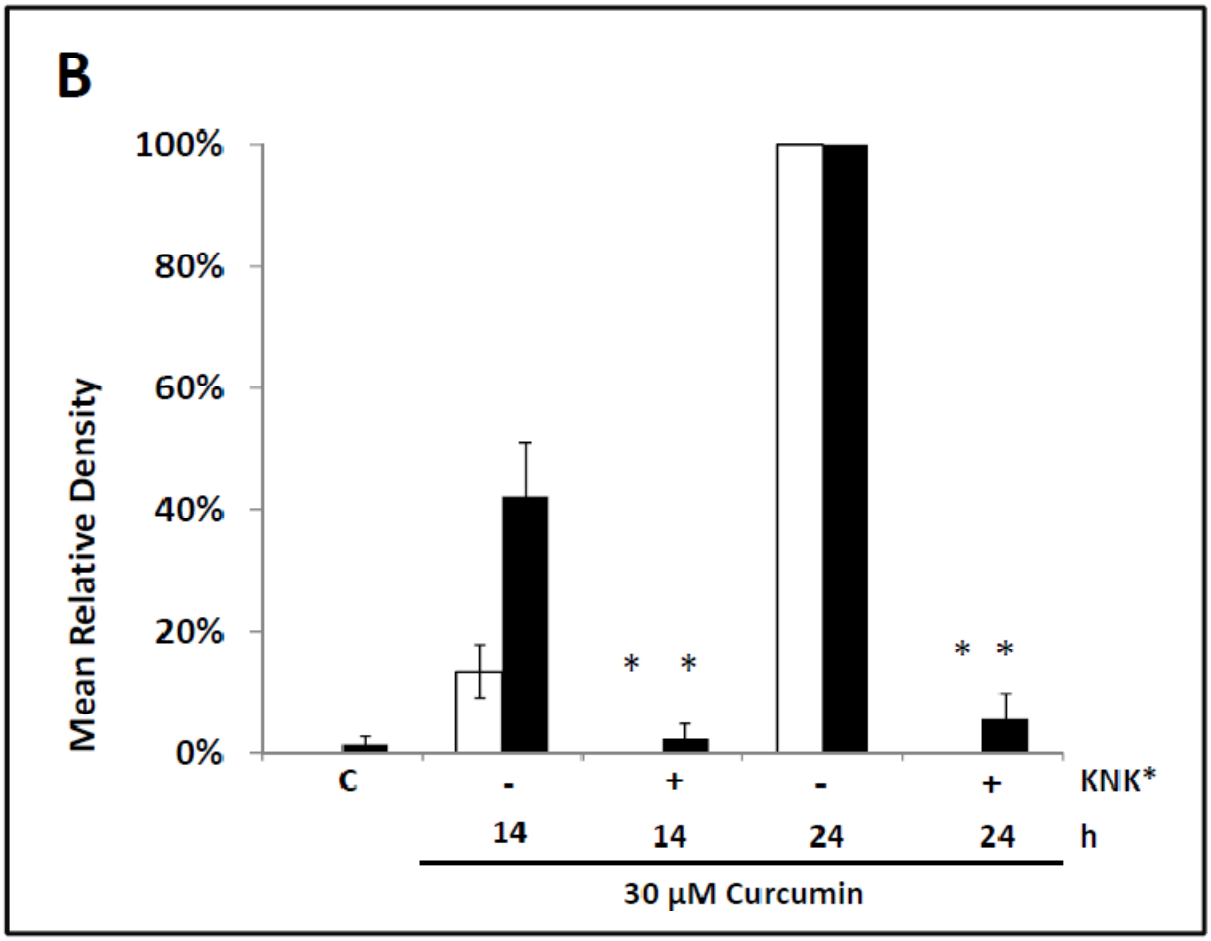
B
100%
80%
60%
40%
20%
0%
Mean Relative Density
* *
* *
C
-
+
-
+
KNK*
14
14
24
24
h
30 µM Curcumin

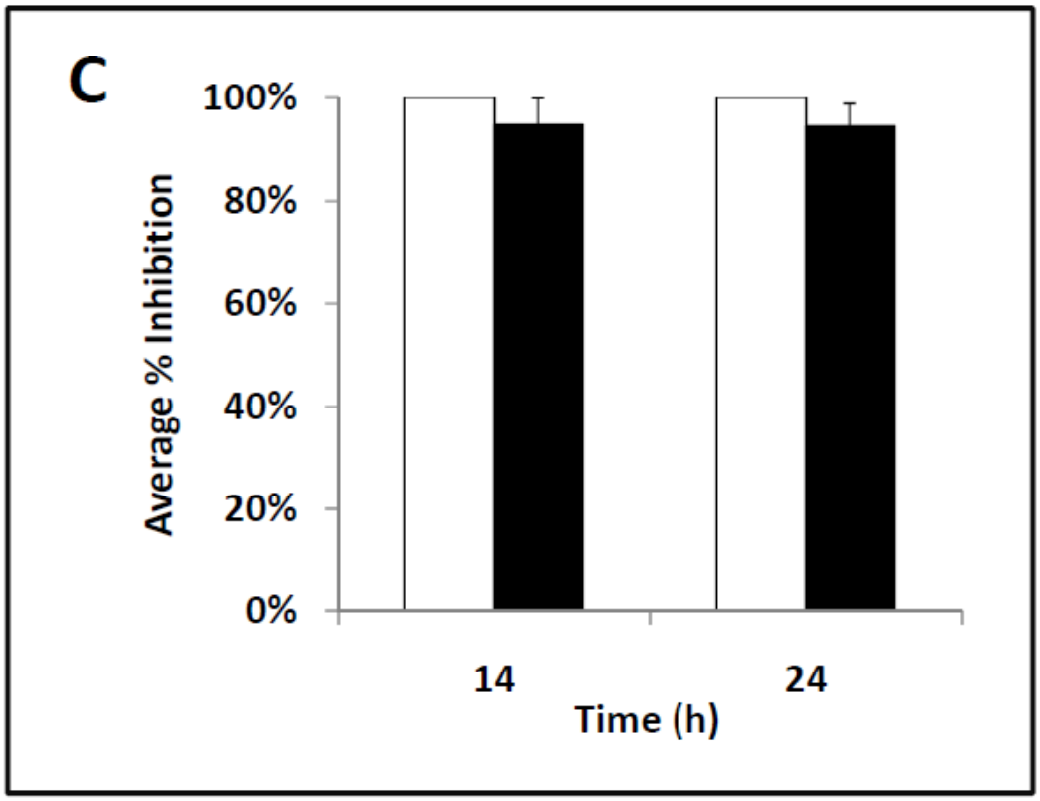
C
100%
80%
60%
40%
20%
0%
Average % Inhibition
14
24
Time (h)

Figure 12. Analysis of HSP30 and HSP70 accumulation in A6 cells treated simultaneously with curcumin plus mild heat shock. [A] Cells were maintained at 22 °C, or exposed to 10 μM curcumin either singly or in combination with a 30 °C for 6 h followed by a 2 h recovery period at 22 °C. Cells were harvested and total protein was isolated and analyzed by immunoblotting using anti-HSP30, anti-HSP70 or anti-actin polyclonal antibodies as described in Material and methods. **[B]** Image J software was used to perform densitometric analysis of the signal intensity for HSP30 (white) and HSP70 (black) protein bands of western blot images. The data are expressed as a percentage of the maximum band (simultaneous treatment of 10 μM curcumin plus 30 °C for 6 h for HSP30 and HSP70) while the standard error is represented by vertical error bars. The level of significance of the differences between samples was calculated by one-way ANOVA with a Tukey's post-test. Significant differences between the maximum signal and other treatments are indicated as * ($p < 0.05$). These results are representative of 3 separate experiments.

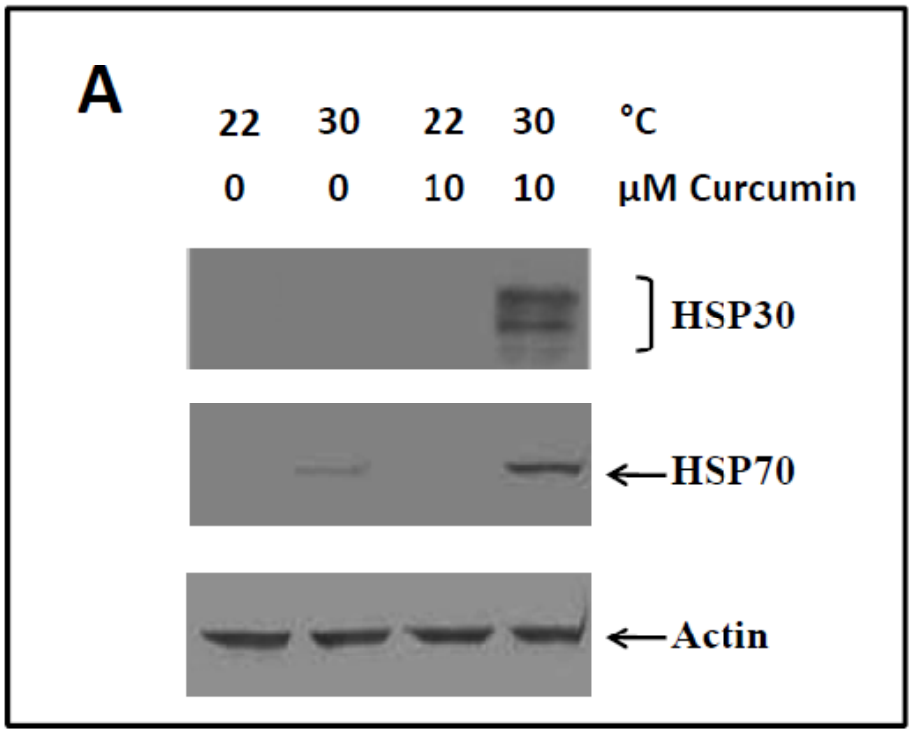
A
22 30 22 30 °C
0 0 10 10 μM Curcumin
HSP30
HSP70
Actin

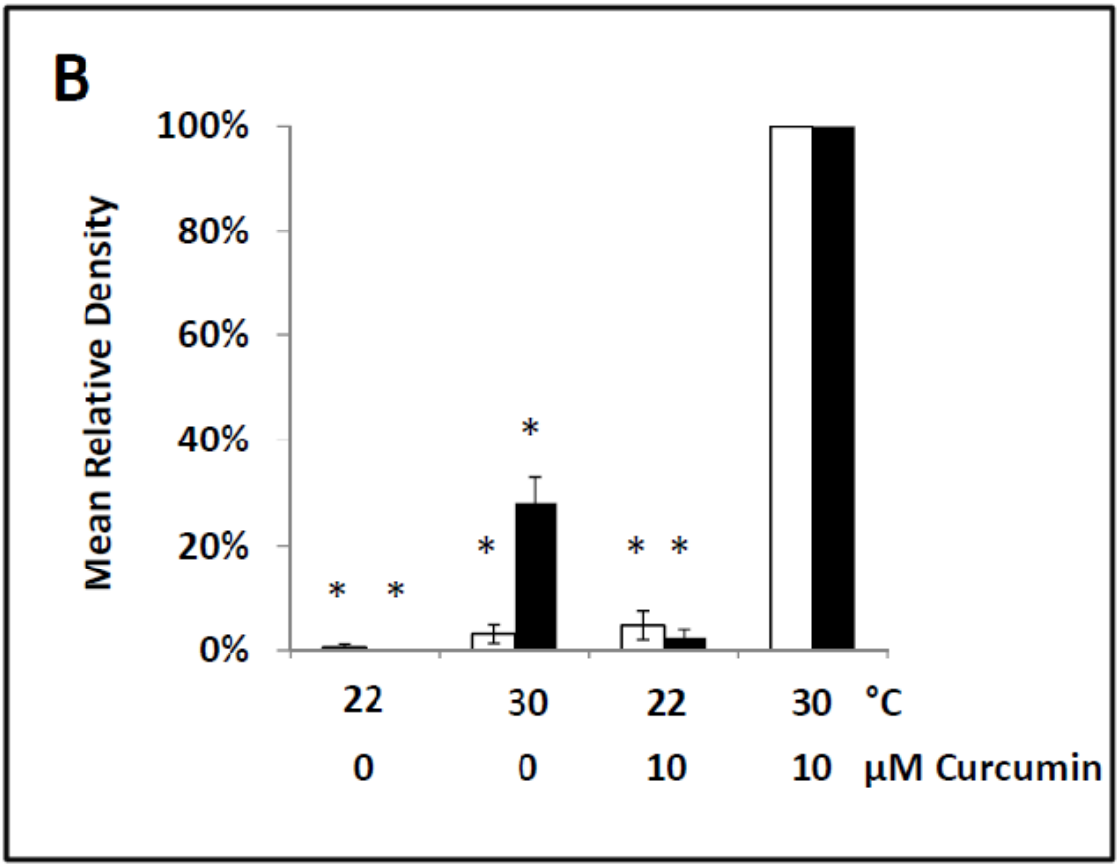
B
Mean Relative Density
100%
80%
60%
40%
20%
0%
22 30 22 30 °C
0 0 10 10 μM Curcumin

shock for 6 h or a 10 μM curcumin treatment for 6 h, a combination of the two stressors resulted in a higher accumulation of HSP70. Actin levels remained relatively unchanged for all the treatments. Densitometric analysis revealed that in comparison to cells treated with curcumin for 6 h by itself, a 20-fold increase in HSP30 accumulation occurred in cells treated simultaneously with curcumin and a mild heat shock (Fig. 12B). Similarly, HSP70 increased 42.7-fold in cells treated simultaneously with curcumin and mild heat shock when compared to curcumin treated cells.

A time course of HSP30 and HSP70 accumulation in A6 cells exposed to concurrent curcumin plus elevated temperature is shown in Figure 13. A6 cells were treated simultaneously with 10 μM curcumin plus a 30 ºC heat shock for time periods ranging from 2 to 24 h (Fig. 13A). In cells treated with concurrent curcumin and elevated temperature the accumulation of HSP30 and HSP70 gradually increased from 2 to 6 h of treatment, after which there was a decrease in accumulation up to 24 h. Densitometric analysis demonstrated a 2.5 fold increase in HSP30 levels from 2 to 6 h of concurrent curcumin and mild temperature treatment of cells.

3.8. Localization of HSP30 in heat shock and curcumin-treated A6 cells

The effect of heat shock and curcumin on the localization of HSP30 in A6 cells was determined by immunocytochemistry and laser scanning confocal microscopy (LSCM). HSP70 was not investigated using this methodology since the affinity-purified, polyclonal anti-HSP70 antibody, which was utilized successfully in western blot analysis, was unable to specifically detect HSP70 by immunocytochemistry (Gauley et al., 2008). As shown in Figure 14, heat shock treatment of cells resulted in the localization of HSP30 in the cytoplasm in a granular or punctuate pattern. HSP30 was not detectable in control cells maintained at 22 °C. Relatively low

Figure 13. Time course of HSP30 and HSP70 accumulation in A6 cells treated with concurrent curcumin and mild heat shock. [A] Cells were maintained at 22 °C, or exposed to 10 μM curcumin in combination with a 30 °C for 2, 6, 10, 14, 18 or 24 h followed by a 2 h recovery period at 22 °C in fresh L-15 media. Cells were harvested and total protein was isolated and analyzed by immunoblotting using anti-HSP30, anti-HSP70 or anti-actin polyclonal antibodies as described in Material and methods. **[B]** Image J software was used to perform densitometric analysis of the signal intensity for HSP30 (white) and HSP70 (black) protein bands of western blot images. The data are expressed as a percentage of the maximum band (simultaneous treatment of 10 μM curcumin plus 30 °C for 6 h for HSP30 and HSP70) while the standard error is represented by vertical error bars. The level of significance of the differences between samples was calculated by one-way ANOVA with a Tukey's post-test. Significant differences between the control and other treatments are indicated as * ($p < 0.05$) or Δ ($p < 0.1$). These results are representative of 3 separate experiments.

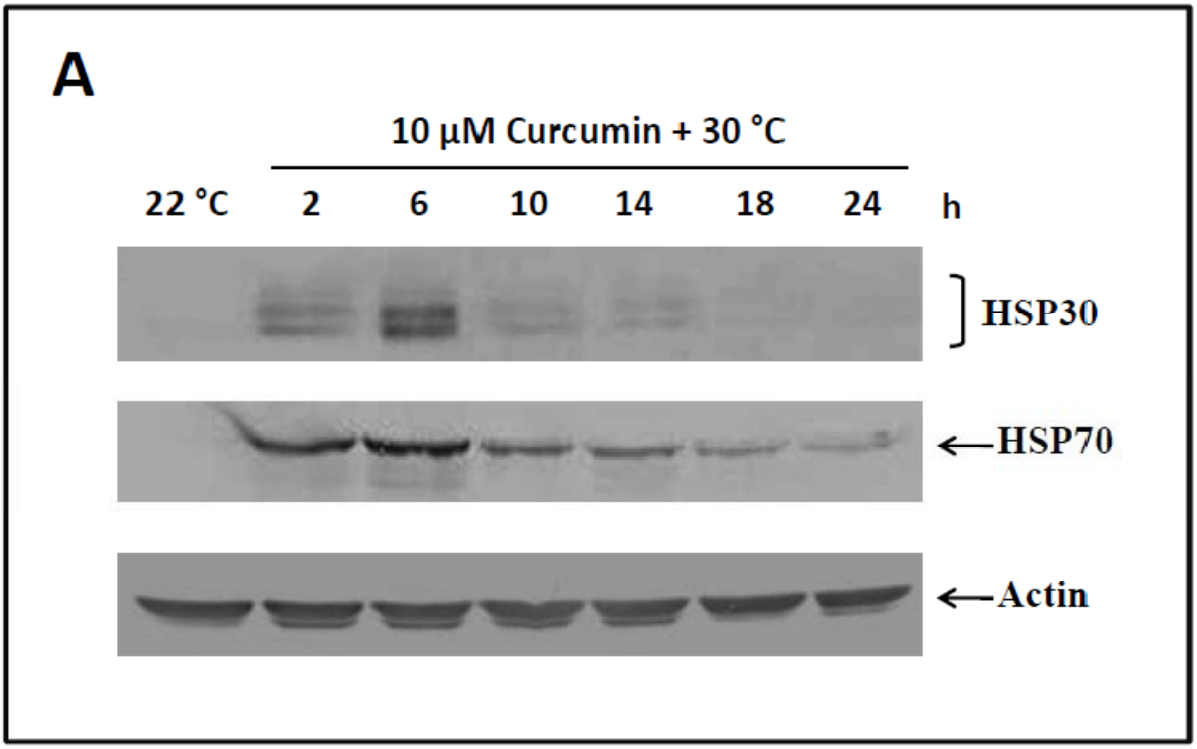
A
10 μM Curcumin + 30 °C
22 °C
2
6
10
14
18
24
h
HSP30
HSP70
Actin

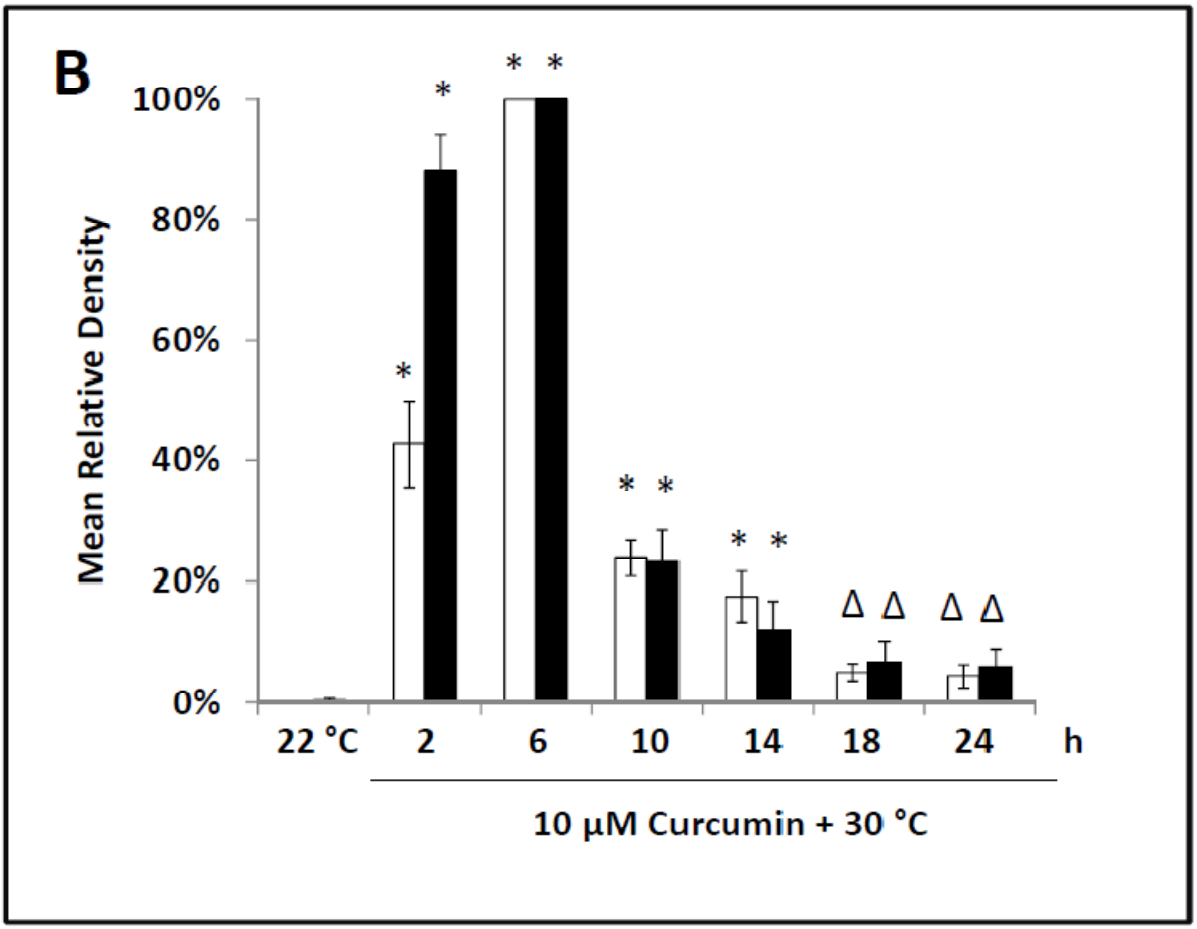
B
Mean Relative Density
100%
80%
60%
40%
20%
0%
22 °C
2
6
10
14
18
24
h
10 μM Curcumin + 30 °C

Figure 14. Immunocytochemical detection of intracellular HSP30 accumulation in A6 cells exposed to two different heat shock temperatures. Cells were grown on glass coverslips in L-15 media and were either maintained at 22 °C or heat shocked at 30 °C for 6 h or 33 °C for 2 h, followed by a 2 h recovery period at 22 °C. Actin and nuclei were stained directly with phalloidin conjugated to TRITC (red) and DAPI (blue), respectively. HSP30 was detected indirectly using an anti-HSP30 antibody and Alexa-488 secondary antibody conjugate (green). From left to right the columns display fluorescence detection channels for actin, HSP30 and merger of actin, DAPI and HSP30. The 20-μm white scale bar bars are indicated at the bottom right section of each panel. These results are representative of 3 different experiments.

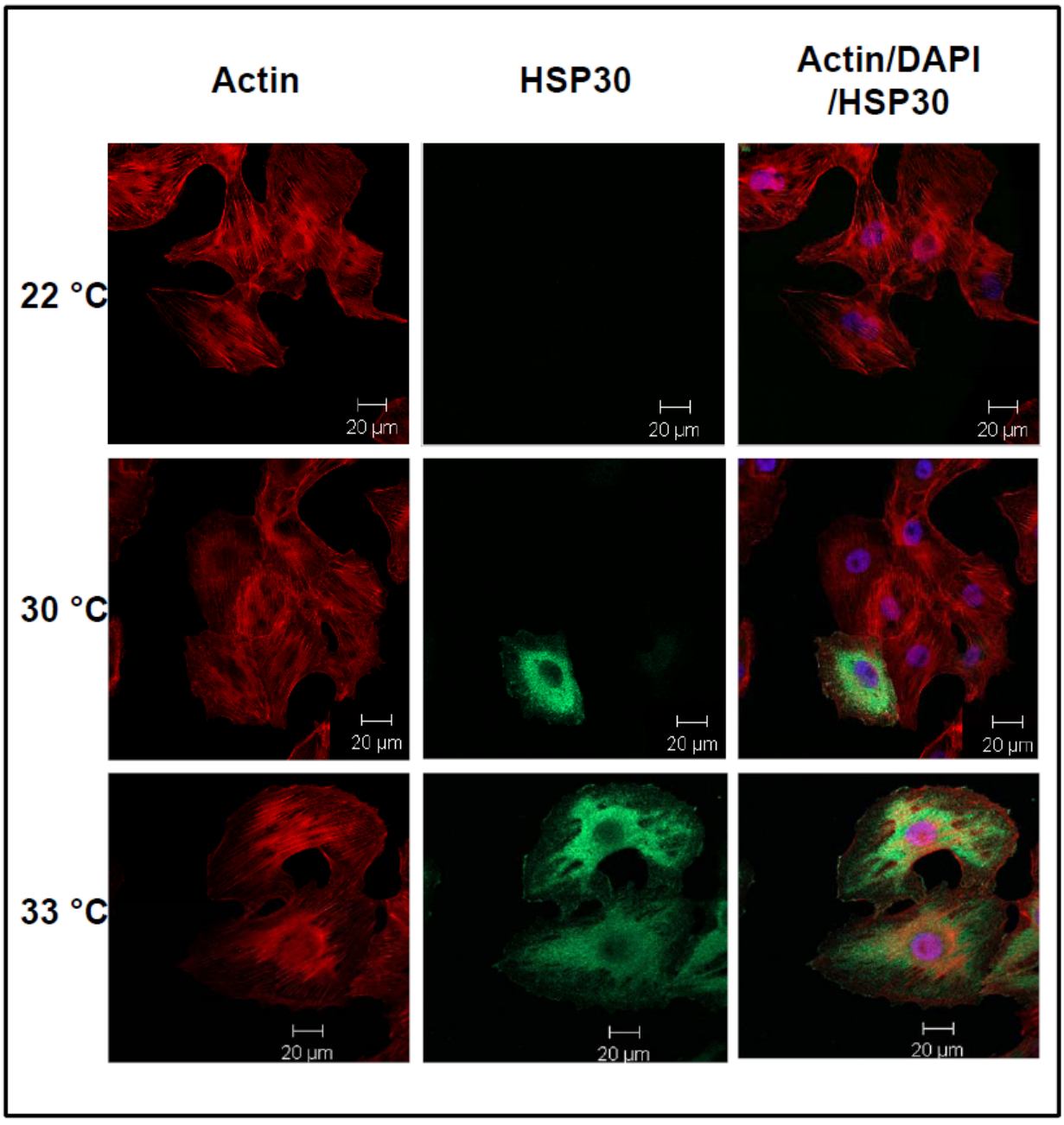
Actin
HSP30
Actin/DAPI
/HSP30
22 °C
30 °C
33 °C
20 µm

amounts of HSP30 accumulation were detected in 30 % of cells incubated at 30 °C for 6 h (Fig. 14). However, HSP30 did accumulate in 90 % of the cells exposed to a 33 °C heat shock.

When A6 cells were treated with curcumin, HSP30 was localized primarily in the cytoplasm in a punctuate pattern. Curcumin-induced HSP30 accumulation was detected in approximately 10 % and 75 % of total cells treated for 14 h with 10 μM and 30 μM curcumin, respectively (Fig. 15). An increase in curcumin concentration up to 30 μM curcumin had no visible effects on the actin cytoskeleton.

Combined treatment of cells with 10 μM curcumin and mild heat shock at 30 °C for 2 h, followed by a 2 h recovery at 22 °C resulted in an increase in HSP30 accumulation in 40 % of the cells with no visible effects on the actin cytoskeleton as indicated by the presence of control-like stress fibers (Fig. 16). A 1.5 and 2-fold increase in HSP30 accumulating cells was observed for 4 and 6 h treatments, respectively, with no detrimental effect on the actin cytoskeleton (Fig. 17).

3.9. The effect of curcumin and mild heat shock on the acquisition of thermotolerance in A6 cells

In a previous study, it was established that pre-treatment of A6 cells with a 33 ºC heat shock resulted in the accumulation of HSPs and an acquired state of thermotolerance (Manwell and Heikkila, 2007). In the present study, A6 cells were pretreated with curcumin prior to a thermal challenge at 37 ºC to assess whether this agent can produce thermotolerance. Shifting the incubation temperature of cells from 22 °C directly to a 37 °C thermal challenge for 1 h resulted in the collapse of the actin cytoskeleton (Fig. 18A). However, 80 % of cells pretreated with a 33

Figure 15. Intracellular localization of curcumin-induced HSP30 accumulation. Cells were grown on glass coverslips and were maintained at 22 °C (Control) or treated with 10 or 30 μM curcumin for 2 or 14 h at 22 °C. Actin and nuclei were stained directly with phalloidin conjugated to TRITC (red) and DAPI (blue), respectively. HSP30 was indirectly detected with an anti-HSP30 antibody and a secondary antibody conjugated to Alexa-488 (green). From left to right the columns display fluorescence detection channels for actin, HSP30 and merger of actin, DAPI and HSP30. The 20-μm white scale bars are indicated at the bottom right section of each panel. These results are representative of 3 different experiments.

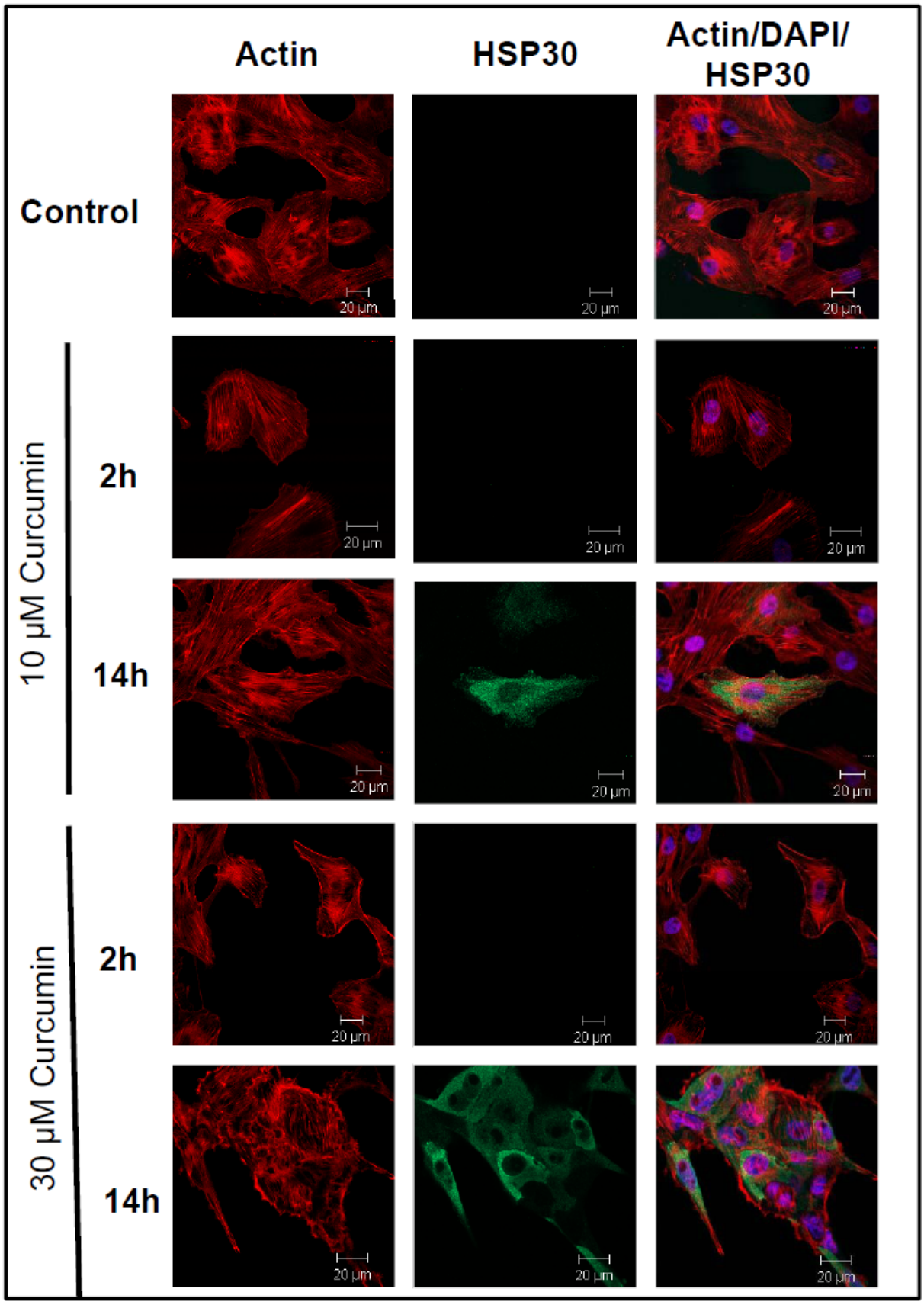
Actin
HSP30
Actin/DAPI/
HSP30
Control
10 μM Curcumin
2h
14h
30 μM Curcumin
2h
14h
20 μm

Figure 16. Localization of HSP30 accumulation in A6 cells treated singularly or simultaneously with a mild heat shock plus curcumin. Cells were grown on glass coverslips in L-15 media at 22 °C. Cells were maintained at 22 °C (Control), treated with 10 μM curcumin (Cur) or a 30 °C heat shock for 2 h individually or in combination, followed by a 2 h recovery at 22 °C. Actin and nuclei were stained directly with phalloidin conjugated to TRITC (red) and DAPI (blue), respectively. HSP30 was indirectly detected with an anti-HSP30 antibody and Alexa-488 secondary antibody conjugate (green). From left to right the columns display fluorescence detection channels for actin, HSP30 and merger of actin, DAPI and HSP30. The 20 μm white scale bar is indicated at the bottom right corner of each panel. These results are representative of 3 different experiments.

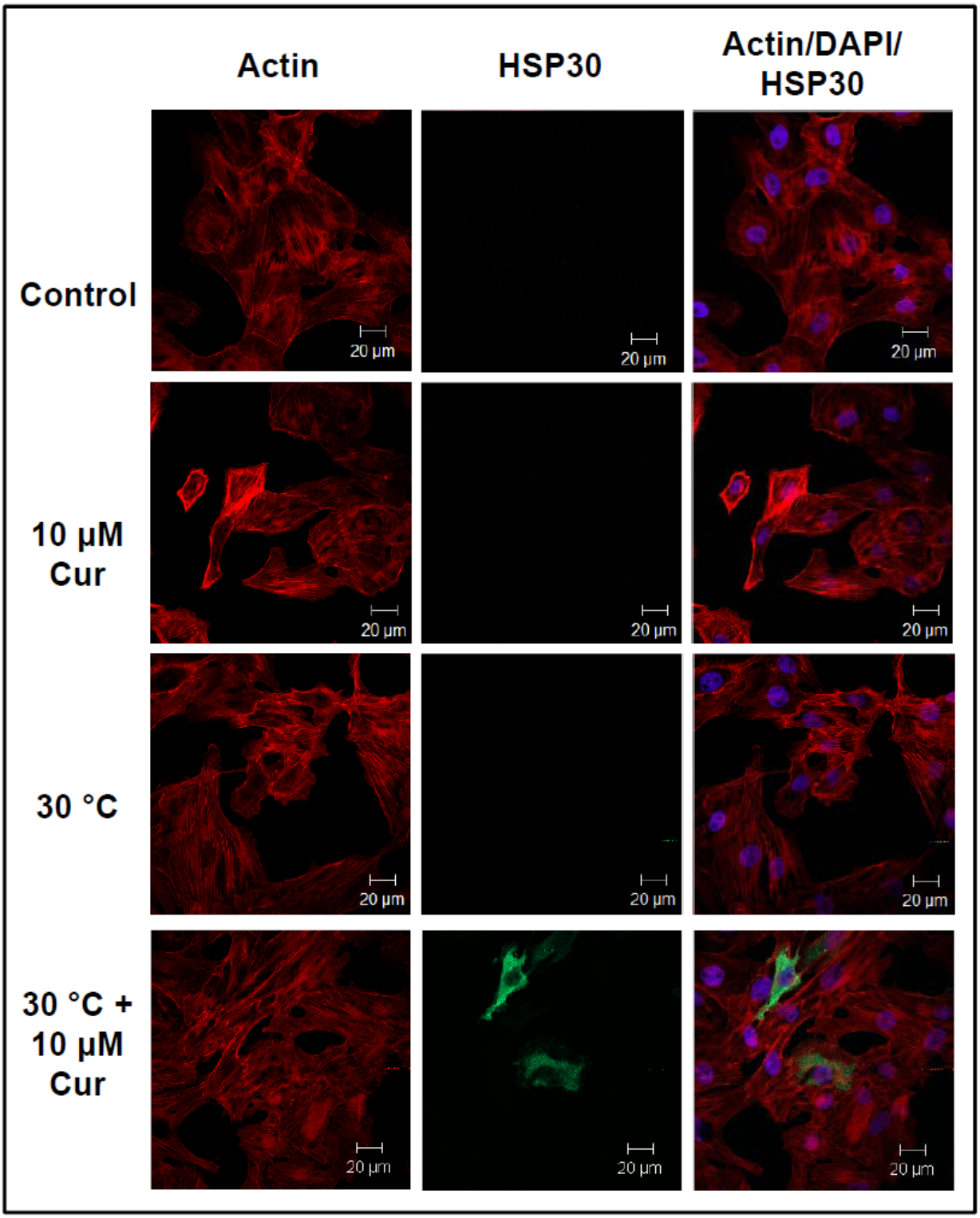
Actin
HSP30
Actin/DAPI/
HSP30
Control
10 µM
Cur
30 °C
30 °C +
10 µM
Cur
20 µm

Figure 17. Time course of intracellular HSP30 accumulation in A6 cells treated with a mild heat shock plus curcumin treatment. Cells were grown on glass coverslips in L-15 media at 22 °C. Cells were maintained at 22 °C (Control) or simultaneously treated with a 30 °C heat shock and 10 μM curcumin treatment for 2, 4 or 6 h followed by a 2 h recovery at 22 °C. Actin and nuclei were stained directly with phalloidin conjugated to TRITC (red) and DAPI (blue), respectively. HSP30 was indirectly detected with an anti-HSP30 antibody and Alexa-488 secondary antibody conjugate (green). From left to right the columns display fluorescence detection channels for actin, HSP30 and merger of actin, DAPI and HSP30. The 20 μm white scale bar is indicated at the bottom right corner of each panel. These results are representative of 3 different experiments.

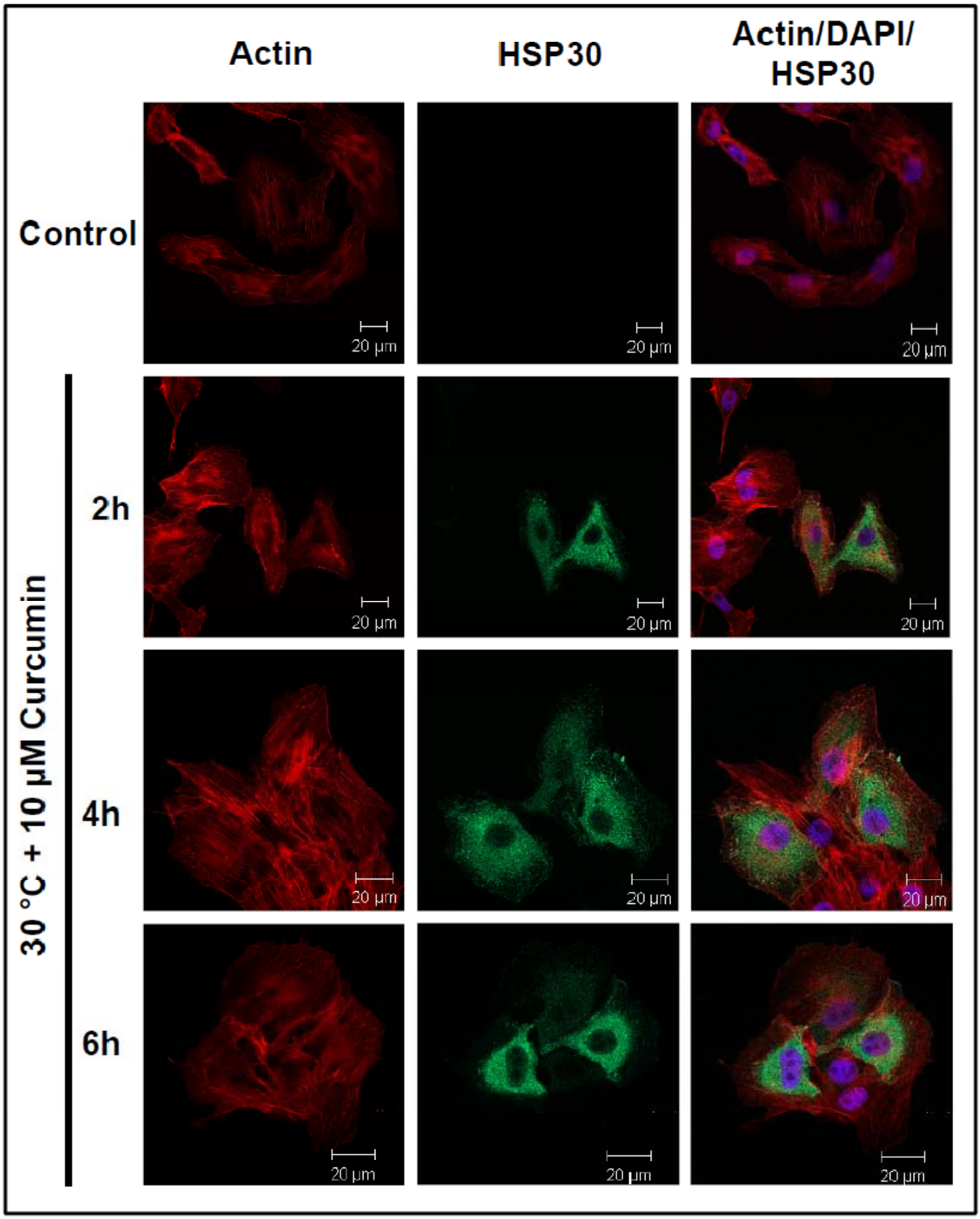
Actin
HSP30
Actin/DAPI/
HSP30
Control
30 °C + 10 µM Curcumin
2h
4h
6h
20 µm

Figure 18. Cytoprotective effects of pre-treating A6 cells with heat shock prior to a 37 ºC thermal challenge. Cells were grown on glass coverslips and were maintained at 22 ºC, subjected to a 37 ºC thermal challenge or heat shocked at 33 ºC prior to a 37 ºC thermal challenge for 1 h. A6 cells were also pretreated with 100 μM KNK437 for 6 h before exposure to a 33 ºC heat shock and subsequent thermal challenge. Heat shocks at 33 ºC and thermal challenges at 37 ºC were followed by either a 2 h recovery period or 6 h recovery period at 22 ºC, respectively. Actin and nuclei were stained directly with TRITC (red) and DAPI (blue), respectively. HSP30 was indirectly detected with an anti-HSP30 antibody and a secondary antibody conjugated to Alexa-488 (green). From left to right the columns display fluorescence detection channels for actin, HSP30 and merger of actin, DAPI and HSP30. The 20 μm white scale bar is indicated at the bottom right corner of each panel. These results are representative of 3 different experiments.

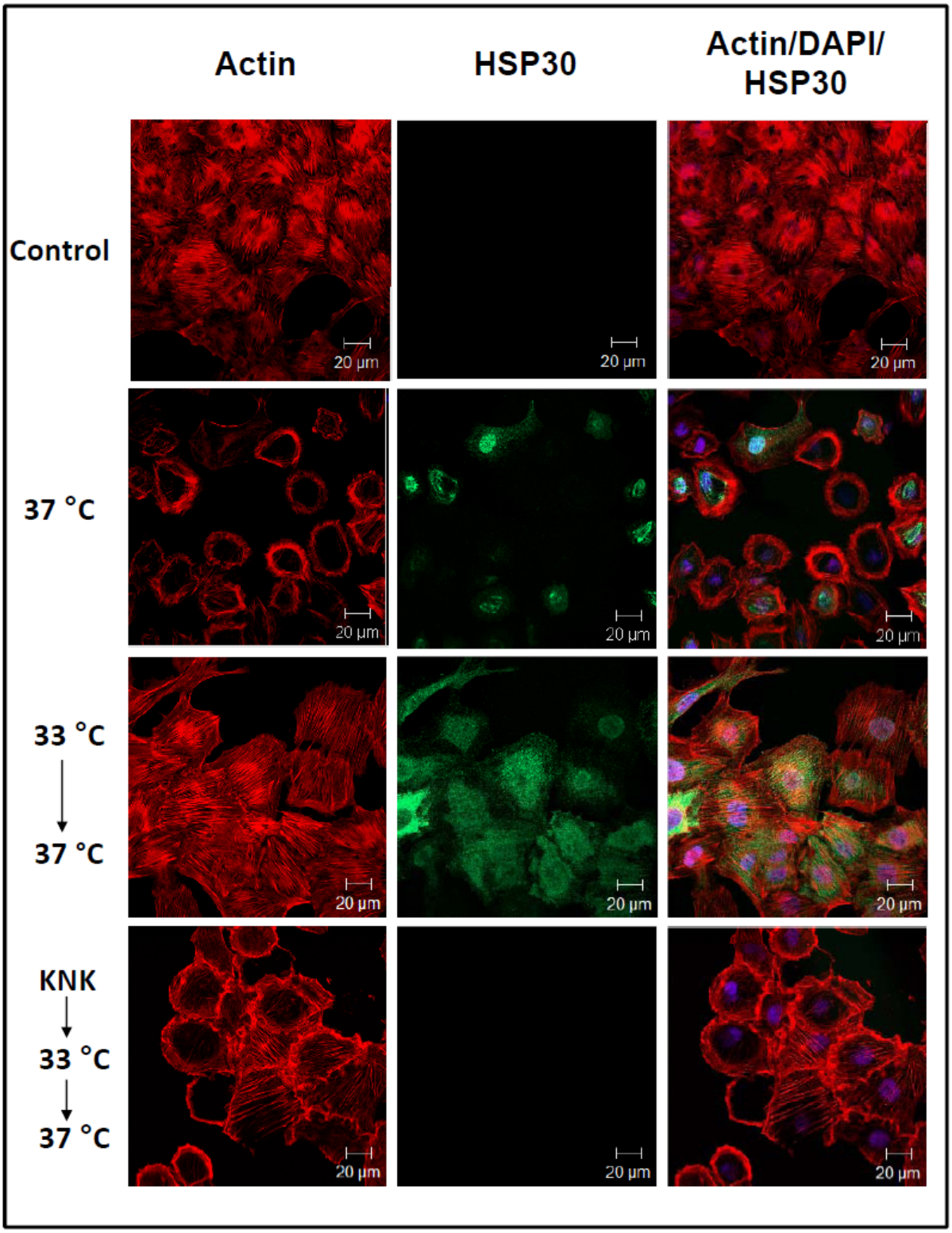
Actin
HSP30
Actin/DAPI/
HSP30
Control
37 °C
33 °C
37 °C
KNK
33 °C
37 °C
20 μm

ºC heat shock prior to the thermal challenge exhibited a normal actin cytoskeleton with intact stress fibers (Fig. 18A).

As noted previously, cells treated with 30 μM curcumin for 24 h had an optimal level of HSP30 accumulation. Therefore these conditions were employed in the present thermotolerance studies. As shown in Figure 19A, 90 % of the cells pretreated with 30 μM curcumin for 24 h prior to a thermal challenge did not have a collapsed actin cytoskeleton and displayed control-like stress fibers. Thus, curcumin was effective in conferring thermotolerance in A6 cells. The accumulation of HSPs in A6 cells may be responsible for this acquired state of thermotolerance by curcumin since KNK437 pre-treatment, which inhibited the accumulation of HSP30 and HSP70, also resulted in cytoskeletal collapse (Fig. 19A, last row). Relatively large circular HSP30 staining structures were observed in the cytoplasm of 25% of cells pretreated with curcumin prior to a thermal challenge (Fig. 19B).

Finally, I examined whether simultaneous exposure to curcumin and heat shock, which induced the accumulation of HSP30 and HSP70, could also acquire thermotolerance. Cells treated singly with a 30 °C heat shock or 10 μM curcumin prior to the 37 °C thermal challenge for 1 h displayed a cytoskeletal collapse. However, pre-treatment with curcumin plus mild heat shock before the thermal challenge resulted in 90% of cells displaying intact stress fibers and no cytoskeletal collapse (Fig 20). Thus, curcumin plus mild heat shock pre-treatment was effective at conferring thermotolerance in A6 cells.

Figure 19. Cytoprotective effects of pre-treating A6 cells with curcumin prior to a 37 ºC thermal challenge. [A] Cells were grown on glass coverslips and were maintained at 22 ºC, subjected to a 37 ºC thermal challenge or exposed to 30 μM curcumin (Cur) for 24 h prior to a 37 ºC thermal challenge for 1 h. A6 cells were also pretreated with 100 μM KNK437 for 6 h before exposure to 30 μM Cur for 24 h and subsequent thermal challenge. Thermal challenges at 37 ºC were followed by 6 h recovery period at 22 ºC. Actin and nuclei were stained directly with TRITC (red) and DAPI (blue), respectively. HSP30 was indirectly detected with an anti-HSP30 antibody and a secondary antibody conjugated to Alexa-488 (green). From left to right the columns display fluorescence detection channels for actin, HSP30 and merger of actin, DAPI and HSP30. The 20 μm white scale bar is indicated at the bottom right corner of each panel. These results are representative of 3 different experiments. **[B]** Enlargements of the HSP30 localization patterns observed in A6 cells treated with 30 μM Cur for 24 h prior to a 37 ºC thermal challenge for 1 h. The bottom image is magnification of the area within the red box. The white arrow indicates large circular cytoplasmic foci of HSP30 accumulation. Actin and nuclei were stained directly with TRITC (red) and DAPI (blue), respectively. HSP30 was indirectly detected with an anti-HSP30 antibody and a secondary antibody conjugated to Alexa-488 (green).

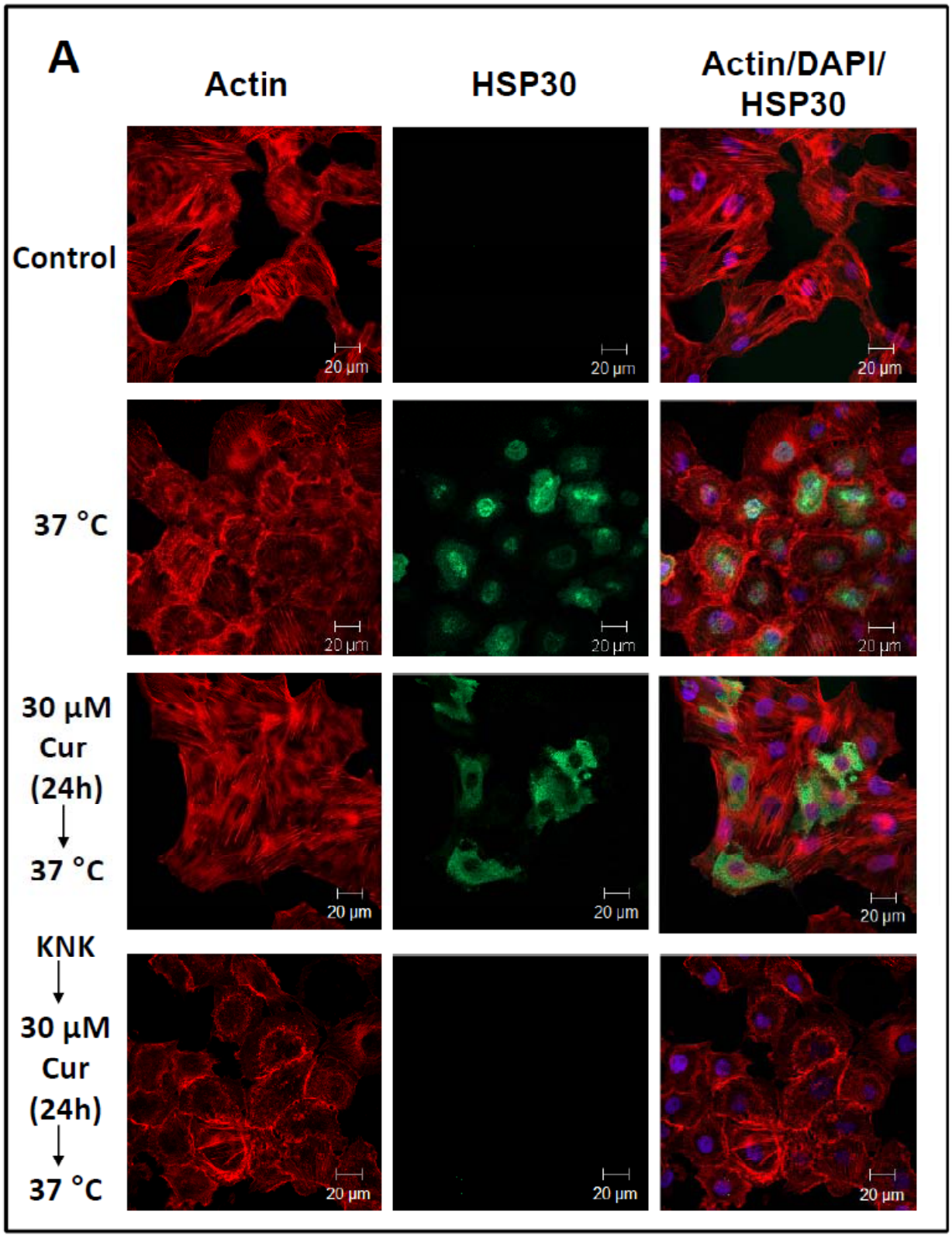
A
Actin
HSP30
Actin/DAPI/
HSP30
Control
37 °C
30 µM
Cur
(24h)
37 °C
KNK
30 µM
Cur
(24h)
37 °C
20 µm

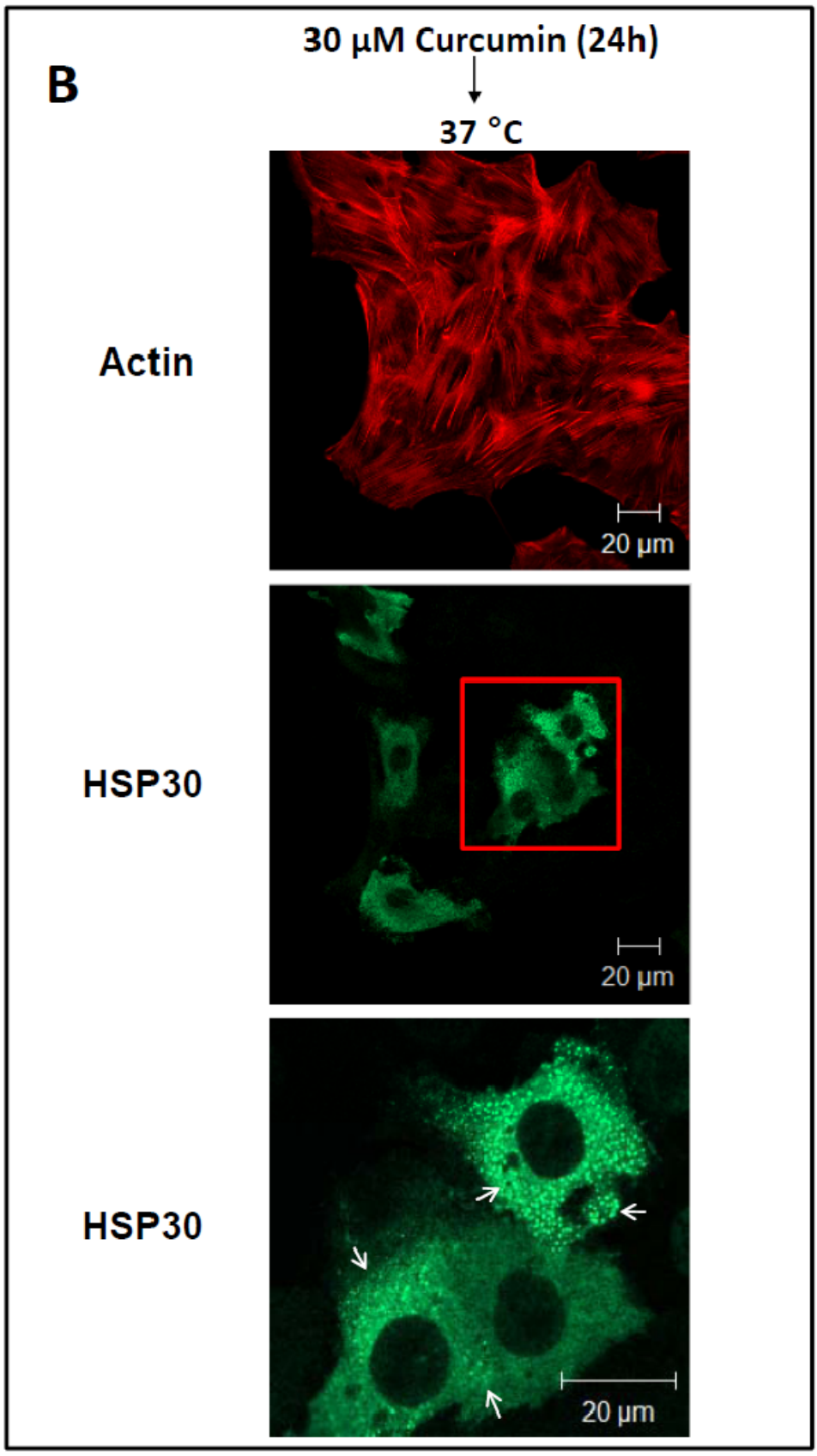
B
30 µM Curcumin (24h)
37 °C
Actin
20 µm
HSP30
20 µm
HSP30
20 µm

Figure 20. Cytoprotective effects of pre-treating A6 cells simultaneously with a mild heat shock plus curcumin prior to a 37 ºC thermal challenge. Cells were grown on glass coverslips and were maintained at 22 ºC, subjected to a 30 ºC heat shock or 10 μM curcumin (Cur) for 4 h treatment individually or in combination, prior to a 37 ºC thermal challenge for 1 h. Heat shocks, curcumin treatments and thermal challenges were followed by a 2 h recovery period. Actin and nuclei were stained directly with TRITC (red) and DAPI (blue), respectively. HSP30 was indirectly detected with an anti-HSP30 antibody and a secondary antibody conjugated to Alexa-488 (green). From left to right the columns display fluorescence detection channels for actin, HSP30 and merger of actin, DAPI and HSP30. The 20 μm white scale bar is indicated at the bottom right corner of each panel. These results are representative of 3 different experiments.

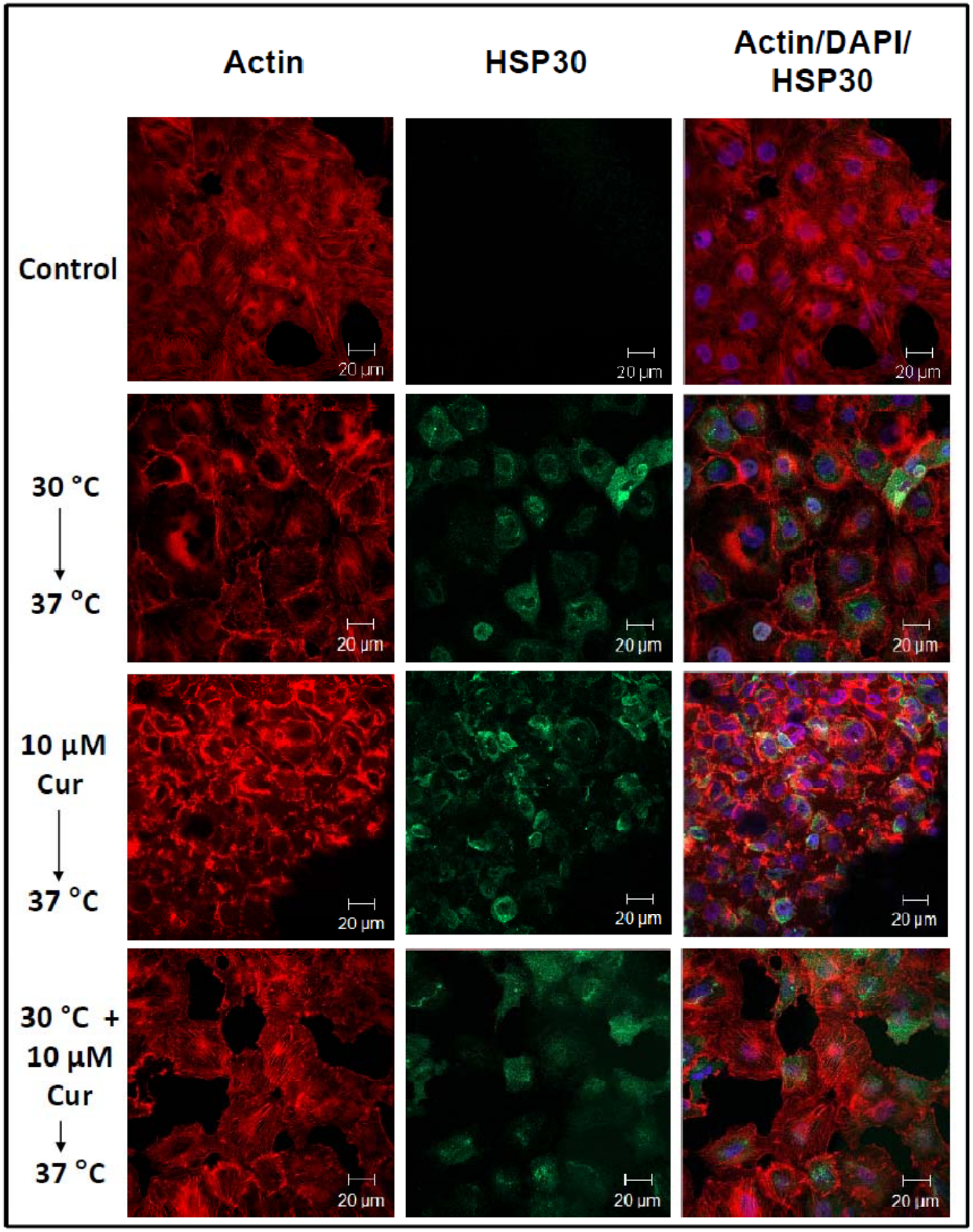
Actin
HSP30
Actin/DAPI/
HSP30
Control
30 °C
37 °C
10 µM
Cur
37 °C
30 °C +
10 µM
Cur
37 °C
20 µm

4. Discussion

The present study has shown that curcumin inhibited the chymotrypsin-like activity of the 26S proteasome, enhanced accumulation of ubiquitinated protein and induced *hsp30* and *hsp70* gene expression in *Xenopus laevis* A6 kidney epithelial cells. Initial studies demonstrated that exposure of A6 cells to curcumin enhanced the relative levels of ubiquitinated protein. These results were comparable to MG132-induced ubiquitinated protein accumulation presented in this study and previously in our laboratory (Young and Heikkila, 2010). Moreover, A6 cells treated with 30 μM curcumin for 14 or 24 h exhibited a 24 and 76 % decrease, respectively, in chymotrypsin (CT)-like activity when compared to control cells. It has been shown in previous studies that MG132, a known proteasome inhibitor, and celastrol inhibited CT-like activity in A6 cells (Walcott and Heikkila, 2010). Taken together, the curcumin-induced increase in the accumulation of ubiquitinated proteins and the decrease in CT-like activity was suggestive of curcumin-induced proteasomal inhibition. Similar findings have been described in mammalian cells. For example, curcumin inhibited proteasome activity and increased protein ubiquitination in HCT-116 and SW480 human colon cancer cell lines *in vitro* and *in vivo* (Milacic et al., 2008). Additionally, curcumin treated human keratinocytes had a 46 % decrease in chymotrypsin-like activity when compared to untreated cells (Ali and Rattan, 2006).

In *Xenopus laevis* A6 cells, like other eukaryotic systems, the ubiquitin-proteasome system (UPS) is the primary degradation pathway for misfolded or damaged proteins (Lee and Goldberg, 1998b; Malik et al., 2001). Previous studies have demonstrated that proteasome inhibition results in the accumulation of ubiquitinated cellular protein targeted for degradation within the cytosol (Bush et al., 1997; Lee and Goldberg, 1998b; Malik et al., 2001; Liao et al., 2006). Since these misfolded proteins possess exposed hydrophobic amino acid residues,

increased cellular concentrations of these non-native proteins by means of proteasomal inhibition can result in aggregate formation, which is detrimental to cell function (Hartl, 1996; Lee and Goldberg, 1998b; Hartl and Hayer-Hartl, 2009).

As previously mentioned, this study has shown, for the first time in amphibians, that treatment of A6 cells with curcumin resulted in the accumulation of HSP30 and HSP70 protein. In these experiments, curcumin had no detectable effect on actin accumulation. The curcumin concentrations (10 to 30 μM) employed in the present study were similar to those employed in mammalian cell line studies that induced *hsp* gene expression (Kato et al., 1998; Chen et al., 2001; Dunsmore et al., 2001; Ali and Rattan, 2006; Kanitkar and Bhonde, 2008; Teiten et al.,. 2009). For example, 10 to 30 μM curcumin stimulated heat- and stress-induced HSP27, HSP70 and αB crystallin accumulation in C6 rat glioma cells (Kato et al., 1998). Also, Dunsmore et al. (2001) demonstrated that up to 20 μM curcumin-induced HSP70 accumulation in HeLa cells in a time and dose-dependent manner. Additionally, Ali and Rattan (2006) showed significantly increased HSP90 and HSP70 accumulation in human keratinocytes treated with 10 μM curcumin in comparison to untreated cells. Finally, 20 μM curcumin also induced *hsp70* gene expression in human colorectal cancer cells and human leukemia K562 cells (Chen et al., 2001; Teiten et al., 2009).

In *Xenopus*, the stress-induced expression of *hsp* genes is mediated by HSF1-HSE binding activity (Heikkila, 2003; Voellmy, 2004). Although, the mechanism by which HSF1 is activated is unknown, it is thought that this process is triggered by the accumulation of misfolded or damaged proteins in the cytosol (Morimoto and Santoro, 1998; Voellmy, 2004; Morimoto, 2008). The current study determined that pretreatment of A6 cells with the HSF1 inhibitor, KNK437, prior to the application of curcumin repressed the accumulation of both HSP30 and

HSP70. This suggested that curcumin-induced *hsp* gene expression in *Xenopus* A6 cells was likely controlled, at least in part, at the level of transcription through the activation of the HSE-binding activity of HSF1. Previous studies have also investigated the effect of curcumin on HSF1 activity in rat and human cells (Kato et al., 1998; Dunsmore et al., 2001; Teiten et al., 2009). For example, Kato et al. (1998) demonstrated using gel mobility shift assays that curcumin prolonged the stress-induced activation of the HSE-binding activity of the HSF1 in C6 rat glioma cells. Additionally, studies using electromobility shift assays demonstrated that curcumin induced activation of HSF1 in HeLa cells (Dunsmore et al., 2001). Recently, Teiten et al. (2009) also demonstrated that curcumin induced nuclear translocation of HSF-1 and increased its binding ability to HSE present on the *hsp70* promoter. Lastly, these results are in agreement with previous studies in *Xenopus*, illustrating that pretreatment with KNK437, inhibited heat shock, chemical stress, MG132 and celastrol-induced *hsp* gene expression (Manwell and Heikkila, 2007; Voyer and Heikkila, 2008; Walcott and Heikkila, 2010; Young and Heikkila, 2010). The molecular and cellular mechanisms that lead to stress-inducible *hsp* gene expression as a result of proteasomal inhibition are unclear. Since the proteasome degrades approximately 90% of all proteins, inhibition of this process results in a substantial increase in the concentration of total cellular protein including misfolded or damaged proteins that would normally get degraded by the proteasome (Lee and Goldberg, 1998b). The accumulation of unfolded cellular protein by proteasomal inhibition may therefore trigger the activation of HSF1. This possibility is supported by previous studies in our laboratory, which demonstrated that proteasome inhibition by MG132, lactacystin and celastrol induced *hsp30* and *hsp70* gene expression in A6 cells (Walcott and Heikkila, 2010; Young and Heikkila, 2010).

In time course studies HSP30 and HSP70 were first detectable in A6 cells after 10 h of 30 μM curcumin treatment. HSP30 levels increased over time with maximal accumulation between 18 and 24 h. Similarly, HSP70 levels increased as the length of curcumin exposure was increased from 10 to 24 h. In contrast, continuous exposure of A6 cells to heat shock induced detectable levels of HSP30 and HSP70 after 1 h and maximal levels of HSP accumulation were observed after 2 h (Darasch et al., 1988). Reasons for the different temporal patterns of HSP accumulation in A6 cells subjected to heat shock and curcumin are not completely understood. It is possible that the delay in maximal HSP accumulation in A6 cells treated with curcumin may be due to the time required for curcumin to enter the cells and to increase the level of non-native protein by proteasomal inhibition in order to activate HSE-HSF1 binding activity. In support of this possibility a delayed accumulation of HSPs compared to heat shock was observed in A6 cells subjected to sodium arsenite, cadmium chloride, MG132, or celastrol (Gauley and Heikkila, 2006; Woolfson and Heikkila, 2009; Walcott and Heikkila, 2010; Young and Heikkila, 2010). For example, A6 cells exposed to 2.5 μM celastrol displayed detectable levels of HSP70 and HSP30 initially after 2 and 6 h of treatment, respectively, with maximal levels occurring after 18 h (Walcott and Heikkila, 2010). Also, MG132-treated A6 cells displayed enhanced levels of HSP70 and HSP30 after 4 and 8 h, respectively, with maximal HSP accumulation occurring after 24 h (Young and Heikkila, 2010).

The present study also investigated the pattern of HSP accumulation in *X. laevis* A6 cells recovering from curcumin treatment. Cells treated with 30 μM curcumin for 14 h had a relatively low accumulation of HSP30 and HSP70, which increased significantly for up to 24 h after the removal of curcumin. At 36 and 48 h post-treatment, the relative levels of HSPs decreased substantially. These findings were similar to results described in A6 cells recovering from

MG132 or celastrol, in which the relative levels of HSP30 and HSP70 remained elevated for up to 24 h (Walcott and Heikkila, 2010; Young and Heikkila, 2010). Additionally, a prolonged accumulation of HSPs was reported in rat neonatal cardiomyocytes recovering from proteasomal inhibition (Stangl et al., 2002). It is possible that elevated levels of HSPs are beneficial to curcumin-treated cells since relatively high concentrations of ubiquitinated cellular proteins that accumulate within the cytosol as a result of proteasomal inhibition may require an extended amount of time to re-establish protein homeostasis by degradation (Bush et al., 1997; Lee and Goldberg, 1998b; Liao et al., 2006).

In *X. laevis* A6 cells, concurrent treatment with mild heat shock and low concentrations of curcumin induced elevated levels of HSP30 and HSP70 accumulation. In fact, the relative levels of HSP30 and HSP70 in cells treated with both stressors were greater than the sum of the values found with each stressor individually. This result is supported by the finding that curcumin acted as a potent stimulator of heat shock-induced accumulation of HSP27 and αB crystallin in C6 rat glioma cells, BRL-3A rat liver cells and Swiss 3T3 mouse fibroblasts (Kato et al., 1998). Similarly, increased levels of HSP30 were observed in A6 cells treated concurrently with mild heat shock and relatively low concentrations of celastrol (Walcott and Heikkila, 2010). Moreover, increased levels of HSP30 and HSP70 accumulation were observed in *Xenopus* A6 cells treated concurrently with MG132 and mild heat shock temperatures (Young and Heikkila, 2010). Additionally, our laboratory also reported increases in *hsp* gene expression in A6 cells when a mild heat shock was combined with low concentrations of cadmium chloride, sodium arsenite, herbimycin A or hydrogen peroxide (Heikkila et al., 1987; Briant et al., 1997; Muller et al., 2004; Woolfson and Heikkila, 2009). The mechanism responsible for increased levels of HSP30 and HSP70 in A6 cells concurrently exposed to curcumin and mild heat shock is not

known. As mentioned previously, curcumin can induce an increase in the relative levels of ubiquitinated protein destined for degradation by proteasomal inhibition. Additionally, heat shock can induce a generalized unfolding of intracellular proteins. Thus, it is possible in A6 cells, that a combined mild heat shock and curcumin treatment will elevate the total level of non-native protein to a threshold level required for HSF1 activation. Evidence supporting the existence of a threshold level for HSF1 activation has been described in a number of systems including mouse T-lymphocytes and testis, intertidal mussels, HeLa cells and *Xenopus* (Sarge, 1995; Lee et al., 1995; Ali et al., 1997; Buckley et al., 2001; Gothard et al., 2003).

Immunocytochemistry and LSCM was employed to determine the localization of HSP30 in A6 cells exposed to heat shock or curcumin. Cells exposed to these stressors displayed HSP30 accumulation primarily in the cytoplasm in a granular or punctate pattern with a lesser amount in the nucleus. The punctate pattern of HSP30 accumulation may represent the stress-induced formation of HSP30 multimeric structures that are required for sHSP function (Ohan et al., 1998; MacRae, 2000; Van Montfort et al., 2001). Curcumin-induced HSP30 protein accumulation increased in a concentration- and time-dependent manner with no visible effects on the actin cytoskeleton, which has been used as an indicator of cellular viability and health (Wiegant et al., 1987; Ohtsuka et al., 1993). This was in contrast to treatment of A6 cells with celastrol, which resulted in a disruption of the actin cytoskeleton with most cells displaying a rounder morphology compared to control cells (Walcott and Heikkila, 2010).

Immunocytochemistry and LSCM revealed an enhanced accumulation of HSP30 in A6 cells treated concurrently with low curcumin concentrations and a mild heat shock compared to the stresses individually. HSP30 was readily detected in the cytoplasm in a granular pattern in cells treated with 10 μM curcumin at 30 °C for 2 h with a 2 h recovery with no visible effects on

the actin cytoskeleton. This pattern of enhanced accumulation of HSP30 in response to a combined stress increased over time with no detrimental effects on the actin cytoskeleton. These results are in agreement with previous studies in *Xenopus*, which illustrated that concurrent treatments with low concentrations of sodium arsenite (5 – 10 μM) and mild heat shock at 30 °C resulted in enhanced accumulation of HSP30 in the cytoplasm in a granular pattern (Young et al., 2009).

Some A6 cells pretreated with curcumin for 24 h displayed relatively large cytoplasmic foci containing HSP30 accumulation. Similar structures were reported in A6 cells exposed to cadmium chloride, sodium arsenite, MG132 or celastrol (Voyer and Heikkila, 2008; Woolfson and Heikkila, 2009; Walcott and Heikkila, 2010; Young and Heikkila, 2010). Although the identity of these large structures is currently unknown, it has been suggested that they are inclusion bodies containing HSP30 bound to unfolded proteins and may be associated with the molecular chaperone function of HSP30 (Fernando and Heikkila, 2000; Heikkila, 2004; Heikkila, 2010; Young and Heikkila, 2010). In support of this concept, previous studies determined that proteasome inhibition significantly increased the formation of cytosolic aggresomes that are composed of smaller protein aggregates also known as inclusion bodies (Garcia-Mata et al., 1999). Previous studies with A6 cells determined that these foci also occurred in response to high concentrations of MG132 or celastrol (Walcott and Heikkila, 2010; Young and Heikkila, 2010).

The present study also determined for the first time that cells acquire a state of thermotolerance when treated with curcumin. In the present study, curcumin-induced *hsp* gene expression was required for this state of thermotolerance since it was repressed by KNK437. In previous studies in A6 cells, our laboratory reported that a 33 ºC heat shock resulted in HSP-

mediated acquisition of thermotolerance as determined by cytoprotection of the actin cytoskeleton (Manwell and Heikkila, 2007). Together these findings suggest that heat shock and curcumin-induced HSP accumulation can protect cells from injury or other stresses based on the preservation of the cytoskeletal actin filaments and cellular morphology. It can be hypothesized that the accumulation of HSPs as a result of curcumin treatment increases the overall level of molecular chaperones in cells such that they can protect vital cellular proteins including those associated with the maintenance of the cytoskeleton. Additionally, this study determined that treatment of A6 cells with concurrent low concentrations of curcumin plus mild heat shock induced the accumulation of HSPs and conferred a state of thermotolerance. This result, which was not observed when the cells were treated with the stresses individually, was repressed by KNK437 (data not shown). The ability of A6 cells to respond to two relatively mild stresses and produce an enhanced accumulation of HSPs and a state of stress resistance is advantageous for survival since these chaperones can prevent or ameliorate the deleterious effects of stress-induced misfolded, damaged or aggregated protein. Additionally, the concept of using two relatively mild stressors to induce an enhanced level of *hsp* gene expression may be a strategic method to elevate HSP levels with minimal cellular damage. This is of importance given that upregulation of cellular HSPs has been proposed as a possible therapeutic strategy for protein conformational diseases (Westerheide and Morimoto, 2005).

In summary, the present study has shown for the first time in an amphibian system, that curcumin inhibited chymotrypsin-like activity of the proteasome, induced enhanced accumulation of ubiquitinated proteins and induced HSP30 and HSP70 accumulation in A6 cells with no detrimental effect on the actin cytoskeleton. Understanding the effect that curcumin has on *Xenopus hsp* gene expression is of importance given the potential therapeutic role for HSPs in

various human neurological disorders. Therefore, further analysis on the relationship between curcumin-induced proteasome inhibition and the accumulation of HSPs is required. Future studies should compare the effects of chronic versus acute stress imposed on A6 cells through curcumin treatments. Since many mammalian studies have suggested that proteasome inhibition may have an impact on molecular chaperones in the endoplasmic reticulum and HSP90 (Bush et al., 1997; Banerji, 2009); another avenue of future research is to investigate the effect of curcumin on other *Xenopus hsp* genes such as *BiP*, *hsp47*, *hsp90* and *hsp110*. Also the effect of proteasome inhibition on *hsp* gene expression during animal development has not been investigated. Given the advantages of the *Xenopus* embryonic system including microinjections and transgenic methodology, future experiments should examine the effects of curcumin on *hsp* gene expression during early development. Recently, curcumin has also been shown to induce apoptosis in human leukemia K562 cells at high concentrations of 80 – 100 μM (Teiten et al., 2009). Therefore, the potential induction of apoptosis in curcumin-treated *Xenopus* A6 cells and embryos should also be investigated. For example, the use of apoptotic cell based assays or utilizing Hoechst 33258 with immunocytochemistry and LSCM would help to determine if A6 cells are undergoing apoptosis in response to higher concentrations of curcumin.

References

Abdulle, R., Mohindra, A., Fernando, P., Heikkila, J.J. 2002. *Xenopus* small heat shock proteins, Hsp30C and Hsp30D, maintain heat- and chemically denatured luciferase in a folding-competent state. Cell Stress Chaperones 7, 6-16.

Abe, Y., Hashimoto, S., Horie, T. 1999. Curcumin inhibition of inflammatory cytokine production by human peripheral blood monocytes and alveolar macrophages. Pharmacol. Res. 39, 41-47.

Adhikari, A.S., Sridhar-Rao, K., Rangaraj, N., Parnaik, V.K., Mohan-Rao, C. 2004. Heat stress-induced localization of small heat shock proteins in mouse myoblasts: intranuclear lamin A/C speckles as target for alphaB-crystallin and Hsp25. Exp. Cell Res. 299, 393-403.

Aggarwal, B.B., Kumar, A., Bharti, A.C. 2003. Anticancer potential of curcumin: Preclinical and clinical studies. Anticancer Res. 23, 363-398.

Ali, A., Salter-Cid, L., Flajnik, M., Heikkila, J.J. 1996a. Isolation and characterization of a cDNA encoding a *Xenopus* 70-kDa heat shock cognate protein, Hsc70.I. Comp. Biochem. Physiol. B Biochem. Mol. Biol. 113, 681-687.

Ali, A., Salter-Cid, L., Flajnik, M., Heikkila, J.J. 1996b. Molecular cloning of a cDNA encoding a *Xenopus* laevis 70-kDa heat shock cognate protein, hsc70.II. Biochim. Biophys. Acta. 1309, 174-178.

Ali, A., Fernando, P., Smith, W.L., Ovsenek, N., Lepock, J.R. and Heikkila, J.J. 1997. Preferential activation of HSF-binding activity and *hsp70* gene expression in *Xenopus* heart after mild hyperthermia. Cell Stress Chaperones 2, 229-237.

Ali, R.E., Rattan, S.I. 2006 Curcumin's biphasic hormetic response on proteasome activity and heat-shock protein synthesis in human keratinocytes. Ann. N.Y. Acad. Sci. 1067, 394-399.

Ammon, H.P., Wahl, M.A. 1991. Pharmacology of *Curcuma longa*. Planta Med. 57, 1-7.

Anckar, J., Hietakangas, V., Denessiouk, K., Thiele, D.J., Johnson, M.S., Sistonen, L. 2006. Inhibition of DNA binding by differential sumoylation of heat shock factors. Mol. Cell Biol. 26, 955-964.

Arrigo, A-P., Landry, J. 1994. Expression and function of the low-molecular weight heat shock proteins. In: The Biology of Heat Shock Proteins and Molecular Chaperones. Cold Spring Harbor Laboratory Press, Cold Spring Harbor, N.Y.

Arrigo, A-P. 1998. Small stress proteins: chaperones that act as regulators of intracellular redox state and programmed cell death. J. Biol. Chem. 379, 19-26.

Balch, W.E., Morimoto, R.I., Dillin A., Kelly J.W. 2008. Adapting proteostasis for disease intervention. Science 319, 916-919.

Banerji, U. 2009. Heat shock protein 90 as a drug target: Some like it hot. Clin. Cancer Res. 15, 9-14.

Beere, H.M., Wolf, B.B., Cain, K., Mosser, D.D., Mahboubi, A., Kuwana, T., Tailor, P., Morimoto, R.I., Cohen, G.M., Green, D.R. 2000. Heat-shock protein 70 inhibits apoptosis by preventing recruitment of procaspase-9 to the apaf-1 apoptosome. Nat. Cell Biol. 2, 469-475.

Bienz, M. 1984. Developmental control of the heat shock response in *Xenopus*. Proc. Natl. Acad. Sci. USA. 81, 3138-3142.

Birnbaum, G., Kotilinek, L. 1997. Heat shock or stress proteins and their role as autoantigens in multiple sclerosis. Ann. N.Y. Acad. Sci. 835, 157-167.

Boorstein, W.R., Ziegelhoffer, T., Craig, E.A. 1994. Molecular evolution of the HSP70 multigene family. J. Mol. Evol. 38, 1-17.

Briant, D., Ohan, N., Heikkila, J.J. 1997. Effect of herbimycin A on *hsp30* and *hsp70* heat shock protein gene expression in *Xenopus* cultured cells. Biochem. Cell Biol. 75, 777-782.

Brodsky, J.L., Chiosis, G. 2006. Hsp70 molecular chaperones: emerging roles in human disease and identification of small molecule modulators. Curr. Top. Med. Chem. 6, 1215-1225.

Buchner, J., Ehrnsperger, M., Gaestel, M., Walke, S. 1998. Purification and characterization of small heat shock proteins. Methods Enzymol. 290, 339-349.

Buckley, B.A., Owen, M-E., Hofmann, G.E. 2001. Adjusting the thermostat: the threshold induction temperature for the heat-shock response in intertidal mussels (genus *Mytilus*) changes as a function of thermal history. J. Exp. Biol. 204, 3571-3579.

Burggren, W.W, Warburton, S. 2007. Amphibians as animal models for laboratory research in physiology. Institute of Laboratory Animal Resources J. 48, 260-269.

Bush, K.T., Goldberg, A.L., Nigam, S.K. 1997. Proteasome inhibition leads to a heat-shock response, induction of endoplasmic reticulum chaperones, and thermotolerance. J. Biol. Chem. 272, 9086-9092.

Campbell, F.C., Collett, G.P. 2005. Chemopreventive properties of curcumin. Future Oncol. 1, 405-414.

Chen, H.W., Yu, S.L., Chen, J.J., Li, H.N., Lin, Y.C., Yao, P.L., Chou, H.Y., Chien, C.T., Chen, W.J., Lee, Y.T., Yang, P.C. 2004. Anti-invasive gene expression profile of curcumin in lung adenocarcinoma based on a high throughput microarray analysis. Mol. Pharmacol. 65, 99-110.

Chen, Y.C., Tsai, S.H., Shen, S.C., Lin, J.K., Lee, W.R. 2001. Alternative activation of extracellular signal-regulated protein kinases in curcumin and arsenite-induced HSP70 gene expression in human colorectal carcinoma cells. Eur. J. Cell Biol. 80, 213-221.

Ciechanover, A. 1998. The ubiquitin-proteasome pathway: on protein death and cell life. EMBO J. 17, 7151-7160.

Ciocca, D.R., Oesterreich, S., Chamness, G.C., McGuire, W.L., Fuqua, S.A. 1993. Biological and clinical implications of heat shock protein 27000 (Hsp27): a review. J. Natl. Cancer Inst. 85, 1558-1570.

Cohen, S., Lahav-Baratz, S., Ciechanover, A. 2006. Two distinct ubiquitin-dependent mechanisms are involved in NF-κB p105 proteolysis. Biochem. Biophys. Res. Commun. 345, 7-13.

Darasch, S., Mosser, D.D., Bols, N.C., Heikkila, J.J. 1988. Heat shock gene expression in *Xenopus laevis* A6 cells in response to heat shock and sodium arsenite treatments. Biochem. Cell Biol. 66, 862-868.

Daugaard, M., Rohde, M., Jäättelä, M. 2007. The heat shock protein 70 family: Highly homologous proteins with overlapping and distinct functions. FEBS Lett. 581, 3702-3710.

Deeb, D.D., Jiang, H., Gao, X., Divine, G., Dulchavsky, S.A., Gautam, S.C. 2005. Chemosensitization of hormone-refractory prostate cancer cells by curcumin to TRAIL-induced apoptosis. J. Exp. Ther. Oncol. 5, 81-91.

Dunsmore, K.E., Chen, P.G., Wong, H.R. 2001. Curcumin, a medicinal herbal compound capable of inducing the heat shock response. Crit. Care Med. 29, 2199 - 2204.

Duvoix, A., Morceau, F., Schnekenburger, M., Delhalle, S., Galteau, M.M., Dicato, M., Diederich, M. 2003. Curcumin-induced cell death in two leukemia cell lines: K562 and jurkat. Ann. N.Y. Acad. Sci. 1010, 389-392.

Feige, U., Morimoto, R.I., Yahara, I., Polla, B.S. 1996. "Stress-inducible cellular responses," Birkhauser Verlag., Basel: Switzerland.

Fernando, P., Abdulle, R., Mohindra, A., Guillemette, J.G., Heikkila, J.J. 2002. Mutation or deletion of the C-terminal tail affects the function and structure of *Xenopus laevis* small heat shock protein, hsp30. Comp. Biochem. Physiol. B Biochem. Mol. Biol. 133, 95-103.

Fernando, P., Heikkila, J.J. 2000. Functional characterization of *Xenopus* small heat shock protein, Hsp30C: The carboxyl end is required for stability and chaperone activity. Cell Stress Chaperones 5, 148-159.

Freeman, B.C., Yamamoto, K.R. 2002. Disassembly of transcriptional regulatory complexes by molecular chaperones. Science 296, 2232-2235.

Ganea, E. 2001. Chaperone-like activity of α-crystallin and other small heat shock proteins. Curr. Protein Pept. Sci. 2, 205-225.

Garcia-Mata, R., Bebok, Z., Sorscher, E.J., Sztul, E.S. 1999. Characterization and dynamics of aggresome formation by a cytosolic GFP-chimera. J. Cell Biol. 146, 1239-1254.

Garg, A.K., Buchholz, T.A., Aggarwal, B.B. 2005. Chemosensitization and radiosensitization of tumors by plant polyphenols. Antioxid. Redox. Signal. 7, 1630-1647.

Gauley, J., Heikkila, J.J. 2006. Examination of the expression of the heat shock protein gene, *hsp110*, in *Xenopus laevis* cultured cells and embryos. Comp. Biochem. Physiol. A Mol. Integr. Physiol. 145, 225-234.

Gauley, J., Young, J.T.F., Heikkila, J.J. 2008. Intracellular localization of the heat shock protein, HSP110, in *Xenopus laevis* A6 kidney epithelial cells. Comp. Biochem. Physiol. A Mol. Integr. Physiol. 151, 133-138.

Gellalchew, M., Heikkila, J.J. 2005. Intracellular localization of *Xenopus* small heat shock protein, hsp30, in A6 kidney epithelial cells. Cell Biol. Int. 29, 221-227.

Gothard, L.Q., Ruffner, M.E., Woodward, J.G., Park-Sarge, O-K. and Sarge, K.D. 2003. Lowered temperature set point for ativation of the cellular stress response in T-lymphocytes. J. Biol. Chem. 278, 9322-9326.

Groll, M., Ditzel, L., Lowe, J., Stock, D., Bochtler, M., Bartunik, H.D., Huber, R. 1997. Structure of 20S proteasome from yeast at 2.4 A resolution. Nature 386, 463-471.

Guerra, L., Favia, M., Fanelli, T., Calamita, G., Svetlo, M., Bagorda, A., Jacobson, K.A., Reshkin, S.J., Casavola, V. 2004 Stimulation of *Xenopus* P2Y1 receptor activates CFTR in A6 cells. Pflugers Arch. 449, 66-75.

Hartl, F.U. 1996. Molecular chaperones in cellular protein folding. Nature 381, 571-579.

Hartl, F.U, Hayer-Hartl, M. 2009. Converging concepts of protein folding in vitro and in vivo. Nat Struct. Mol. Biol. 16, 574-581.

Haslbeck, M. 2002. SHsps and their role in the chaperone network. Cell Mol. Life Sci. 59, 1649-1657.

Heikkila, J.J. 2003. Expression and function of small heat shock protein genes during *Xenopus* development. Semin. Cell Dev. Biol. 14, 259-266.

Heikkila, J. J. 2004. Regulation and function of small heat shock protein genes during amphibian development. J. Cell Biochem. 93, 672-680.

Heikkila, J.J. 2010. Heat shock protein gene expression and function in amphibian model systems. Comp. Biochem. Physiol. A Mol. Integr. Physiol. 156, 19-33.

Heikkila, J.J., Ohan, N., Tam, Y., Ali, A. 1997. Heat shock protein gene expression during *Xenopus* development. Cell Mol. Life Sci. 53, 114-121.

Heikkila, J.J., Kaldis, A., Morrow, G., Tanguay, R.M. 2007. The use of the *Xenopus* oocyte as a model system to analyze the expression and function of eukaryotic heat shock proteins. Biotechnol. Adv. 25, 385-395.

Hershko, A., Ciechanover, A. 1998. The ubiquitin system. Ann. Rev. Biochem. 67, 425-479.

Holmberg, C.I., Tran, S.E., Eriksson, J.E., Sistonen, L. 2002. Multisite phosphorylation provides sophisticated regulation of transcription factors. Trends Biochem. Sci. 27, 619-627.

Hong, Y., Rogers, R., Matunis, M.J., Mayhew, C.N., Goodson, M.L., Park-Sarge, O.K., Sarge, K.D. 2001. Regulation of heat shock transcription factor 1 by stress-induced SUMO-1 modification. J. Biol. Chem. 276, 40263-40267.

Ikuzawa, M., Akiduki, S., Asashima, M. 2007. Gene expression profile of *Xenopus* A6 cells cultured under random positioning machine shows downregulation of ion transporter genes and inhibition of dome formation. Adv. Space Res. 40, 1694-1702.

Jolly, C., Morimoto, R.I. 2000. Role of the heat shock response and molecular chaperones in oncogenesis and cell death. J. Natl. Cancer Inst. 92, 1564-1572.

Kanitkar, M., Bhonde, R.R. 2008. Curcumin treatment enhances islet recovery by induction of heat shock response proteins, Hsp70 and heme oxygenase-1, during cryopreservation. Life Sci. 82, 182-189.

Kato, K., Ito, H., Kamei, K., Iwamoto, I. 1998. Stimulation of the stress-induced expression of stress proteins by curcumin in cultured cells and in rat tissues in vivo. Cell Stress Chaperones, 3, 152-160.

Katschinski, D. M. 2004. On heat and cells and proteins. News Physiol. Sci. 19, 11-15.

Klemenz, R., Andrews, A-C, Frohli, E., Schafer, R., Aoyama, A. 1993. Expression of the murine small heat shock proteins hsp25 and αB crystalline in the absence of stress. J. Cell Biol. 120, 639-645.

Koegl, M., Hoppe, T., Schlenker, S., Ulrich, H.D., Mayer, T.U., Jentsch, S. 1999. A novel ubiquitination factor, E4, is involved in multiubiquitin chain assembly. Cell 96, 635-644.

Krone, P., Heikkila, J.J. 1988. Analysis of *hsp30*, *hsp70*, and ubiquitin gene expression in *Xenopus laevis* tadpoles. Development 103, 59-67.

Krone, P.H., Snow, A., Ali, A., Pasternak, J.J., Heikkila, J.J. 1992. Comparison of regulatory and structural regions of the *Xenopus laevis* small heat-shock protein-encoding gene family. Gene 110, 159-166.

Lambert, H., Charette, S.J., Bernier, A.F., Guimond, A., Landry, J. 1999. HSP27 multimerization mediated by phosphorylation-sensitive intermolecular interactions at the amino terminus. J. Biol. Chem. 274, 9378-9385.

Landis-Piwowar, K.R., Milacic, V., Chen, D., Yang, H., Zhao, Y., Chan, T.H., Yan, B., Dou, Q.P. 2006. The proteasome as a potential target for novel anticancer drugs and chemosensitizers. Drug Resist. Updat. 9, 263-273.

Lang, L., Miskovic, D., Fernando, P., Heikkila, J.J. 1999. Spatial pattern of constitutive and heat shock-induced expression of the small heat shock protein gene family, Hsp30, in *Xenopus laevis* tailbud embryos. Dev. Genet. 25, 365-374.

Lang, L., Miskovic, D., Lo, M. Heikkila, J.J. 2000. Stress-induced, tissue-specific enrichment of *hsp70* mRNA accumulation in *Xenopus laevis* embryos. Cell Stress Chaperones 5, 36-44.

Lee, D.H., Goldberg, A.L. 1998a. Proteasome inhibitors: valuable new tools for cell biologists. Trends Cell Biol. 8, 397-403.

Lee, D.H., Goldberg, A.L. 1998b. Proteasome inhibitors cause induction of heat shock proteins and trehalose, which together confer thermotolerance in *Saccharomyces cerevisiae.* Mol. Cell Biol. 18, 30-38.

Lehman, N.L. 2009. The ubiquitin proteasome system in neuropathology. Acta Neuropathol. 118, 329-347.

Liao, W., Li, X., Mancini, M., Chan, L. 2006. Proteasome inhibition induces differential heat shock protein response but not unfolded protein response in HepG2 cells. J. Cell Biochem. 99, 1085-1095.

Lindquist, S. 1986. The heat-shock response. Annu. Rev. Biochem. 55, 1151-1191.

Lopes, U.G., Erhardt, P., Yao, R., Cooper, G.M. 1997. p53-dependent induction of apoptosis by proteasome inhibitors. J. Biol. Chem. 272, 12893-12896.

MacRae, T.H. 2000. Structure and function of small heat shock/α-crystallin proteins: Established concepts and emerging ideas. Cell Mol. Life Sci. 57, 899-913.

Maheshwari, R.K., Singh, A.K., Gaddipati, J., Srimal, R.C. 2006. Multiple biological activities of curcumin: A short review. Life Sci. 78, 2081-2087.

Malik, B., Schlanger, L., Al-Khalili, O., Bao, H.F., Yue, G., Price, S.R., Mitch, W.E., Eaton, D.C. 2001. Enac degradation in A6 cells by the ubiquitin-proteosome proteolytic pathway. J. Biol. Chem. 276, 12903-12910.

Malusecka, E., Zborek, A., Krzyzowska-Gruca, S., Krawczyk, Z. 2001. Expression of heat shock proteins HSP70 and HSP27 in primary non-small cell lung carcinomas. an immunohistochemical study. Anticancer Res. 21, 1015-1021.

Mani, A., Gelmann, E.P. 2005. The ubiquitin-proteasome pathway and its role in cancer. J. Clin. Oncol. 23, 4776-4789.

Manwell, L.A., Heikkila, J.J. 2007. Examination of KNK437- and quercetin-mediated inhibition of heat shock-induced heat shock protein gene expression in *Xenopus laevis* cultured cells. Comp. Biochem. Physiol. A Mol. Integr. Physiol. 148, 521-530.

Masliah, E., Rockenstein, E., Veinbergs, I., Mallory, M., Hashimoto, M., Takeda, A., Sagara, Y., Sisk, A., Mucke, L. 2000. Dopaminergic loss and inclusion body formation in alpha-synuclein mice: Implications for neurodegenerative disorders. Science 287, 1265-1269.

Melendez, K., Wallen, E.S., Edwards, B.S., Mobarak, C.D., Bear, D.G., Moseley, P.L. 2006. Heat shock protein 70 and glycoprotein 96 are differentially expressed on the surface of malignant and nonmalignant breast cells. Cell Stress Chaperones 11, 334-342.

Milacic, V., Banerjee, S., Landis-Piwowar, K.R., Sarkar, F.H., Majumdar, A.P.N., Dou, Q.P. 2008. Curcumin inhibits the proteasome activity in human colon cancer cells in vitro and *in vivo*. Cancer Res. 68, 7283-7292.

Miskovic, D., Salter-Cid, L., Ohan, N., Flajnik, M., Heikkila, J.J. 1997. Isolation and characterization of a cDNA encoding a *Xenopus* immunoglobulin binding protein, BiP (grp78). Comp. Biochem. Physiol. B Biochem. Mol. Biol. 116, 227-34.

Morimoto, R.I. 1998. Regulation of the heat shock transcriptional response: Cross talk between a family of heat shock factors, molecular chaperones, and negative regulators. Genes Dev. 12, 3788-3796.

Morimoto, R.I, Santoro, M.G. 1998. Stress-inducible responses and heat shock proteins: New pharmacologic targets for cytoprotection. Nat. Biotechnol. 16, 833-838.

Morimoto, R.I. 2008. Proteotoxic stress and inducible chaperone networks in neurodegenerative disease and aging. Genes Dev. 22, 1427-1438.

Mosser, D.D., Caron, A.W., Bourget, L., Meriin, A.B., Sherman, M.Y., Morimoto, R.I., Massie, B. 2000. The chaperone function of hsp70 is required for protection against stress-induced apoptosis. Mol. Cell Biol. 20, 7146-7159.

Muller, M., Gauley, J., Heikkila, J.J. 2004. Hydrogen peroxide induces heat shock protein and proto-oncogene mRNA accumulation in *Xenopus laevis* A6 kidney epithelial cells. Can. J. Physiol. Pharmacol. 82, 523-529.

Nakai, A. 1999. New aspects in the vertebrate heat shock factor system: HSF3 and HSF4. Cell Stress Chaperones 4, 86-93.

Nylandsted, J., Brand, K., Jaattela, M. 2000. Heat shock protein 70 is required for the survival of cancer cells. Ann. N.Y. Acad. Sci. 926, 122-125.

Ohan, N.W., Tam, Y., Fernando, P., Heikkila, J.J. 1998. Characterization of a novel group of basic small heat shock proteins in *Xenopus laevis* A6 kidney epithelial cells. Biochem. Cell Biol. 76, 665-671.

Ohtsuka, K., Liu, Y.C., Kaneda, T. 1993. Cytoskeletal thermotolerance in NRK cells.Int J Hyperthermia 9, 115-124.

Ostling, P., Bjork, J.K., Roos-Mattjus, P., Mezger, V., Sistonen, L. 2007. Heat shock factor 2 (HSF2) contributes to inducible expression of *hsp* genes through interplay with HSF1. J. Biol. Chem. 282, 7077-7086.

Ovsenek, N., Heikkila, J.J. 1990. DNA sequence-specific binding activity of the heat shock transcription factor is heat-inducible before midblastula transition of early *Xenopus* development. Development 110, 427-433.

Phang, D., Joyce, E.M., Heikkila J.J. 1999. Heat shock-induced acquisition of thermotolerance at the levels of cell survival and translation in *Xenopus* A6 kidney epithelial cells. Biochem. Cell Biol. 77, 141-151.

Pirkkala, L., Nykanen, P., Sistonen, L. 2001. Roles of the heat shock transcription factors in regulation of the heat shock response and beyond. Fed. Am. Soc. Exp. Biol. J. 15, 1118-1131.

Rafferty, K.A. 1968. Mass culture of amphibian cells: methods and observations concerning stability of cell type. In Biology of Amphibian Tumors (ed. M Mizzel), pp. 52-81. New York, NY, USA: Springer Verlag.

Rallu, M., Loones, M., Lallemand, Y., Morimoto, R.I., Morange, M., Mezger, V. 1997. Function and regulation of heat shock factor 2 during mouse embryogenesis. Proc. Natl. Acad. Sci. U.S.A. 94, 2392-2397.

Ross, C.A., Pickart, C.M. 2004. The ubiquitin–proteasome pathway in Parkinson's disease and other neurodegenerative diseases. Trends Cell Biol. 14, 703-711.

Sambrook, J., Russell, D.W. 2001. Molecular cloning: A laboratory manual. Cold Spring Harbor Laboratory Press, Cold Spring Harbor, N.Y.

Sarge, K.D. 1995. Male germ cell-specific alteration in temperature set point of the cellular stress response. J. Biol. Chem. 270, 18745-18748.

Shishodia, S., Amin, H.M., Lai, R., Aggarwal, B.B. 2005. Curcumin (diferuloylmethane) inhibits constitutive NF-kappaB activation, induces G1/S arrest, suppresses proliferation, and induces apoptosis in mantle cell lymphoma. Biochem. Pharmacol. 70, 700-713.

Smith, J.C., Tata, J.R. 1991. *Xenopus* cell lines. In “Methods in cell biology” 36, pp. 635-654, Academic Press, Inc., London, England.

So, A., Hadaschik, B., Sowery, R., Gleave, M. 2007.The role of stress proteins in prostate cancer. Curr. Genomics 8, 252-261.

Sreedhar, A.S., Csermely, P. 2004. Heat shock proteins in the regulation of apoptosis: new strategies in tumor therapy: a comprehensive review. Pharmacol. Ther. 101, 227-257.

Stangl, K., Gunther, C., Frank, T., Lorenz, M., Meiners, S., Ropke, T., Stelter, L., Moobed, M., Baumann, G., Kloetzel, P.M., Stangl, V. 2002. Inhibition of the ubiquitin-proteasome pathway induces differential heat-shock protein response in cardiomyocytes and renders early cardiac protection. Biochem. Biophys. Res. Commun. 291, 542-549.

Stromer, T., Ehrnsperger, M., Gaestel, M., Buchner, J. 2003. Analysis of the interaction of small heat shock proteins with unfolding proteins. J. Biol. Chem. 278, 18015-18021.

Takemoto, L., Emmons, T., Horwitz, J. 1993. The C-terminal region of α- crystallin: involvement in protection against heat-induced denaturation. Biochem. J. 294, 435-438.

Tanabe, M., Sasai, N., Nagata, K., Liu, X.D., Liu, P.C., Thiele, D.J., Nakai, A. 1999. The mammalian HSF4 gene generates both an activator and a repressor of heat shock genes by alternative splicing. J. Biol. Chem. 274, 27845-27856.

Teiten, M., Reuter, S., Schmucker, S., Dicato, M., Diederich, M. 2009. Induction of heat shock response by curcumin in human leukemia cells. Cancer Lett. 279, 145-154.

Van Montfort, R., Slingsby, C., Vierling, E. 2001. Structure and function of the small heat shock protein/alpha-crystallin family of molecular chaperones. Adv. Protein Chem. 59, 105-156.

Venkatesan, N., Chandrakasan, G. 1995. Modulation of cyclophosphamide-induced early lung injury by curcumin, an anti-inflammatory antioxidant. Mol. Cell Biochem. 142, 79-87.

Voellmy, R. 2004. On mechanisms that control heat shock transcription factor activity in metazoan cells. Cell Stress Chaperones 9, 122-133.

Voyer, J., Heikkila, J.J. 2008. Comparison of the effect of heat shock factor inhibitor, KNK437, on heat shock- and chemical stress-induced *hsp30* gene expression in *Xenopus laevis* A6 cells. Comp. Biochem. Physiol. A Mol. Integr. Physiol. 151, 253-261.

Walcott, S.E., Heikkila, J.J. 2010. Celastrol can inhibit proteasome activity and upregulate the expression of heat shock protein genes, *hsp30* and *hsp70*, in *Xenopus laevis* A6 cells. Comp Biochem Physiol A Mol Integr Physiol.156, 285-293.

Wang, J., Zhang, Z., Chou, C., Liang, Y., Gu, Y., Ma, H. 2009. Cyclosporine stimulates the renal epithelial sodium channel by elevating cholesterol. Am. J. Physiol. Renal Physiol. 296, F284-F290.

Westerheide S.D., Morimoto, R.I. 2005. Heat shock response modulators as therapeutic tools for diseases of protein conformation. J. Biol. Chem. 280, 33097-33100.

Westerheide, S.D., Bosman, J.D., Mbadugha, B.N., Kawahara, T.L., Matsumoto, G., Kim, S., Gu, W., Devlin, J.P., Silverman, R.B., Morimoto, R.I. 2004. Celastrols as inducers of the heat shock response and cytoprotection. J. Biol. Chem. 279, 56053-56060.

Whitesell, L., Mimnaugh, E.G., De Costa, B., Myers, C.E., Neckers, L.M. 1994. Inhibition of heat shock protein HSP90-pp60v-src heteroprotein complex formation by benzoquinone ansamycins: Essential role for stress proteins in oncogenic transformation. Proc. Natl. Acad. Sci. U.S.A. 91, 8324-8328.

Wiegant, F.A., van Bergen en Henegouwen, P.M., van Dongen, G., Linnemans, W.A. 1987. Stress-induced thermotolerance of the cytoskeleton of mouse neuroblastoma N2A cells and rat Reuber H35 hepatoma cells. Cancer Research 47, 1674-1680.

Woolfson, J.P., Heikkila, J.J. 2009. Examination of cadmium-induced expression of the small heat shock protein gene, *hsp30*, in *Xenopus laevis* A6 kidney epithelial cells. Comp. Biochem. Physiol. A Mol. Integr. Physiol. 152, 91-99.

Yamamoto, N., Takemori, Y., Sakurai, M., Sugiyama, K., Sakurai, H. 2009. Differential recognition of heat shock elements by members of the heat shock transcription factor family. FEBS. J. 276, 1962-1974.

Yang, H., Landis-Piwowar, K.R., Chen, D., Milacic, V., Dou, Q.P. 2008. Natural compounds with proteasome inhibitory activity for cancer prevention and treatment. Curr. Protein Pept. Sci. 9, 227-239.

Young, J.T.F., Gauley, J., Heikkila, J.J. 2009. Simultaneous exposure of *Xenopus* A6 kidney epithelial cells to concurrent mild sodium arsenite and heat stress results in enhanced *hsp30* and *hsp70* gene expression and the acquisition of thermotolerance. Comp. Biochem. Physiol. A Mol. Integr. Physiol. 153, 417-424.

Young, J.T., Heikkila, J.J. 2010. Proteasome inhibition induces *hsp30* and *hsp70* gene expression as well as the acquisition of thermotolerance in *Xenopus laevis* A6 cells. Cell Stress Chaperones 15, 323-334.

Zhang, Y.Q., Sarge, K.D. 2007. Celastrol inhibits polyglutamine aggregation and toxicity though induction of the heat shock response. J. Mol. Med. 85, 1421-1428.